11-1-2008

Gamut extension algorithm development and evaluation for the mapping of standard image content to wide-gamut displays

Stacey E. Casella

Gamut Extension Algorithm Development and Evaluation for the Mapping of Standard Image Content to Wide-Gamut Displays.

Stacey E. Casella

MUNSELL COLOR SCIENCE LABORATORY
CHESTER F. CARLSON CENTER FOR IMAGING SCIENCE
COLLEGE OF SCIENCE
ROCHESTER INSTITUTE OF TECHNOLOGY
ROCHESTER, NEW YORK

Accepted by:
Mark D. Fairchild, Advisor, M.S. Program Coordinator
James S. Ferwerda, Reviewer

Gamut Extension Algorithm Development and Evaluation for the Mapping of Standard Image Content to Wide-Gamut Displays

Stacey E. Casella

ABSTRACT

Wide-gamut display technology has provided an excellent opportunity to produce visually pleasing images, more so than in the past. However, through several studies, including Laird and Heynderick, 2008, it was shown that linearly mapping the standard sRGB content to the gamut boundary of a given wide-gamut display may not result in optimal results. Therefore, several algorithms were developed and evaluated for observer preference, including both linear and sigmoidal expansion algorithms, in an effort to define a single, versatile gamut expansion algorithm (GEA) that can be applied to current display technology and produce the most preferable images for observers. The outcome provided preference results from two displays, both of which resulted in large scene dependencies. However, the sigmoidal GEAs (SGEA) were competitive with the linear GEAs (LGEA), and in many cases, resulted in more pleasing reproductions. The SGEAs provide an excellent baseline, in which, with minor improvements, could be key to producing more impressive images on a wide-gamut display.

ACKNOWLEDGEMENT

To my advisor, Dr. Mark Fairchild- Thank you for all of your support and guidance throughout my Master's degree at RIT. I sincerely appreciate the opportunity you provided me to work on this thesis project. I have truly enjoyed the entire process, through which I have learned more than I ever expected.

I would like to express my sincere gratitude to Dr. Roy Berns for additionally providing me with the unforgettable opportunity to join the Color Science community. Also, thank you to the rest of the Munsell Color Science Laboratory faculty, present during my degree: Dr. Ethan Montag, Dr. David Wyble, Lawrence Taplin, Dr. James Ferwerda and Dr. Mitchell Rosen. I am reminded everyday in my professional career how much knowledge I obtained from all of you, and am incredibly grateful to have had that opportunity.

I also owe a special thanks to Dr. Rodney Heckaman. Rod—you kept me inspired throughout this program, bringing a smile to my face everyday. I owe much of my degree to your encouragement and support throughout my research, and am so fortunate to have your invaluable friendship to take with me. Also, to the two classmates I owe my survival of first year to- Shen and Nanette. We were an excellent team and I cannot express enough gratitude to both of you for all of your support. In addition, thank you to my best observer/recruiter –Erin. You helped me in so many ways this past year, taking my experiment and recruiting others, as well as being an excellent friend. Thank you to the rest of the Color Science family during my time at MCSL: Val, Colleen, Ben, Jonathan, Justin, Sunghyun, Abhijit, Philipp, Ying, Yang, Cathy, Tim, Mahdi, Mahnaz, Iris, Stefan, Susan, YK, to name a few! You all have provided me with such fond memories to remember my years at RIT by.

This research was made possible by Sony Corporation, in which I owe particular thanks to Masato Sakurai, Takehiro Nakatsue and Yoshihide Shimpuku for their guidance, contributions and cooperation throughout this collaborative research.

Last, but certainly not least, my family to which I owe so much thanks. To my husband, Michael—You have provided me with more love and encouragement than I could have ever wished for. Thank you for always supporting me, and enabling me to be a better person. To my incredibly supportive family: Mom and Dad, my siblings, Kristen and Tyler, my grandparents, Gram and Grandpa, Nana and Papa and my parents-in-law, Bob and Mary—You have provided me with the means to pursue all of my dreams. Without any of one of you I would not be the person I am today.

Table of Contents

List of Figures

List of Tables

1. Introduction

The success of digital image rendering is dependent on several variables, including the display the output is viewed on. Current display technology has enabled the goal of expanding the colorfulness of images to become a reality. However, the standard means by which this occurs has yet to be established. Enlarged color gamuts provide greater opportunity for implementing various rendering intents, while allowing more room for creativity on the production side. However, based on past research, it appears the mechanism in which current image and media content is mapped to an enlarged color gamut needs to be carefully considered in order to avoid unpleasing results. Therefore, multiple gamut expansion algorithms (GEAs) should be considered such that the legacy sRGB content (Rec. 709) is expanded in the most preferable manner.

Overall, the development of GEAs has the potential to dramatically enhance the consumers experience with wide-gamut displays, provided appropriate transformations of the data take place. This research delves into suggestions for these transformations to assist in improving the consumer's viewing experience.

2. Motivation: Wide Gamut Displays

A collaborative, necessary effort between Sony's Standard Systems Development Department, Sony Corporation, and the Munsell Color Science Laboratory (MCSL) at the Rochester Institute of Technology (RIT) focused on enhancement of digital image content under existing standards by exercising wide color gamuts. This research will provide guidance on the enhancement of image content, so that both the production and consumption sides of the display industry will benefit. Specifically, the aim of this research is to devise a gamut expansion strategy that is most visually pleasing to the average observer.

With the display technology present today, expanding the colorfulness of images is no longer a challenge. However, current research [Heckaman et al.; 2007, Laird and Heynderickx; 2008] indicates that observer preference does not necessarily increase monotonically with color. Heckaman et al. reported consistent results that observers enjoyed increased colorfulness and lightness contrast with wide gamut displays; however, this effect was scene-dependent. Laird and Heynderickx attributed this scene-dependency to the naturalness of an image, and through their research, established perceptually optimal boundaries for extended gamut displays. In an effort to attain ideal preference results across all images, gamut expansion methods have been, and continue to be, developed and analyzed for their effectiveness in mapping image content under current existing standards (e.g. Rec. 709, YCC) to extended gamut color spaces such as xvYCC [IEC; 2006, Stokes et al.; 1996]. Therefore, through this research, the capabilities of enhancement algorithms will be better understood, such that suggestions will be made regarding the implementation of gamut extension mapping algorithms.

3. Background

The display technology facilitates the rendering capabilities under the given GEAs. Therefore, it is necessary to fully understand the limitations due to the display itself in order to provide greater opportunity to incorporate a successful mapping strategy.

3.1 Gamut Mapping

The phrase, "a picture is worth a thousand words," stems back to an article written by Fred Barnard in 1921, although increases in value still today. Imagery enables stories to be told, concepts to be made, and even, surgeries to be conducted. Technology has certainly aided this proverb throughout the years, and continues to have a large influence over images. With the introduction of digital photography, for example, cross-media processing can easily take place. However, working with different media introduces new challenges.

With each type of device, and each company responsible for designing and producing the devices, different specifications are set. Therefore, when converting data formulated for one device to a second device, it is necessary to bring the data in sync with the latter device's specifications so that the image will look reasonable. This happens to be a complicated process in the color field.

Each device maintains a unique set of primaries, and hence, the number of reproducible colors a particular device can display is also unique [Wen; 2005]. Therefore, additional considerations need to be taken in order to adequately display an image on multiple devices. This process is commonly referred to as gamut mapping. A gamut describes the three-dimensional space, which encompasses a device's reproducible colors. An important distinction, however: a gamut is not a two-dimensional

representation on a chromaticity diagram, as this does not account for varying luminance. Therefore a "gamut" depicted on a chromaticity diagram will be noted as a chromaticity gamut.

Typically in the situation where an image is obtained on an input device, and converted to an output device, there are three unique gamuts involved: the input, output and image gamut [Stone et al.; 1988]. Therefore, when information is transferred between devices, the image gamut is correspondingly adjusted based on the rendering intent: generally the objective is to obtain either the most accurate, or most preferable reproduction. Once the image has been rendered, this reproduction will correspond with the output device, as desired.

Despite the details behind the mapping, color appearance attributes guide the transformation between spaces. Considering a display, without considering the appearance attributes of that display is meaningless. Therefore, an optimal color space to perform color transformations would be a color appearance space, as this space would be "perceptually meaningful" [Fairchild; 2005]. Using a color appearance space allows lightness, chroma and hue to be manipulated independently, so the input gamut can be mapped in the best possible manner. There are several color appearance spaces, however, to choose from.

3.1.1. Color Appearance Spaces

To date, research has been conducted in several unique color appearance spaces: the research incorporating CIELUV, CIELAB, CIECAM97s and CIECAM02 will be explained further. It is common knowledge that CIELAB has significant hue nonlinearities in the blue region (Braun et al.; 1998, Hung and Berns; 1995, Montag and

Fairchild; 1998). However, prior to these references and other research that incorporated results from both CIELAB and CIELUV, there were several gamut mapping algorithms designed using CIELUV color space.

3.1.1.1. CIELUV

CIELUV as a color appearance space intuitively made sense; CIELUV space was theoretically perceptually uniform, and therefore, was expected to make a good color appearance space. Wolski et al., 1994, chose CIELUV over CIE's XYZ, xyY, and CIELAB based on the perceptual uniformity characteristics of the spaces [Wolski et al.; 1994]. In addition, Gentile et al. noted CIELUV provided a better space to conduct gamut mapping methods under ("color gamut mismatch compensation") compared to RGB [Gentile et al.; 1990]. Therefore, when choosing from limited color spaces to begin with, CIELUV seemed to be the best available space resembling a color appearance type space. There were a variety of best-performing algorithms, however, Wolski et al. concluded that different areas of the color space resulted in different preferred mapping directions [Wolski et al.; 1994]. Due to the lack of consistency amongst results, research began to focus on other color appearance spaces in search of a more reliable results.

3.1.1.2. CIELAB

CIELAB was also a reasonable choice, as past research has shown simple models hold up considerably well as color appearance spaces. Montag and Fairchild (1996) used CIELAB based on this prior knowledge along with its ability to be inverted and its correlation with perceived lightness, chroma and hue. In addition to several other conclusions, the authors noted CIELAB resulted in better performance than CIELUV as a color appearance space. Montag and Fairchild (1998) later added CIELAB was used for its prevalence within the market and its applicability to appearance gamuts. However,

despite the ability of CIELAB to be used as a color appearance space, perceived hue is not linearly related to lines of constant metric hue angle [Braun, Fairchild and Ebner; 1998]. As a result, although CIELAB performs well in areas excluding the blue region, this region proved reason enough to explore gamut mapping in other color appearance spaces.

3.1.1.3. CIECAM97s

Prior to 2002, CIECAM97s was the latest and most robust color appearance space that existed; it was recommended by the CIE committee in 1997 as a means for describing color appearance while defining cross-media conditions. Although CIECAM97s required some revisions and improvements (predominantly in regard to simplification), this color space far surpassed CIELAB and CIELUV in terms of describing the working conditions of conversions occurring cross-media.

Morovic and Luo performed an evaluation of specific gamut mapping algorithms in CIECAM97s, given the uniformity of the hue predictor was improved from that under CIELAB. They reported that the blue region performed significantly better using CIECAM97s because of the hue nonlinearities prevalent in CIELAB for this region. However, CIECAM97s resulted in hue shifts in the red/yellow range, an effect absent from the results under CIELAB. Overall, the results from CIECAM97s were comparable to the previously made CIELAB manipulations, with varying advantages and disadvantages.

3.1.1.4. CIECAM02

After the revisions and simplifications were made to CIECAM97s, CIECAM02 stepped in as the most recent color appearance space. Unlike CIELAB, CIECAM02 can predict luminance-dependent effects prevalent in displays (CIELAB does not have any

dependence in absolute luminance). In addition, CIECAM02 improves hue constancy significantly. In Moroney and Zeng's article, "Field trials of CIECAM02 color appearance model" published on Hewlett Packard's website, both CIELAB and CIECAM02 coordinates of OSA Color Scales are represented in Figures 3.1 and 3.2.

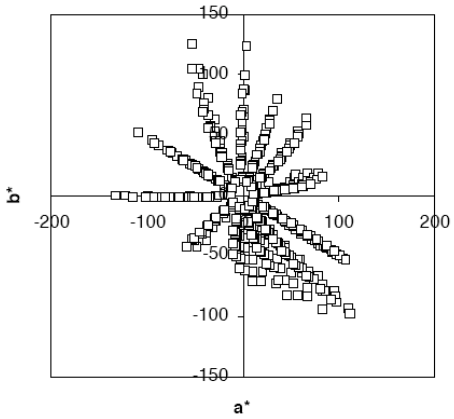

Figure 3.1. CIELAB coordinates of OSA color scales sampling.

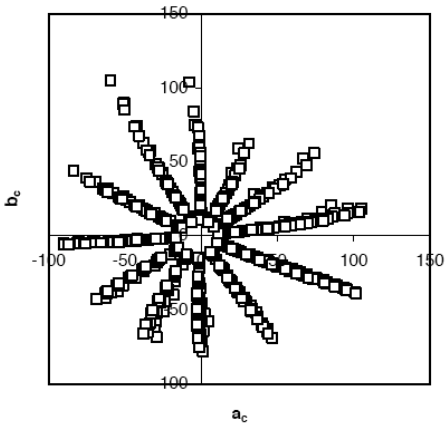

Figure 3.2. CIECAM02 coordinates of OSA color scales sampling.

The improvement of hue linearity for CIECAM02, compared to CIELAB, is quite evident through Figures 3.1 and 3.2. In these figures, color scales in the applicable color space are represented, where lightness increases into the page. The color scales break down in Figure 3.1 under CIELAB in the blue region, whereas this is significantly improved under CIECAM02.

In all of the above research conditions, a common conclusion was drawn: the output reproductions resulting from gamut mapping were dependent on the appearance space used. In addition, another factor is the intent of the gamut mapping. As mentioned above, two clear distinctions were either obtaining an accurate reproduction, or a most pleasing rendering. Each rendering intent is a unique motive for the gamut mapping algorithms.

3.1.1.5. Rendering for accuracy

Obtaining an accurate color appearance to the original proved to be challenging. Morovic and Luo attempted to find a universal, robust gamut mapping algorithm that provides the most accurate color reproduction. More specifically, enhancement was not desired. Both CIECAM97s and CIELAB were incorporated into a psychophysical analysis, so that a comparison between the two methods could be made. The gamut mapping algorithms incorporated lightness and/or chroma compression, while preserving hue. There were five specific algorithms evaluated, each that performed specific operations relative to the output gamut size.

A few observations were made; CIECAM97s resulted in wider lightness contrast ratios than CIELAB did. Since the output gamut was smaller than the original gamut, a prevalent consequence of compression is loss of lightness contrast. However, to retain the original look, it is important to retain as much of the lightness contrast as possible. Therefore, based solely on this reasoning, one may predict the CIECAM97s manipulations would better resemble the original. However, the authors reported similar results between the two color spaces, as noted above. In addition, Morovic and Luo found it more critical to maintain chroma, even when that meant perceived lightness takes the hit. In addition, the most accurate renderings resulted from the algorithms that affected the perceptual attributes the least. And so, without many solid conclusions, gamut mapping remains the key focus.

3.1.2. Compression Versus Expansion

It was reiterated throughout the studies that the outcome of the gamut mapping algorithm (GMA) is largely dependent on both the color space it is performed in, the

rendering intent, as well as the individual device gamuts involved. The output gamut size relative to the input gamut takes a large toll on the design of the GMA. Historically, compression explained every GMA. However, with the new technology available today, compression in many cases is no longer applicable. Gamut expansion has become of interest with the introduction of the new technology as color becomes a large focus for displays. Imagery has in the past, and continues to strive to represent what the human visual system can perceive. Therefore, color management has become a high priority in display devices. Hence, with better display capabilities comes the ability to display a greater range of colors. Although compression may no longer be the focus of GMAs, these algorithms serve as an excellent baseline to derive gamut mapping methodologies.

3.1.2.1. Compression Algorithms

Many GMAs are designed for compression due to the limited output gamut size. It is clear that a reproduction resulting in reduced color and reduced lightness contrast is no longer a goal; however, with a limited output gamut volume, this may become the inherent result.

When mapping is conducted in color appearance spaces, and thus, perceptual attributes are manipulated, it proves valuable to perform psychophysical experiments on the rendered images to determine the strategies that resulted in the best reproductions. Gentile et al. studied color gamut mismatch compensation in 1990, where their focus was on creating brighter, more colorful colors in both display and printing applications: a focus that is still, eighteen years later, a high priority.

Using CIELUV space, ten algorithms were evaluated, such that both clipping and compression techniques were incorporated into variations of lightness, hue and saturation coordinates. The major difference between clipping and compression was the retention

of the relationship between colors. Compression works harder to retain the general relationships, and therefore, may compress the attributes more than necessary in doing so [Gentile et al.; 1990]. Thus, they found clipping was preferred unanimously. In addition, the algorithms that preserved lightness, or lightness and hue attributes in combination, were consistently preferred as well. Overall, the best performing algorithm clipped chroma, while maintaining lightness and hue.

Similarly, Wolski et al., 1994, investigated compression techniques and noted global compression resulted in a loss of lightness contrast. A soft compression technique was implemented to bypass this negative consequence. The conclusions, supported by the results from previous research, focused on the significant image and color space dependencies. The technique introduced in this article focused on incorporating these dependencies into an automatic algorithm for gamut mapping. This algorithm considered the color coordinates within the specified color space, and manipulated those coordinates correspondingly. The goal was to design a computer-generated, universal algorithm that could incorporate specific attributes of an image into the process. In the end, the authors were not convinced that the one universal algorithm sought out for is even attainable. It seemed the image dependencies may be too large to create the versatile algorithm intended.

Montag and Fairchild, 1996, also reported scene dependencies. They performed gamut mapping using both clipping and linear mapping in piece-wise segments on simple images, where the mapping depended on the color content: red, green, blue, cyan, magenta, yellow, and neutral skin tones. For simplicity, mapping was performed under

artificial boundary conditions. Again, the most preferred method maintained hue and lightness, and clipped the out-of-gamut chroma coordinates.

When Montag and Fairchild, 1998, evaluated chroma clipping for three unique output gamuts, hue and lightness dependencies were prevalent. The best method varied depending on the lightness extremes (top or bottom of the gamut). At the higher lightness values, a soft-clipping or knee compression function applied to lightness values was preferred such that chroma was reduced to maintain constant saturation. In contrast, the darker regions were rendered well under clipping of the lightness values to maintain saturation. Overall, for lightness mapping, it was critical that saturation was maintained. This was not the case for chroma mapping, however. Straight clipping was preferred for this mapping, as other studies have shown as well.

In 2000, Braun and Fairchild developed algorithms for gamut mapping that again, incorporated soft-clipping or knee-functions. These functions make a slower transition to the output gamut, compared to clipping or straight compression. The reported results correlated well with previous studies: compression caused an undesired, dramatic change. The linear lightness compression resulted in lighter renderings that displayed lower contrast. In addition, the linear chromatic compression reduced chromatic contrast, and as a result, flesh tones appeared washed out. Using a soft-clipping or knee-function allowed the transformation to take place gradually, so that lightness and chromatic contrast was maintained from the original.

MacDonald et al., 2000, recognized the image-dependencies, as well as the hue- and lightness-dependencies noted above, however, took a slightly different approach to account for them. MacDonald et al. developed a GMA that entailed a core gamut

boundary (Figure 3.3) on the lightness/chroma plane such that, colors within the boundary were held constant. Mapping was only applied to those colors outside the core gamut boundary as an effort to maintain low chromatic colors. The core gamut boundary was defined so that the cusp was located at the lightness value that corresponded to the destination gamut cusp. Then, using a chroma-scaling constant, generally between 0.7 and 0.9, the core boundary was defined [MacDonald et al.; 2000].

In addition to the defined core boundary, the algorithm incorporated a bilinear function. This function extended colors outside of the core along the designated mapping directions to the destination gamut, according to the range of lightness values the coordinate fell into. This method, in addition to three other GMAs comprised of varying techniques, was psychophysically evaluated. Although the topographical method was ranked high, MacDonald et al. noted important improvements necessary in order to increase the GMA's performance.

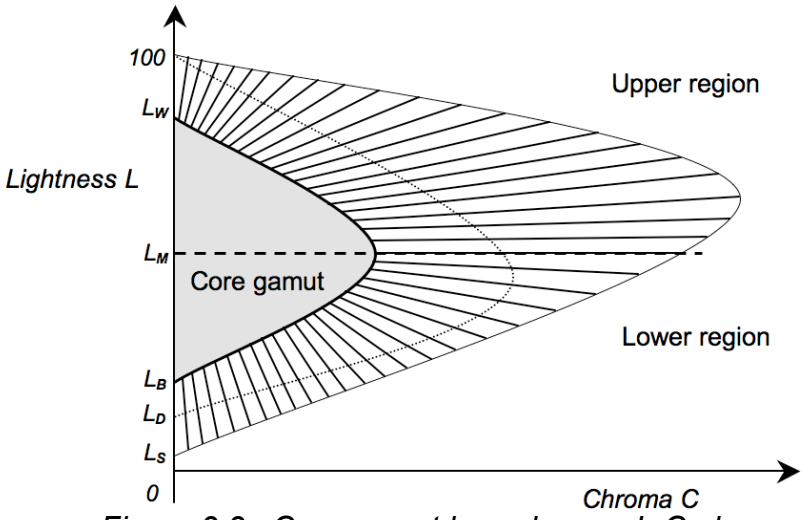

Figure 3.3. Core gamut boundary on L-C plane.

The second version, featured in [MacDonald et al.; 2001] incorporated the lighter colors into the gamut mapping region. This is conveyed through Figure 3.3, where the original

GMA had both the core gamut and destination gamuts "coterminous" at a lightness value of 100. In addition, the mapping chords were comprised of a soft-clipping function to accommodate the colors outside the source gamut boundary. These alterations dramatically improved the results, as this topographical method was now most preferred by observers when compared with the same three algorithms.

Obvious trends in the above studies have become apparent through this review. Much of the research conducted on gamut mapping strategies often manipulates similar attributes, while maintaining others. Since a universal gamut mapping algorithm is an important goal, specific manipulations can be noted in which should be included in a final algorithm.

The most pronounced objective, common among many researchers, is the requirement for constant perceived hue. Unfortunately, perceived hue often does not directly correlate to constant metric hue. Some appearance spaces are better than others in this respect, and thus, this objective is limited to the capabilities of the color space chosen for manipulating the data. In addition, the range of lightness and colorfulness, or achromatic/chromatic contrast, should be preserved if possible. By maintaining both lightness and colorfulness contrast, the relationships between objects within the image can be retained, thus, preventing a decrease in preference. In addition, maintaining a constant saturation was found to influence observer preference. By preserving saturation, particularly in regions of low chroma, the appearance of a "washed out" image or desaturated features was avoided.

Although many of the published results correlate with one another, one specific algorithm has not been defined for a wide range of situations. Since the success of gamut

mapping algorithms is largely dependent on both the color space and image content, improvements are still currently of interest to encompass more images and conditions.

The research described above presents a range of alternatives to mapping image content to a smaller gamut (often to the gamut of a printer), and thus, incorporated both clipping and compression techniques. However, with the addition of wide-gamut display technology, the focus is aimed toward gamut mapping algorithms used to expand the input image content. This objective is newer, however, progress has already been made.

As previously mentioned, Fedorovskaya et al., 1996, evaluated perceptual quality, colorfulness and naturalness for reproductions created through chroma variations on multiple scenes. The results displayed a direct correlation between perceptual quality and naturalness, however, the more profound conclusion from this study entailed colorfulness. Colorfulness was found to be the most significant factor effecting image quality, out of the two evaluated.

3.1.2.2. Expansion Algorithms

Keeping consistent with the conclusion from Fedorovskaya et al., that colorfulness is the primary perceptual attribute effecting image quality, Sakurai et al., 2007, reported that colorfulness is the most sensitive attribute to change in color gamut volume. In addition they found that perceived lightness contrast increases at a decreasing rate, with larger color gamut volumes, whereas colorfulness increases monotonically with increasing gamut volume. Despite these clear trends, the influence of the color space on determining the relationship between color appearance and color gamut volume is apparent. Future work will most definitely include gamut mapping in terms of gamut expansion. The compression algorithms serve as a strong baseline for objectives in

manipulating color appearance attributes, and can now be incorporated into the research conducted on expanding the input gamut.

Now that gamuts are getting wider, the issue has changed from gamut compression to gamut expansion. However, applying the knowledge gained from the former objective can aid in the research towards establishing a robust gamut expansion algorithm.

3.1.2.2.1 Naturalness: An Influential Attribute

The complex nature of color is a result of the uniqueness of human visual perceptions. For imagery purposes, color variations have been studied for both quality and preference as an effort toward creating more visually satisfying images. Fedorovskaya, Ridder and Blommaert (1997) evaluated the effects of chroma variations, in CIELUV color space, within natural scenes on perceptual quality, colorfulness and naturalness. As previously mentioned, gamut mapping algorithms are driven by one of two motives: accuracy or pleasantness. In other words, if an algorithm is driven toward accuracy, the reproduction may not necessarily be the most preferred. Similarly, if an algorithm is based on preference, the result may not be accurate according to the spectral properties of the objects within the image. This is largely influenced by memory colors, and the fact that the average observer sees given memory colors as a specific color name, regardless of the illumination of the scene or spectral properties of the objects.

When mapping to a display with extended primaries, visual accuracy may not be achievable. Therefore, many researchers [Federovskaya et al.; 1997, Ridder and Blommaert; 1995] agree a third attribute, the naturalness of an image, may be an important constraint on color reproduction.

Fedorovskaya et al. claim an observer inherently compares the scene at hand with an "internal reference" or "memory representation". Therefore, an image worthy of high image quality ratings must be perceived as natural. Ridder and Blommaert concur that the naturalness of an image, which largely affects image quality, also depends on the familiar memory colors. Most research conducted on gamut mapping algorithms has focused on mapping complex images, and therefore, generally the scenes are of natural context (one notable exception will be discussed later [Laird and Heynderickx; 2008]).

3.1.2.2.2. Gamut Expansion Mapping in Various Color Spaces

Color has two attributes: saturation and chroma. In a natural scene, all objects are similarly illuminated, and therefore, saturation remains constant since the objects in the scene are present under the same reference white. However, maintaining a constant hue and lightness over two uniquely colored regions results in color differences due to chroma variation (Eqn. 3.1.), in CIELUV space [Federoskaya et al. 1997].

$$\Delta E^*_{UV} = \sqrt{\left[\left(\Delta L^*\right)^2 + \left(\Delta H^*\right)^2 + \left(\Delta C^*\right)^2\right]} \qquad (3.1)$$

According to Fedorovskaya et al., CIELUV color space was appropriate for this experiment, given it was deemed an important color space for television applications by preceding color scientists (including both Hunt (1992) and De Corte (1986)). However, as was discussed for compression mapping, there have been many color spaces incorporated into gamut mapping studies, and still, no definitive answer for which is best.

Through reproductions based on chroma variations, Fedorovskaya et al. emphasized the capability of colorfulness as a critical attribute effecting image quality. In addition to chroma variations, hue variations have been noted to be equally, if not more, influential over image quality. Ridder and Blommaert found that hue variations

influenced image quality and naturalness more so than chroma variations [Ridder and Blommaert; 1995]. Therefore, both hue and chroma are critical color attributes that influence color reproduction.

3.1.2.2.2.1. Establishing Colorfulness Boundaries

To this, technology has caught on, as it did not take long before the market was inundated with extended gamut displays. Given the importance of color in the processing chain, it only made sense to obtain the most colorful reproduction possible, using the display primaries as the limiting factor. However, the naturalness of an image became of utmost importance, after the images were not performing as expected. To evaluate this further, Laird and Heynderickx evaluated perceptually optimal boundaries and reported an intriguing conclusion about gamut expansion algorithms.

While Laird and Heynderickx discussed the advantages of the current technological advancements in wide-gamut televisions, they also noted that regions of "very intense, bright colors" can be "displeasing" to observers. Using scenes of limited content, predominantly monochromatic in color, and unrelated to memory colors, observers adjusted chroma for given hue and lightness values until the scene appeared unnatural. The purpose was to describe a perceptually optimal boundary within CIELAB space in which, a gamut extension algorithm should not exceed.

Upon analyzing the psychophysical results, Laird and Heynderickx (2008) found an overall preference (despite scene dependencies and inherent hue dependencies) for a gamut extension boundary closer to Rec. 709, or the "EBU" standard [[ITU-R BT.709-5 2002]. Kang et al., 2003, evaluated GEAs based on observer experimental data to validate the advantages of wide gamut display technology.

3.1.2.2.2.2. Determining Influential Attributes

In their evaluation, Kang et al. implemented a computer-controlled, interactive tool that enabled the observer to adjust color regions within a given area to represent a more preferred color reproduction. The observers were first trained to understand lightness, chroma and hue attributes, and then were allowed to manipulate certain color regions within the image content. This method enabled algorithm development designed specifically on the data supplied by the observers.

Based on the first round of experiments, the data supported the conclusions that the algorithm should not incorporate a hue shift. Since the observers did not alter the color region to a significantly different hue, this attribute was not varied within the algorithm. An encouraging result became clear through the second part of the experiment: after observers altered the images, a GEA was developed. In addition, four unique GEAs were developed by varying the degree of chromatic extension, where all were then compared through an overall preference experiment. The results indicated that the extensions applied by the observers in the first experiment were insufficient, in that more dramatic chromatic extensions were preferred when later evaluations were conducted. Therefore, observers actually preferred more colorful images than they originally created. Despite the conclusion Laird and Heynderikx reported, Kang et al. found support for wide gamut technology.

In addition, Kang et al. found their data emphasized a trend on image dependency. Through four unique images, the effect of image content became clear. More specifically, one image was largely comprised of skin tones and the results were significantly different from those of the other three images, all of which maintained a larger average chroma [Kang et al.; 2003]. Kang et al. concluded memory colors largely

impact GEA preference, and thus, should be considered in the algorithm development stages.

An additional consideration to algorithm development should be dynamic range. With the introduction of wide gamut technology comes larger dynamic ranges. In addition to incorporating increased colorfulness into GMAs, Reinhard et al., 2007, remark on the importance of creating GMAs that correspond to high-dynamic range displays. The radical difference between real world illumination and the capabilities of current gamut mapping strategies emphasizes the journey researchers still have to bring these closer together. Reinhard et al. explain that maintaining equal or greater dynamic ranges within a given image content will better ensure success of the reproduction.

3.1.2.2.3. Control Consideration

When analyzing GEAs, it is important to validate the necessity of expanding the gamut from the current EBU standard. Therefore, Muijs et al. (2008) included a true-color representation of the test images in their psychophysical study evaluating observer preference for gamut extension algorithms. A true-color representation displays an EBU input image correspondingly on a wide-gamut display. By accounting for the difference between the input and display primaries, the image is displayed on a wide-gamut monitor within the input gamut. This version serves as a baseline image as it is not expanded beyond the EBU standard.

Also, as mentioned before, when wide gamut technology flooded the market, companies were using the display primaries as the limitation to the GEAs, figuring that the more colorful the images, the better. By directly using the digital counts of standard image content as the output digital counts, an image is linearly stretched to fit the output

display gamut. This theoretically represents a more colorful image. However, this reproduction largely depends on the display technology, and has the potential to drastically alter the overall image appearance. By incorporating true-color representation and the linearly stretched version as the two mapping extremes, proper comparison and analysis of any developed gamut expansion strategies is enabled.

Similar to gamut compression algorithms, GEAs can entail multiple color appearance spaces to perform mapping in. However, the correlation between chroma and colorfulness guides the decision of what space to perform the mapping in. CIELAB is the most common color space GEAs are performed in because it is a perceptually meaningful color space in which, chroma can easily be both calculated and manipulated [Muijs et al.; 2008, Kotera et al.; 2002, Kotera et al.; 2001, Kang et al.; 2005, Kang et al.; 2003, etc.].

Kang et al., 2005, provide an overview to demonstrate the variety among mapping algorithms incorporating CIELAB space. These methods are based on CIELAB attributes, such that both lightness and chroma are mapped using multiple functions. They discuss both linear and non-linear mapping functions as methods conducted in past research. These functions enable a mapping to incorporate attribute dependencies so each CIELAB coordinate is mapped appropriately. This becomes particularly useful when considering memory colors (i.e. skin, blue sky and green grass [Kang et al.; 2005]), as these are fairly unique color regions that need to be carefully mapped in order to satisfy the observer.

3.1.2.2.4. Gamut Expansion Linear Methods

Hoshino, 1994, patented a technique designed to map lightness/chroma

coordinates by incorporating the ratio of the input to output lightness ranges. After calculating the range between the maximum and minimum lightness values for both the input and destination gamut, a ratio between the ranges was obtained. Using this ratio, the expanded, output chroma, C_2 was calculated from a line that was formed between (L_1, C_1) and (L_2, C_2) such that hue was maintained. Therefore, by constraining hue, and using the ratio of dynamic ranges for each gamut, Hoshino successfully linearly expanded the input data to a larger gamut. This concept of mapping lightness/chroma coordinates showed great potential and thus, is commonly incorporated into gamut expansion evaluations.

3.1.2.2.5. Gamut Expansion Non-linear Methods

Muijis et al., 2008, developed three methods (one-linear, two-non-linear), all of which manipulated lightness and/or chroma values to extend along a given direction with a given driving function. One of the methods, denoted wide gamut color mapping, WGCM, was derived as a linear combination of both the true-color mapping and the linearly stretched mapping, where the output was dependent on the input saturation. The idea behind the dependency on saturation was to maintain neutral colors while drastically enhancing highly saturated colors. Through this method, colors of low saturation could retain a reasonable color, while the more chromatic colors were enhanced, so that the full display gamut was utilized.

Muijs et al. also incorporated both a chroma-extension and a lightness-dependent extension in their evaluation. These methods operated under an extension defined by an exponential transfer curve, or a non-linear/ sigmoidal curve. The chroma-extension altered chroma while maintaining lightness and hue; the lightness-dependent extension

varied both chroma and lightness in a lightness-dependent manner, while maintaining hue. Thus, the latter accounted for variations in lightness, particularly at the extremes. As a result, this method balanced contrast enhancement for the bright and dark, low saturated, near-neutral colors with the mid-lightness, highly saturated, chromatic colors [Muijs et al.; 2008].

Through their psychophysical analysis, the only method out of the three developed that was significantly preferred over the true-color mapping was the lightness/chroma mapping. At the lightness extremes, a device's color gamut varies drastically in comparison to mid-lightness values, as typically mid-lightness values enable more chromatic colors to be reproduced. This mapping took this into account by varying the degree of extension based on the lightness values. This was done through a sigmoidal transfer function so that different chroma/lightness combinations resulted in different extensions. Therefore, this method enabled special consideration for memory colors.

Other techniques have been implemented in an effort to control near neutral colors. Bang and Choh, 2007, recognized the need to maintain flesh tones, since "high chromatic skin reduces user preference." A nonlinear look-up table was implemented to slightly reduce the saturation of skin tones, while making them brighter. In addition, greenish and bluish colors are independently controlled through a nonlinear hue correction to account for hue non-linearities in the blue region as a result of using CIELAB. Given this experiment was designed to produce printed images ranging from soft-copy versions to the vivid hard-copy prints, the remaining colors were mapped based on an enhancement of saturation. Ultimately, this innovative gamut mapping method

resulted in a higher user satisfaction index (USI) than the standard mapping solution. This is because in this case, there was additional consideration taken for the expansion methods of specific color regions. The non-linearity of the method enabled a greater degree of specificity for individual color regions, which was highly received according to the observer data.

Simliar to Bang and Choh, Anderson et al., 2007, employed a nonlinear method to avoid the oversaturation of specific color regions (i.e. skin tones, pastels and neutrals) as a result of linearly mapping to an extended destination gamut. Using extended color pair samples provided by color experts, for a given image frame, local linear regression was performed and applied to the scene using multi-dimensional look-up-tables stored in an ICC profile. Based on past research that suggested any GMA developed is inherently image-dependent, Anderson et al. felt this was a reasonable mechanism to better automate the process. Video and image sets were incorporated into the experiment, each with four versions: original, expanded, linearly expanded and mapped via a locally linear LUT. Hue dependencies were evident through the results, however, the locally linear LUT clearly outperformed the other methods. Still, this regression technique was costly since the ground truth from the artistically expanded color pairs was necessary for each individual image set. Therefore, the regression technique has not been actively pursued as of yet.

Kotera et al. took a unique approach to nonlinear gamut extension by entailing histogram specification to drive the mapping. Therefore, unlike the majority of methods that use CIELAB, Kotera et al. converted RGB digital counts to YCC space so that histogram equalization could be performed, thereby leading to natural, pleasing results.

Therefore, they performed a Gaussian histogram on the luminance channel, and followed with separating the chrominance components according to luminance and hue angle. The chroma of each value was then extended by the Gaussian histogram, while maintaining hue. This type of gamut algorithm is an automated approach to an image-dependent algorithm. Therefore, this is a method to use in place of the development of a cumbersome image-dependent algorithm, and as a result, it has more potential to be accepted as a standard GMA than it otherwise would have had.

3.1.2.2.6. Gamut Expansion via a Mapping Direction

Aside from the general basis behind the GEA (linear or sigmoidal), an additional consideration should be taken to address the direction of the mapping. MacDonald et al., 2001, commented on directional mapping for compression toward a specified cusp, given their mapping chords were required to be defined extending to and from specific directions. Kang et al., 2005, distinguish between mapping function and direction in their description of chroma mapping. Maintaining a constant lightness is common amid past research [Montag and Fairchild; 1996, Gentile et al.; 1990, Morovic and Luo; 2001, Wolski et al.; 1994]. In addition, however, mapping to/from a specified point can also prove very useful.

Lee et al. proposed a GMA that incorporated variable anchor points on the lightness axis. Although maintaining, or increasing contrast was not a requirement, as they were mapping to limited gamut sizes, the concept remains applicable to gamut extension. The first of several directions evaluated mapped towards the central point of the lightness axis, for a given hue value. One disadvantage encountered with this method was the decrease in contrast, as the brighter coordinates were decreased and the darker

coordinates increased. However, with gamut expansion, in which, mapping would extend away from the anchor point, this was not an issue. This method, therefore, served as an excellent baseline, which was further expanded on to include a second variable point to be evaluated. Overall, the SGEAs were evaluated extending from L* equal to zero, L* equal to fifty, in addition to maintaining lightness values.

3.2 Extended Gamut Displays

Gamut mapping algorithms that extend the input color values become pertinent for extended gamut displays. The limitation of enhanced color reproductions is dependent on the gamut of an extended-gamut display. Current technology boasts expanded primaries, thanks to the advancement of light-emitting diodes (LEDs). Since 2006, LEDs have become increasingly prevalent in a number of technologies, gaining advocates for their increased color output and efficiency.

In regard to displays (both liquid-crystal displays, LCD, and digital-light processing, DLP displays), LEDs offer color stability and control, color rendering capability and luminous efficacy. The narrow band spectrum of an LED is similar to that of a high power laser, enabling its high stability [Holleman et al.; 2001]. The color rendering capability depends on the material compound of each primary involved. The most common display design incorporates three (red, green and blue) LEDs (Figure 3.4) and through deflection of their narrow-band spectra, results in additive color mixing with a high degree of color control.

Figure 3.4. Red, Green and Blue LEDs [P.Namek, Wikipedia, 2008]

In addition, the luminous efficacy associated with LEDs is due to the extra light per watt produced, in comparison with an incandescent bulb. Therefore, this capability earns the efficiency label.

Often the light source within a display is referred to as a "backlight". This component of the display technology entails two main layers: the LCD panel and a reflector. Overall, the component works to distribute the diffused light in an optimal manner. In order to achieve this, the backlight relies on various diffusers and reflectors to guide the light successfully towards the display viewer [3M; 2008]. The reflectors minimize the amount of wasted light, while the diffusers uniformly distribute the reflected light. All of these components that makeup the framework for the display's backlight were designed to optimally present a signal to the viewer. With LEDs as the light source, viewers of both LCD and DLP displays will experience the benefits.

3.2.1. LCD with LED Backlight

Large scale LCDs have recently adopted LED backlights for their efficiency and large color gamuts. However, due to the cost of this technology, the trend has been somewhat slow coming. While the commercial market gets up to speed, research has been actively pursuing these displays.

LCDs were designed based on the physical, optical and electronic properties of liquid crystal molecules [3M; 2008]. There a multiple layers: liquid crystal material sandwiched between two transparent electrodes and two outer polarizing filters and a color filter, where each component plays an intricate role in the display.

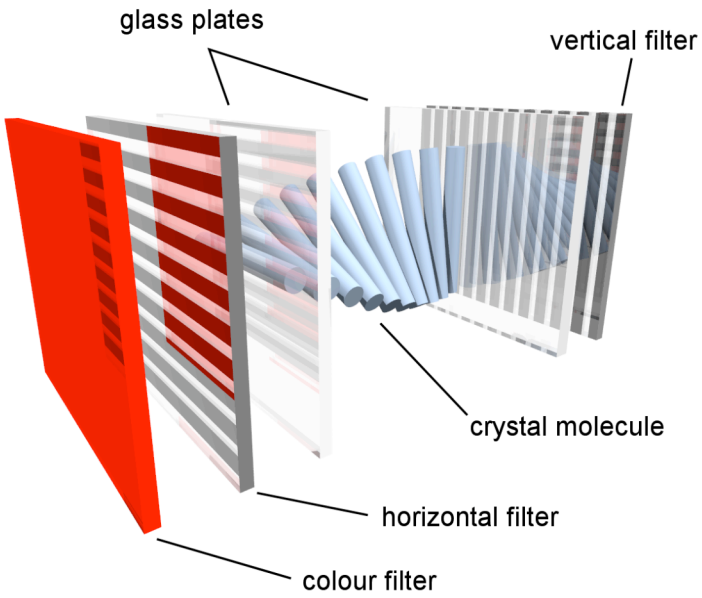

Figure 3.5 A subpixel in a LCD [M. Raaijmakers, Wikipedia, 2008].

One-third of a pixel, or a display subpixel, is represented in Figure 3.5. This figure demonstrates the capability of the crystal molecules to orient in a given direction, where the direction is determined by both the electrical charge and the orientation of the filters. Since the filters are aligned orthogonally to one another, the liquid crystal twists through the thickness of the display to match the orientation of each filter [3M; 2008].

However, when an electronic voltage is applied, the molecules will alter their orientation to match that of the electronic field. Therefore, through an applied charge, the molecules will adjust to either match the orientation of each filter by twisting (the orientation of that in Figure 3.5), denoted as “ON”, or matching only the orientation of

the first filter (orthogonal to the second polarizer), and thus, denoted as “OFF”. This is the process in which modulates the light intensity of the subpixel.

In addition, color is added by placing either a red, green or blue colored filter outside of the second polarizer, where a pixel is represented by one of each red, green and blue subpixels (Figure 3.6).

Figure 3.6. Simulated depiction of LCD pixels operating together to display an image [V. Ezekowitz, Wikipedia, 2008].

In Figure 3.6, the pattern of subpixels is displayed. Altering the light intensity of the LED backlight for a given subpixel results in millions of producible colors.

3.2.1.1 Sony Prototype, 40 inch, LED backlit, 1080p, LCD

Sony has produced a prototype LCD with LED backlit, for research purposes, that was incorporated into this study. The display primaries are represented in Figure 3.7.

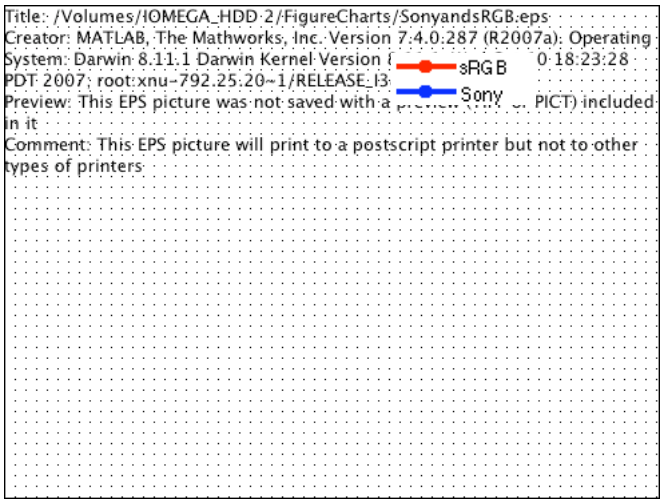

Figure 3.7 Red, Green and Blue primaries for the display gamut (Sony) and the input (sRGB) gamut.

The chromaticity gamut area of the Sony is much larger than that of the standard, sRGB, space. The screen size of the display is 40 inches. The maximum luminance of the display was measured at 418.8 cd/m^2, with a contrast of 445:1, under a gray surround of the viewing condition in this experiment.

3.2.2 DLP with LED primaries

LED technology has also influenced to digital light processing displays, or DLPs. As current technology continues to evolve, DLP displays have actively improved as well. This technology refers to projection technology as a means for displaying image content and relies on a digital micromirror device (DMD) invented by Larry Hornbeck of Texas Instruments in 1987 [TI; 2008].

Figure 3.8. DMD representation.

This device, represented in Figure 3.8, contains an array of mirrors, each of which correspond to a given region of projected light on the display. The process begins with a digital signal, applied to an electrode beneath each mirror.

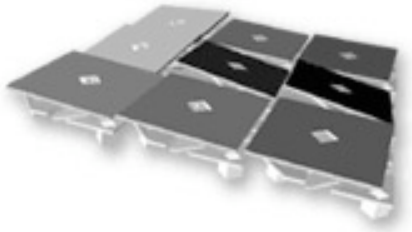

Figure 3.9. Microscopic mirrors within DLP device.

The voltage signal causes the electrode to tilt toward or away from the light source. If the mirror is tilted toward the light source, the light will be reflected onto the screen (denoted as "ON"). When the mirror tilts away from the light source, that specific mirror's pixel space will remain dark (denoted as "OFF") [TI; 2008]. By varying the mirror's degree of tilt at a high frequency, various light intensities are obtained and displayed on the screen. This process enables the projection of a grayscale image.

Color is added via the light source in DLPs with LED illumination. Figure 3.10 represents the process taken to add color to the equation.

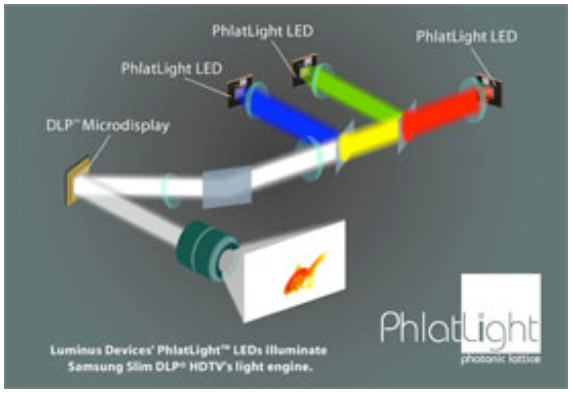

Figure 3.10. Process of projecting an image on a DLP HDTV with LED illumination [TI; 2008].

Since DLP displays are now incorporating LED primaries, many of the negative characteristics of this technology are addressed. For example, one major change that has taken place was that the color wheel was replaced with the adoption of LED technology. The result is an extended gamut display that will no longer experience color break-up artifacts when displaying moving targets.

3.2.2.1 Samsung HLT5087s, 50 inch, slim LED Engine, 1080p, DLP

After researching several different displays, the extended color gamut display chosen was the Samsung HLT5087S 50" Slim LED Engine 1080p DLP HDTV. A DLP display was elected as the perfect candidate, due to the gamut expansion capabilities. The display is comprised of LED primaries, (red, green and blue), which are brighter, and thus, enable a wider gamut. Replacing the color wheel, a characteristic of the traditional DLP, LED technology provides increased color stability [Hollemann et al.; 2001, Samsung; 2008], wider color gamuts through xvYCC color space [Matsumoto et al.; 2006], and several other promising improvements. This Samsung display was an ideal display, as it incorporates the recent technology to boost colorfulness, displayed in Figure 3.11 in terms of chromaticity gamut areas.

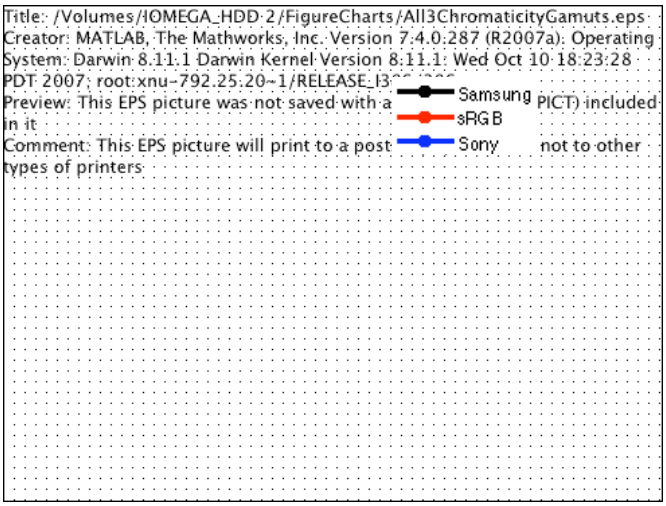

Figure 3.11 Chromaticity gamut areas of the two destination gamuts: Samsung and Sony displays, in comparison to sRGB.

As a consumer purchasing this Samsung display, internal processing procedures that operate to yield the best picture are inherent. Therefore, for research purposes, any apparent controls responsible for this processing were suppressed through the display setup menu. Every setting was set to "Standard", or "Normal", where applicable. The only exception was the "Color Gamut" setting, which was kept at wide, as this research required a wide color gamut. Different contrast and brightness settings were measured, to determine the combination that provided maximum contrast between black and white, where white represented a linear combination of the three- red, green and blue channels.

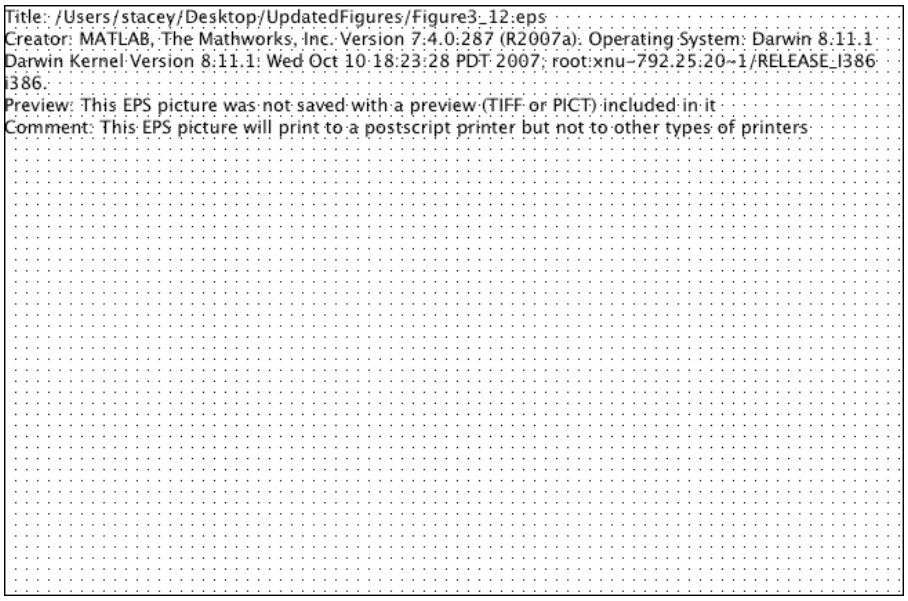

Figure 3.12. The luminance values, of the red channel, from tristimulus measurements for multiple contrast/brightness combinations.

The combination providing the highest luminance value for white, while maintaining a zero luminance for black was the desired choice. From Figure 3.12, the curve most fitting to this description is C75B50 (dotted blue line), which represents contrast at 75, brightness at 50. Therefore, these settings were maintained throughout the research.

Preserving the contrast and brightness settings, the following modes were chosen, as the best attempt to stop any alternative processing of the images.

Table 3.1. Controllable display options and the combinations chosen for analysis.

Display Settings		
Mode	Standard	Movie
Contrast	75	75
Brightness	50	50
ColorTone	Normal	Warm 2
Color Gamut	Wide	Wide

There were five unique color tone settings on this display, ranging from “Cool 2”, to “Normal”, to “Warm2”. The white point for each of the five color tone settings was measured, and compared to CIE’s D65 illuminant.

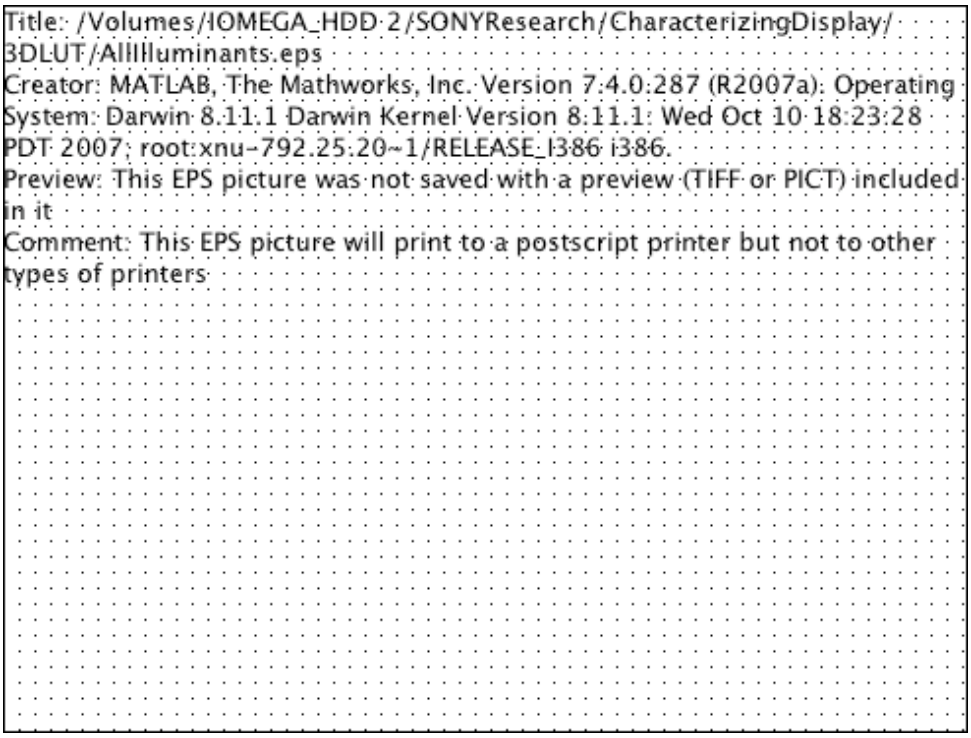

Figure 3.13. Chromaticity diagram with labeled white points from the measured color tone settings, as compared with D65.

As seen in Figure 3.13, the color tone setting, Warm 2, provided a white point closest to D65, or a correlated color temperature nearest to 6500K. This was selected and maintained throughout the research incorporating this display.

3.3 Display Color Spaces

Color management is required on any digital imaging device to convert color information from one device to another. Through color management, the processing of the device and the viewing conditions can be controlled [Hunt; 2004]. Despite identical digital counts sent to a display, each display returns varying outputs, which then affects the color appearance of the content. In addition, when transferring data between devices, viewing conditions might change as well. This situation occurred during the recent time period of the upsurge in computers, and remains an issue. Color management enables the

transfer of digital image content to various displays (performed through image coding [Poynton; 1997]) to go as smoothly as possible.

The differences within each device gamut can be accounted for, despite the number of discernible colors available [Hunt; 2004, Wen; 2005]. This entails the use of a standard color space, in which various content can be mapped to and from devices so that the output across different displays will correlate.

3.3.1. sRGB Color Space

In collaboration, the International Color Consortium (ICC) and the International Electrotechnical Commission (IEC) have devised a "default RGB color space" that is applicable cross-media to serve numerous purposes [ICC; 1996, Stokes et al.; 1996]. The ICC's contribution of the sRGB profile led to the creation of sRGB color space. Originally, the sRGB profile was implemented as a translation between devices; specifically, it was a monitor profile [Nielsen and Stokes; 1998]. Therefore, the need for a more widespread color management system remained until the IEC defined the sRGB color space. By defining a standard RGB color space incorporated into color management, color coordinates became device-independent, and thus, minimized the visually apparent discrepancies between devices [Stokes et al.; 1996].

When incorporating a standardized color space, there are reference display conditions that apply to the conversions between devices. The display white point for sRGB is D65, or the daylight illuminant with a 6500K correlated color temperature. Therefore, when performing a conversion from nonlinear RGB values to 1931 CIE tristimulus values, the D65 illuminant is necessary for correct conversion. A non-linear

transformation matrix is used to convert sRGB digital counts to tristimulus values. Eqns. 2 through 5 describe the overall computations necessary [Stokes et al.; 1996].

$$\begin{aligned} R'_{sRGB} &= R_{8bit} \div 255.0 \\ G'_{sRGB} &= G_{8bit} \div 255.0 \\ B'_{sRGB} &= B_{8bit} \div 255.0 \end{aligned} \qquad (3.2)$$

After applying Eqn. (3.2) to the linear input 8-bit digital counts, constraints are applied to the non-linear sR',G',B' values for optimal performance. If R'_{sRGB}, $G'_{sRGB,}$ B'_{sRGB} is less than or equal to 0.045045 then

$$\begin{aligned} R_{sRGB} &= R'_{sRGB} \div 12.92 \\ G_{sRGB} &= G'_{sRGB} \div 12.92 . \\ B_{sRGB} &= B'_{sRGB} \div 12.92 \end{aligned} \qquad (3.3)$$

Otherwise, Eqn. 3.4 is applied.

$$\begin{aligned} R_{sRGB} &= \left[\frac{\left(R'_{sRGB} + 0.055\right)}{1.055}\right]^{2.4} \\ G_{sRGB} &= \left[\frac{\left(G'_{sRGB} + 0.055\right)}{1.055}\right]^{2.4} \\ B_{sRGB} &= \left[\frac{\left(B'_{sRGB} + 0.055\right)}{1.055}\right]^{2.4} \end{aligned} \qquad (3.4)$$

The final conversion to tristimulus values incorporates the sRGB transformation matrix to linearly relate sRGB values to tristimulus values (XYZ).

$$\begin{bmatrix} X \\ Y \\ Z \end{bmatrix} = \begin{bmatrix} 0.4124 & 0.3576 & 0.1805 \\ 0.2126 & 0.7152 & 0.0722 \\ 0.0193 & 0.1192 & 0.9505 \end{bmatrix} \begin{bmatrix} R_{sRGB} \\ G_{sRGB} \\ B_{sRGB} \end{bmatrix} \qquad (3.5)$$

Using CIE colorimetry, the chromaticity coordinates of sRGB, with consideration for the reference viewing conditions, are linear combinations of the CIE XYZ tristimulus values. Therefore, rearranging these mathematical equations provides the equation necessary to compute XYZ tristimulus values from the encoded colors under sRGB (Eqn 3.5). Once

XYZ space is reached, the data can be manipulated and converted to various devices when necessary.

The sRGB color space has provided an integrated, versatile color space for many applications within color management. Since its proposal, this color space has become widely accepted, for a wide range of devices. However, there are additional systems capable of encoding digital image content.

3.3.2. YCC Color Space

The efficiency of a color space becomes an important factor in obtaining the optimal image specification language. Digital image content typically comes with a hefty file size, and thus, maintaining full R, G, B channel information is excessive. In addition to linear RGB digital counts and nonlinear standard RGB values, YCC encoding represents an effective image specification system. The premise of YCC, short for $Y'C_BC_R$ or $Y'P_BP_R$ for either HDTV (high-definition television) or SDTV (standard definition television) respectively, entails encoding an image in terms of luminance, "Y", and chrominance, "C" and/or "P" [Poynton; 2003].

3.3.2.1. Sensitivity of the Human Visual System to Luminance and Chrominance

The human visual system has varying sensitivities with respect to spatial resolution in the lightness and color channels. The eye has a considerably lower spatial acuity for color information as it does for lightness [Poynton; 2007]. Therefore, systems that operate on luminance/chrominance information have the luxury of compressing the color information without degrading the perceived image quality. With this understanding, the percentage of information carried by each component is evident: the luminance channel stores highly detailed, very useful information, and thus, is required at

full resolution. However, the chrominance component carries information greater than the human eye can perceive, and thus, is compressed so that the color information only accounts for a small percentage of the overall image size, while still retaining the image appearance. Therefore, a generic YCC color space allows for appropriate compression to save on file size.

3.3.2.2. Chromaticity Gamut Area of YCC Color Space

One benefit of YCC color space is that it, in theory, reduces clipping [Samadani and Li; 2005]. RGB spaces operate in 8-bit integers, ranging from either 0 to 1 as normalized integers, or 0-255. Therefore, in the event an out-of-gamut color exists, any RGB space clips this color to the gamut boundary [Zeng; 2005]. YCC, on the other hand, handles colors outside the RGB gamut differently. There are some allowed values in the YCC encoding that would be "out-of-gamut" colors under standard RGB specification. Therefore, when represented on the same figure, YCC corresponds to a larger gamut area than sRGB.

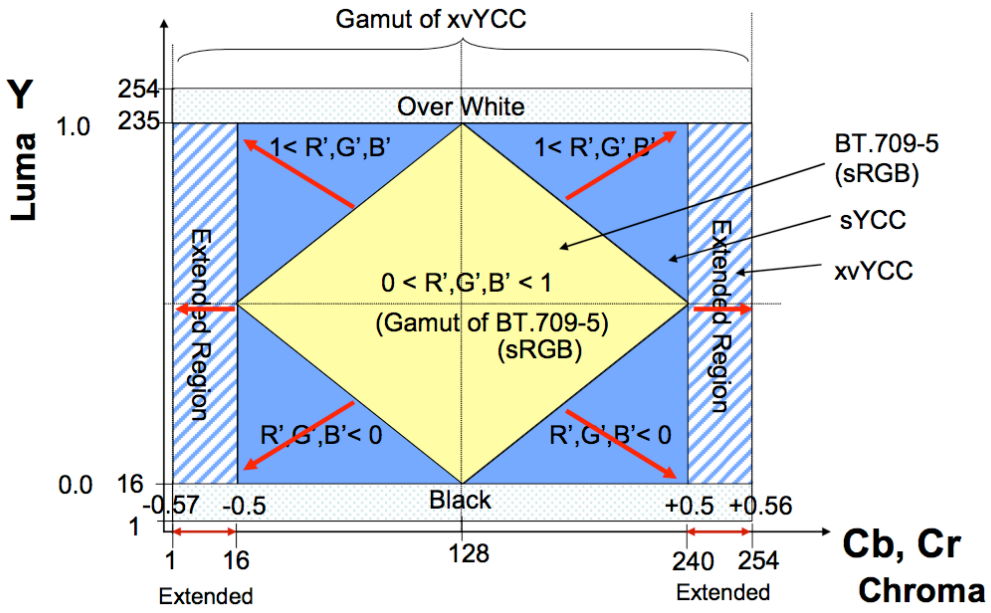

Figure 3.14. Gamut areas of sRGB, YCC and their newly developed, wide-gamut color space, xvYCC [Matsumoto et al., 2006].

In Figure 3.14, a two-dimensional projection of the three-dimensional sRGB gamut is represented, where sRGB values ranging from zero to one are represented on the luma, chroma axes as 0 through 1, -0.5 through 0.5 respectively. These values are also represented as counts 1 through 254, to encompass a digital encoding axis. The color gamut areas corresponding to each color space, shown in Figure 3.14, illustrate the point made about "out-of-gamut" colors. Since the luma component ranges from zero to one, and the chrominance component ranges from -0.5 to 0.5, some unrealizable RGB colors can be represented in terms of YCC coordinates.

There is a version of YCC, denoted as sYCC, which best relates sRGB to YCC. The sYCC color space is defined as a color space in which, YCC is used in the sRGB color space [Kerr; 2005, IEC 61966-2-1 Annex G]. This color space entails the realizable colors of YCC, despite whether those colors are definable within sRGB color space. Therefore, this space can represent negative R,G,B values and values greater than one,

and in the conversion back to sRGB, these out-of-gamut colors can theoretically be processed such that clipping is avoided [Sugiura et al.; 2007]. When transforming 8-bit linearized RGB values to YCC space, the range of data values changes.

As shown in Figure 3.14, when converting to YCC, the chroma axis extends from -0.5 to +0.5. As a result, the RGB cube of data points represents only a portion of the YCC space. However, in YCC space, these values are also termed "invalid" since any region outside of the cube cannot be represented in RGB space. This region of YCC encoded colors provides a great opportunity, should an extended display color space become prevalent. Through processing, every RGB color can be converted to achromatic and chromatic signals, where the input YCC values are color managed to the appropriate hue depending on the existence of a negative sign for that particular value. Therefore, colors can be correctly separated and matrixed to corresponding RGB display digital counts when displayed.

Both YCC and sYCC have larger gamuts than sRGB, however, both are also dependent on the output display gamut. Therefore, if the output display gamut is sRGB, the extended gamut areas are limited to the gamut area of sRGB [Kerr; 2005], and thus, will not affect the output colors. Hence, the need for an extended-gamut color space applicable to monitors becomes imperative to successfully display colors outside the sRGB gamut.

3.3.2.3. The premise of YCC

For simplicity, YCC encompasses both Y'CrCb and Y'PrPb, depending on whether the signal is digital or analog, respectively. However, it is important to refer to Y', as the luma component, rather than as the luminance or Y [Poynton; 1997]. Even though Y' is a video signal representative of luminance, the term luminance corresponds

to the CIE definition of L* under CIELAB, and thus, the term luma is used to directly correspond to the digital video signal [Poynton; 2003].

Although not a complete color space, YCC translates digital count information, where the available colorants determine the color displayed. The luma component is computed in Eqn. 3.6,

$$Y' = K_r * R' + (1 - K_r - K_b) * G' + K_b * B', \qquad (3.6)$$

where constants Kr and Kb are determined based on the applicable color space. Both constants change depending on the definition of the television (HDTV versus SDTV). The chrominance components equal

$$P_b = \frac{1}{2} * \frac{B' - Y'}{1 - K_b}$$
$$P_r = \frac{1}{2} * \frac{R' - Y'}{1 - K_r}, \qquad (3.7) \text{ \& } (3.8)$$

where the result of Eqns. 3.7 and 3.8 (either C_b/C_r or P_bP_r) depend on constants K_r and K_b. R',G',B' are obtained through the opto-electronic transfer function (OETFs) converting from RGB values. The following equations represent the transfer function incorporated into the conversion. For R,G,B less than or equal to -0.018, Eqn. 3.9 is used.

$$R' = -1.099(-R)^{0.45} + 0.099$$
$$G' = -1.099(-G)^{0.45} + 0.099 \qquad (3.9)$$
$$B' = -1.099(-B)^{0.45} + 0.099$$

If R,G,B is less than 0.018, but greater than -0.018, a scaling factor of 4.50 is applied (Eqn. 3.10).

$$R' = 4.50R$$
$$G' = 4.50G \qquad (3.10)$$
$$B' = 4.50B$$

The last case, when R,G,B is greater than or equal to 0.018, Eqn. 3.11 is used.

$$R' = 1.099R^{0.45} - 0.099$$
$$G' = 1.099G^{0.45} - 0.099 \qquad (3.11)$$
$$B' = 1.099B^{0.45} - 0.099$$

Eqns. (3.8) through (3.10) were explained by both Matsumoto et al., 2006, and Poynton, 2003, in more depth, although differed slightly for cases where R,G,B is less than or equal to -0.018. In Figure 3.15, Matsumoto et al., 2006, considers the negative R,G,B values, whereas Poynton addresses only R,G,B, values between zero and one (Figure 3.16).

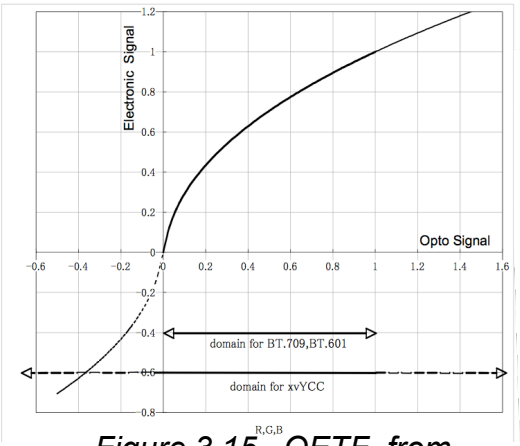

Figure 3.15. OETF, from Matsumoto et al., applied to color information.

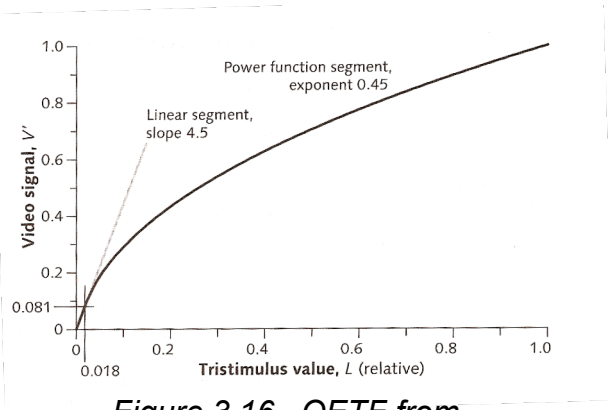

Figure 3.16. OETF from Poynton applied to color information.

In both figures, an OETF applied to color information results in the YCC encoded information. Through additional conversions, digital counts can be recovered, as they are for sRGB space, through YCC decoding followed by a transformation corresponding to the Extended ITU-R BT.709-5 and the appropriate color space conversion [Matsumoto; 2006].

3.3.2.4. ITU Existing Standards

The International Telecommunications Union (ITU) is responsible for standardizing specific broadcast signals. ITU-R BT.709.5 is the current standard for YCC encoding on HDTVs, and ITU-R BT.601.5 represents the standard set for SDTV YCC encoding. For short, further reference to the above standards will be denoted as Rec. 709 and Rec. 601. Under both standards, YCC encoding concludes with a matrix transformation converting R',G',B' to Y'CrCb. The matrix, however, varies between Rec. 601 and Rec. 709 as follows:

$$\begin{bmatrix} Y'_{601} \\ Cb'_{601} \\ Cr'_{601} \end{bmatrix} = \begin{bmatrix} 0.2990 & 0.5870 & 0.1140 \\ -0.1687 & -0.3313 & 0.5000 \\ 0.5000 & -0.4187 & -0.0813 \end{bmatrix} \begin{bmatrix} R' \\ G' \\ B' \end{bmatrix} \qquad (3.12)$$

$$\begin{bmatrix} Y'_{709} \\ Cb'_{709} \\ Cr'_{709} \end{bmatrix} = \begin{bmatrix} 0.2126 & 0.7152 & 0.0722 \\ -0.1146 & -0.3854 & 0.5000 \\ 0.5000 & -0.4542 & -0.0458 \end{bmatrix} \begin{bmatrix} R' \\ G' \\ B' \end{bmatrix} \qquad (3.13)$$

When YCC decoding, the inverse OETFs are used in combination with a color space conversion to obtain digital counts corresponding to the appropriate display.

The above image coding systems, sYCC, YCC and sRGB, incorporate a little 'breathing' room, so to speak, in terms of digital counts, to avoid clipping in either direction. Due to processing by digital and analog filters, and any resulting overshoot or undershoot, it is necessary to incorporate both "headroom" and "footroom" in the digital video standard. Therefore, 8-bit studio standards have 219 steps between reference black and white, where reference black is defined at code value 16, reference white at 235 (Figure 3.14) [Poynton; 2007]. Matsumoto et al., however, investigated the result of incorporating every code value in the digital signal, ranging from 1 through 256, in the display gamut.

3.3.3. Expanded Gamut Color Space (xvYCC)

The sRGB color space is convenient for displaying images accurately on a display (provided the display has sRGB primaries), without additional consideration of the individual display characteristics [Zeng; 2005]. However, with the addition of more recent technology in expanded gamut displays, sRGB color space may be accurate, but not ideal. Both YCC and sYCC are limited by the output display gamut, and therefore, limit the output values as significantly as sRGB does. Zeng addresses the effect of limiting the number of encoded color amounts. Displaying digital media on a larger gamut, a characteristic of many current displays, and encoding the color information with a smaller color space can result in noticeable quantization errors [Zeng; 2005]. Therefore, research has continued with the rising trend in more colorful displays and a corresponding, expanded gamut color space was sought out.

Displaying colors under conventional sRGB gamut standards on wide-gamut display technology cancels out the attractive characteristics the display holds. Therefore, a new standard wide-gamut color space was proposed as a means to present images on these emerging displays. The color space, xvYCC, was defined by the IEC in 2005, published in January 2006, and investigated by Matsumoto et al. in June 2006.

3.3.3.1. Gamut Area of xvYCC

The premise of xvYCC is based on achieving an enhanced color gamut space, one that incorporates both displays and color video imaging. This color space, represented in Figure 3.18, extends the sRGB color space defined in IEC 61966-2-1 and Rec. 709. By extending the digital count range to one through 254 for both the luma and chroma components, the previously "unrealizable" colors can be applied to display technology

with reasonable reproduction. Therefore, when converting from sRGB to xvYCC, the gamut area is inherently expanded, and more saturated colors can be represented [Kim; 2007].

This color space was defined for flat panel displays (IEC 2006), as their existence had become quite prevalent, however, their capabilities were not yet used in their entirety. The YCC color space had only begun to approach the desire for extended output gamuts. The cube of encoded YCC colors, from Suriura et al., is displayed in Figure 3.17.

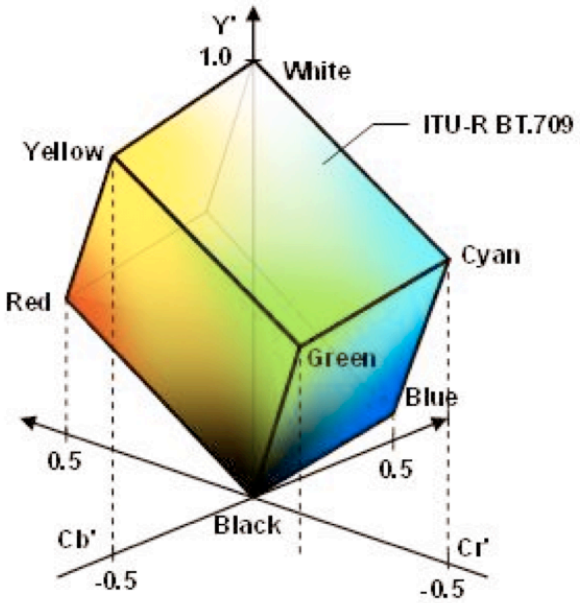

Figure 3.17. The cube of encoded colors that comprise the color space defined by YCC (Rec. 709)

Both "legal" and "illegal" colors are represented in Figure 3.17, according to the definition of the YCC color space [Kim; 2007]. The projections of red, green, blue and white onto the chrominance scale of YCC are represented by the dotted lines. Because Rec. 709 ranges in digital values between zero and one, only the inside cross-section of

the cube is displayed on Figure 3.17, and on a second reproduction of the figure, Figure 3.18. However, YCC theoretically encompasses both negative R,G,B values and values greater than one (denoted as "invalid" colors earlier).

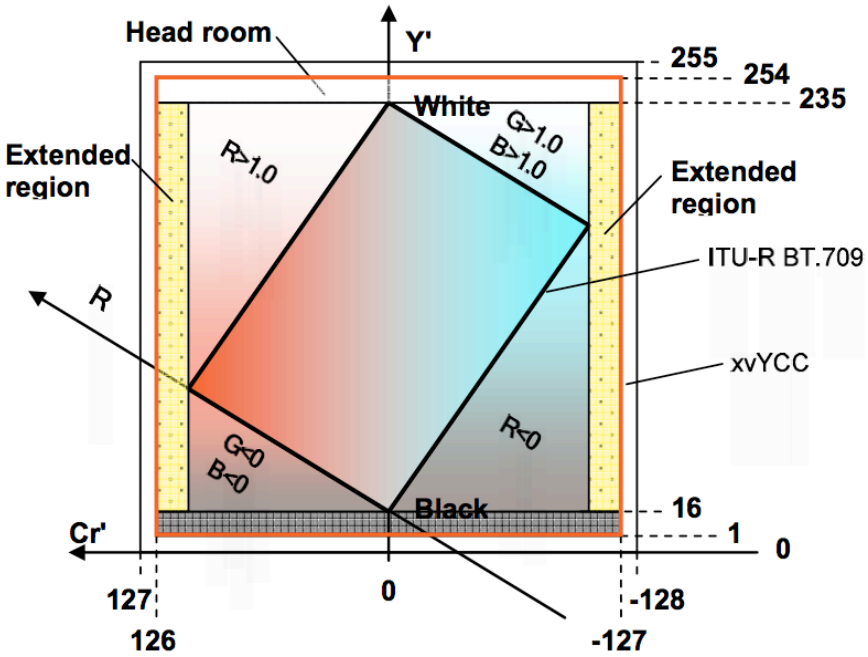

Figure 3.18. The two-dimensional representation of both the space defined by Rec. 709 and the xvYCC color space.

The footroom and headroom spaces, created by the unused digital counts in the extreme regions, are labeled in Figure 3.18. When converting to xvYCC and extending the digital count ranges to span between one and 254, in both the luma and chroma axes, encoding of a greater number of colors is enabled. This extension is a result of the OETF corresponding to xvYCC, such that the transfer function extends the rhombus in Figure 3.18 to incorporate negative values and values greater than one [Kim; 2007]. These values are denoted as invalid in the YCC color space, whereas in xvYCC these values represent the best assets to this extended gamut.

3.3.3.2. Producible Colors in xvYCC

More specifically, when converting to xvYCC, negative R,G,B values are converted to their corresponding complementary hues. Therefore, deeper hues are obtained in xvYCC color space [IEC; 2006]. In addition, RGB signals greater than one are visible colors within xvYCC color space.

The xvYCC color space still has its color limits, however. In the analysis performed by Kim, 2007, the color gamut boundaries of xvYCC were tested. As a result, xvYCC was insufficient in encoding two specific, highly saturated color regions: green-cyan and red-magenta, under lightness values greater than fifty. However, it is more meaningful to address the number of encoded xvYCC colors the output displays can handle. In chapter six of Kim's analysis, this was addressed for various displays. Since xvYCC is an extended space, a wide-gamut display is necessary to obtain optimal results. Both a wide-gamut LCD display, with LED-backlight, and a RGB-laser primary display were incorporated into the analysis, where it was determined that 57.1% and 75.5% of the xvYCC gamut volume could be represented on the respective displays [Kim; 2007]. Given the extension of xvYCC compared to sRGB color space, these percentages of the represented gamut volume are significant.

4. Experiments

The following experiments were conducted with the intent to develop a gamut mapping algorithm in which standard image content is expanded to an extended gamut display in the most preferable manner.

4.1 Display Characterization

Two displays were incorporated into the main algorithm testing experiment to aid in developing a robust expansion algorithm. Including an LCD, backlit with LEDs, and a DLP (with LED primaries) display into the same evaluation, enabled any existing device dependencies to become apparent. In addition, when developing a versatile GEA, robustness is a requirement. Therefore, evaluating multiple display technologies will provide further support for mapping strategies, provided the displays correspond with one another.

In order to properly display images on the different technologies, careful characterization procedures considered each device independently.

4.1.1. One-Dimensional LUT

Day et al., 2004, published a model incorporating three, one dimensional look-up tables (LUTs) as the characterization method corresponding to LCD monitors. The detailed procedure was performed follows: after sufficient warm-up time, a LMT C1210 Colorimeter was calibrated via a Matlab script. The display was presented red, green and blue ramps of equally incremented steps (of fifteen digital counts) ranging from zero to 255, where each channel was incremented individually while the other two were constrained to zero. The script determined the screen size of the display, and displayed

the data on a uniformly gray background in a large circle centered on the display. Neutral patches were also displayed and measured with the colorimeter.

All measurements were taken in dark surround, and for each patch, four measurements were taken and averaged to minimize the measurement error. Once the tristimulus values were measured, each value was normalized by the tristimulus values of the black patch. Each normalized channel was then incorporated into a one-dimensional LUT relating digital counts displayed to red, green and blue scalars.

The relationship between the voltage signals that drive the display and the radiant output of the display needs to be characterized in order to work backwards and determine the signals necessary to produce a given color [Day; 2004]. Because an LCD cannot accurately be characterized via a simple gain-offset-gain model, a LUT is implemented instead to define the nonlinear relationship. In an LCD, the RGB digital counts are converted into the voltages applied to the liquid crystals through a LUT, which can further be converted into tristimulus values through a transformation matrix.

Relating the digital counts displayed to the device to the measured tristimulus values from the color patches sent to the display resulted in transformation matrix. The calculated transformation matrix was then applied to random color patches in order to obtain their corresponding display digital counts. Therefore, using the white point of the monitor, measured by the colorimeter for a white patch, the tristimulus values of the ramp images were converted to RGB values via the inverse of the 3x4 transformation matrix (Eqn. 4.1).

$$\begin{bmatrix} R \\ G \\ B \end{bmatrix} = \begin{bmatrix} X_{r,\max} - X_{k,\min} & X_{g,\max} - X_{k,\min} & X_{b,\max} - X_{k,\min} & X_{k,\min} \\ Y_{r,\max} - Y_{k,\min} & Y_{g,\max} - Y_{k,\min} & Y_{b,\max} - Y_{k,\min} & Y_{k,\min} \\ Z_{r,\max} - Z_{k,\min} & Z_{g,\max} - Z_{k,\min} & Z_{b,\max} - Z_{k,\min} & Z_{k,\min} \end{bmatrix}^{-1} \begin{bmatrix} X - X_{k,\min} \\ Y - Y_{k,\min} \\ Z - Z_{k,\min} \end{bmatrix} \quad (4.1)$$

Once RGB values were obtained, the radiometric scalars were determined by linearly interpolating the LUT for each channel (inverse of Eqn. 4.2).

$$R = LUT(d_r)$$
$$G = LUT(d_g) \quad (4.2)$$
$$B = LUT(d_b)$$

After these scalars were calculated, the signals required to display the corresponding tristimulus values were obtained. This process was implemented to ensure the values were properly displayed and corresponded to the original color patch. (For more information on LCD characterization refer to [Day et al.; 2004]).

4.1.1.1 Sony Display

Using this model, Heckaman et al., 2007, characterized the Sony display and reported the results. The display was characterized with a high degree of success. The display was characterized with an average CIEDE94 value of 1.0 unit, with a standard deviation of 0.67 units [Heckaman et al., 2007]. Therefore, colors mapped to the device are accurately displayed according to their original color values.

4.1.1.2 Samsung Display

The display was characterized by measuring the tristimulus values of the RGB digital count ramps data, under both Standard/Normal (NS) and Movie/Warm 2(MW) modes in order to determine which mode the evaluations would be performed under. The primaries under each mode are represented in Figure 4.1, and demonstrate the correspondence between the chromaticity gamut sizes.

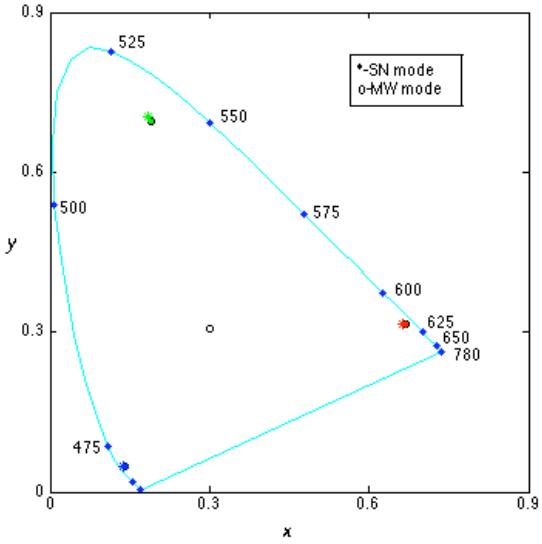

Figure 4.1. Chromaticity diagram with primaries from both SN and MW modes.

This comparison proved both modes provided similar results; however, the closeness between the illuminant under Warm 2 and D65 (Figure 3.13) guided the decision for selecting the mode carried throughout the evaluations.

The ramp measurements were taken according to the procedure described above, and in Day et al., 2004. The red, green and blue ramp chromaticities are displayed in Figure 4.2.

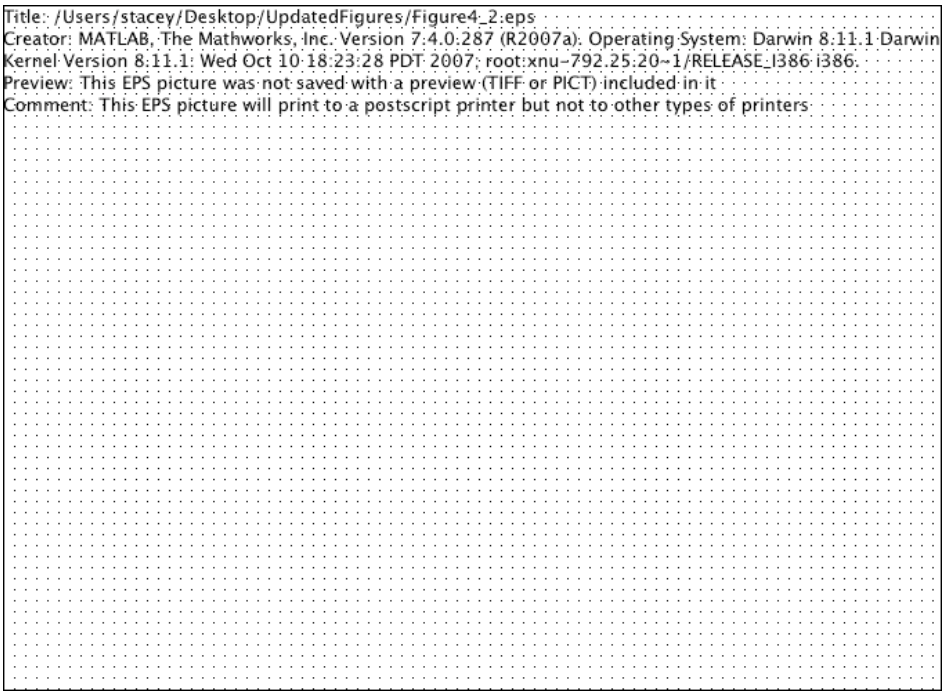

Figure 4.2. Measured tristimulus values converted to chromaticity coordinates, corresponding to the red, green and blue ramp data.

Each channel was offset by the corresponding maximum tristimulus values by subtracting out the tristimulus values for the black patch (the constant background was removed for these values), to result in the RGB values. These RGB values were then converted to obtain linearized display RGB values (scalars) and were interpolated to obtain a full set of scalars: one scalar corresponding to every digital count from zero to 255. This represents the three, one-dimensional LUTs used to convert the tristimulus values to RGB scalars.

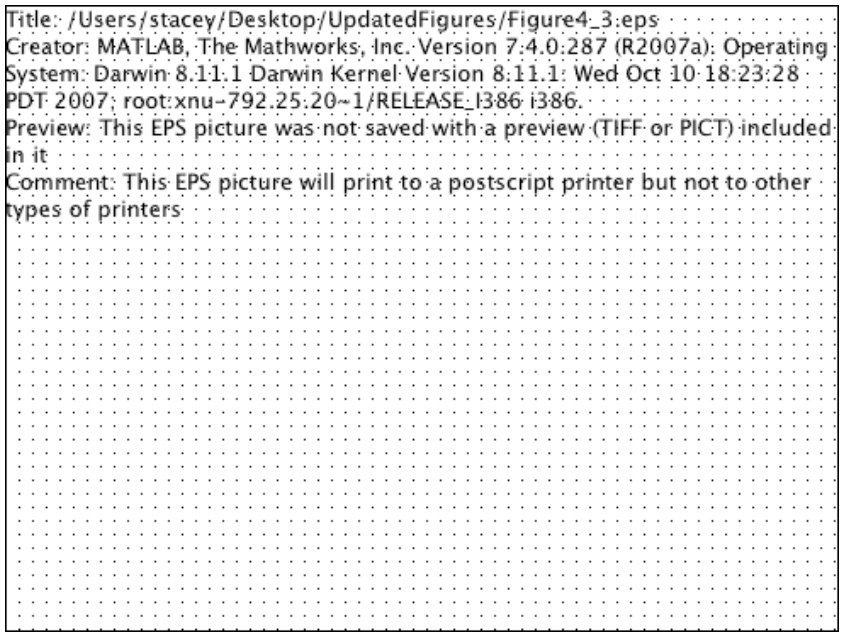

Figure 4.3. Three one-dimensional look-up tables derived from the measured tristimulus values of the RGB ramps and neutral data.

The most efficient method to characterize an LCD with an unknown gamma function, without measuring the gamma curve, is through a LUT. By relating the digital counts presented to the tristimulus values measured, RGB scalars are derived through a LUT to characterize the display. Therefore, using the LUT (Figure 4.3), RGB scalar values corresponding to each of the color patches can be obtained and the color accuracy of the display evaluated. This was first analyzed through a randomly generated set of 100 color samples.

A set of 100 normally distributed, digital counts, randomized for each channel independently, was presented to the display, where the corresponding tristimulus values were measured.

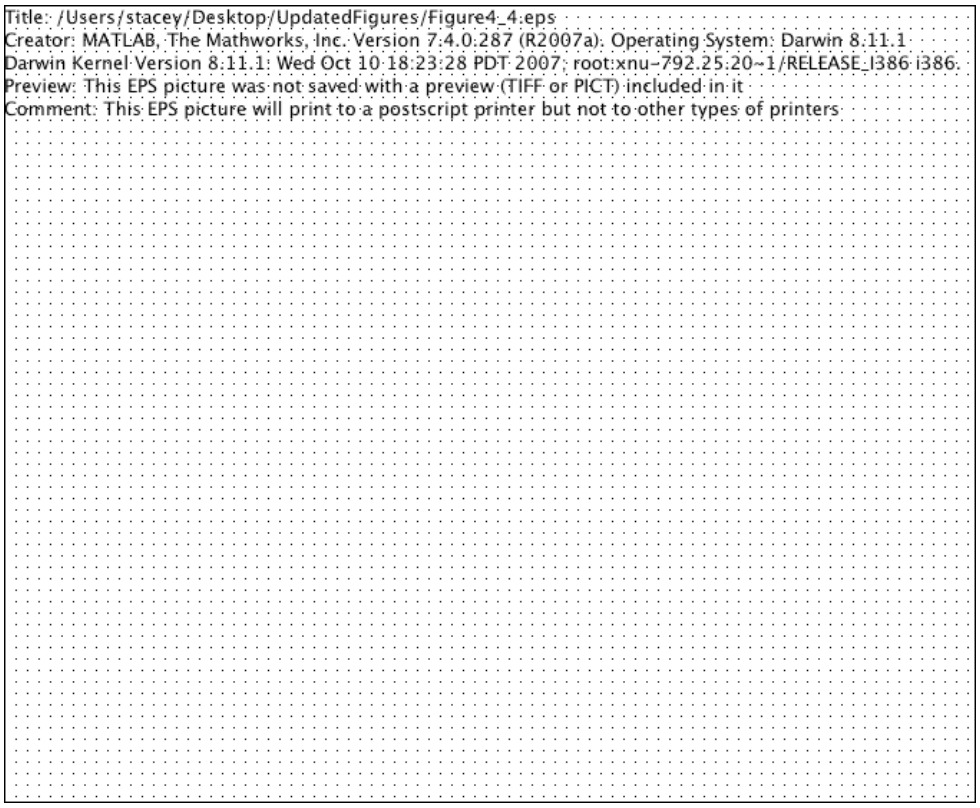

Figure 4.4. 100 randomly generated colors on a chromaticity diagram.

The samples' digital counts were converted to estimated tristimulus values through the transformation matrix derived from the RGB ramp data (Eqn. 4.3).

$$\begin{bmatrix} X \\ Y \\ Z \end{bmatrix} = [M]_{display\,3x4} \begin{bmatrix} R \\ G \\ B \\ 1 \end{bmatrix} \quad (4.3)$$

The transformation matrix in Eqn. 4.3, represents the calculated values for both the Sony and Samsung displays in Eqn. 4.4 and 4.5.

$$M_{Sony} = \begin{bmatrix} 147.524 & 43.019 & 37.382 & 0.39 \\ 61.729 & 152.744 & 21.633 & 0.37 \\ -0.190 & 23.235 & 219.957 & 0.42 \end{bmatrix} \quad (4.4)$$

$$M_{Samsung} = \begin{bmatrix} 51.528 & 15.803 & 17.948 & 0.527 \\ 23.967 & 59.217 & 5.910 & 0.490 \\ 0.714 & 9.194 & 105.571 & 0.704 \end{bmatrix} \quad (4.5)$$

Both sets of tristimulus values, estimated and measured, were converted to CIELAB values using the measured tristimulus values of the white patch at the white point. A mean color difference of 7.70 units, based on CIEDE2000, was calculated.

Based on previous experience with characterizing displays, this result was high. Therefore, using linear regression, the display matrix was optimized using the following equation:

$$M_{display_{3x4}} = \left(\left([RGB1]_{4x3}{}' [RGB1]_{3x4} \right)^{-1} [RGB1]_{4x3}{}' [XYZ]_{3xn} \right)' \quad (4.6)$$

After calculating the display matrix, the procedure was repeated to derive the estimated tristimulus values. A CIEDE2000 color difference of 4.65 was calculated. The improvement of the color differences was expected based on the increased specificity of the calculations. This matrix was used throughout the rest of the calculations as the display matrix.

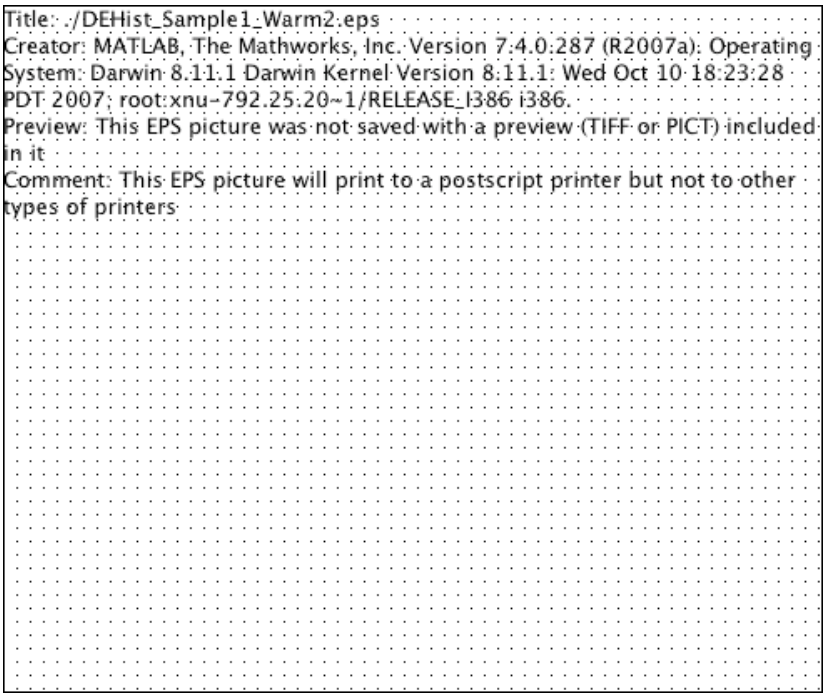

Figure 4.5. CIEDE2000 color difference histogram for the randomly generated set of 100 samples.

The distribution of color differences is displayed in Figure 4.5. The mean CIEDE2000 for the dataset was higher than expected. However, since this characterization procedure was not designed for DLP display technology, in addition to the fact that color reproduction accuracy is not necessary, this result was deemed acceptable.

A color difference vector plot was evaluated, however, to better understand where the differences were occurring.

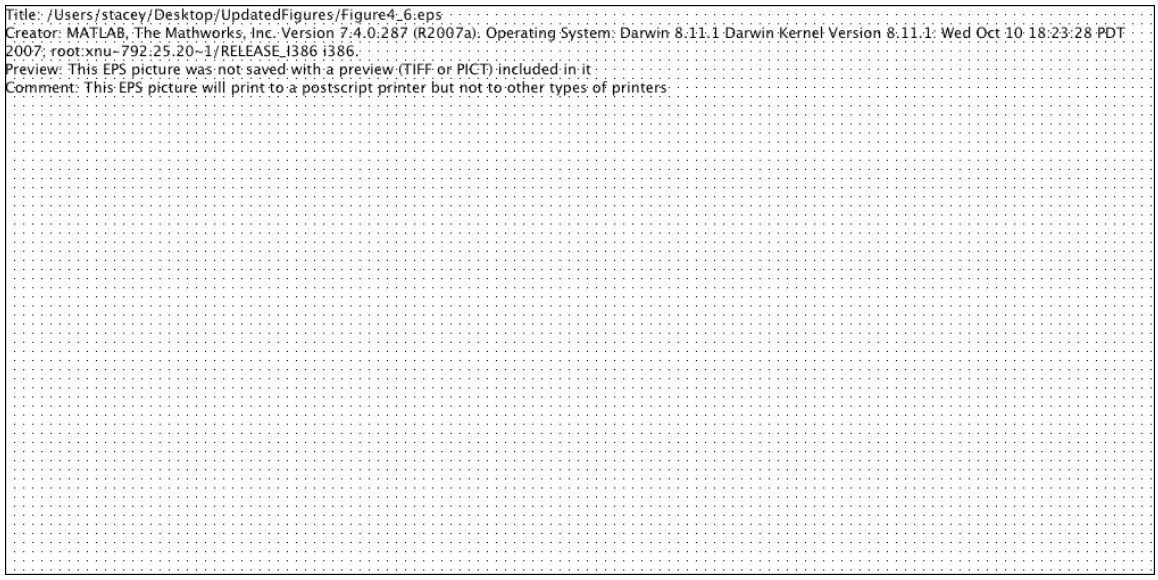

Figure 4.6. Comparison of estimated CIELAB values with the measured CIELAB values, where the arrows run from the measured to estimated values.

In Figure 3.11**,** it is evident that the Samsung gamut is extended slightly in the blue region, in addition to the green region. Therefore, the large color differences in these regions, apparent in Figure 4.6, are explained by the chromaticity gamut of the Samsung display.

Eqn. 4.2 incorporates the RGB scalar values of the sample set into the matrix calculation. Therefore, in order to ensure this estimation process can hold for other sample sets, a second set of 100 randomly generated digital count coordinates were displayed and measured, and a corresponding CIEDE2000 color difference calculated. A color difference, for the second set, of 4.83 units was measured. Therefore, this supports that the display will maintain a color difference approximately ranging between four and five CIEDE2000 units.

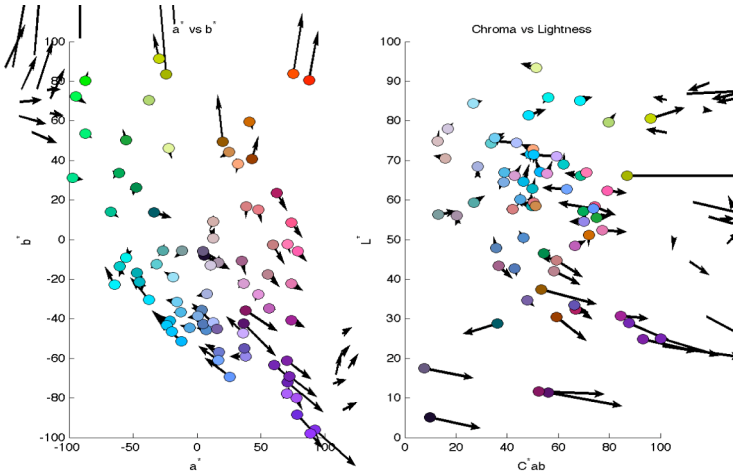

Figure 4.7. CIELAB vector plot for a second randomly generated sample set, where the arrows run from the measured CIELAB values to the estimated values.

Comparing Figures 4.6 and 4.7, the distribution of error in color reproduction occurs in similar regions of (a*,b*) coordinates, and again, in values of high chroma.

Based on the clipping in the blue channel (Figure 4.5) and the higher than expected color differences, further analysis was conducted to examine the hypothesis that the internal processing of the display had not been eliminated. The neutral ramp data of equal digital counts (R=G=B) incremented by fifteen, from 0-255, were measured and the luminance was compared to the resulting luminance values of the ramp data for each of the three channels added together. Theoretically, these ramps should be equal, as the gray ramp is comprised of equal concentrations of red, green and blue.

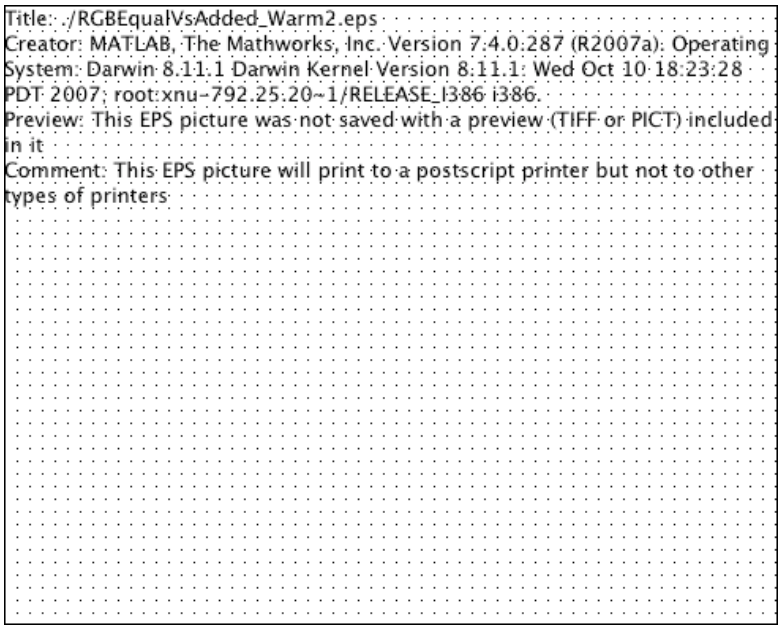

Figure 4.8. Luminance values of the RGB ramps added together compared with the equal digital count ramp (R=G=B).

The disparity between the two curves supports the hypothesis that non-linear processing was occurring, despite the attempt to control all display settings. Since the estimations of the tristimulus values through matrix multiplication resulted in unexpected results, a few other characterization methods were exhausted before settling on the simple characterization model described above.

One alteration was the display mode, as the above procedure was conducted under HDMI mode. The measurements were also conducted under "PC" mode, meaning the display was directly connected to the computer, where the content transmitted was under appropriate standards, or was compressed. This is compared to the HDMI connection, in which uncompressed high-definition material can be digitally sent to the display.

The corresponding LUT under PC mode is displayed in Figure 4.9.

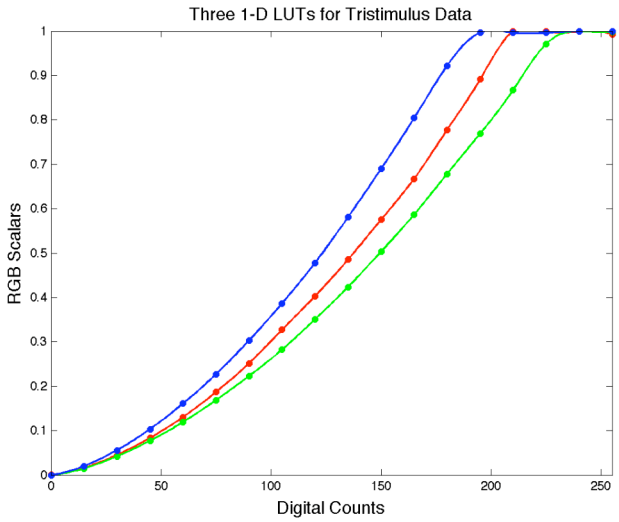

Figure 4.9. Three one-dimensional look-up tables derived from the measured tristimulus values of the RGB ramps and neutral data (in PC mode).

The ramps in Figure 4.9 are distinct, in that each ramp has additional clipping. The blue ramp, in particular, is clipped to a scalar of one at a digital count of approximately 190 through 255. Therefore, much of the information from the blue channel will be effected, based on this LUT. The same set of 100 samples, evaluated in HDMI mode, were used again to compute estimated tristimulus values, and resulting CIELAB values from the original digital counts. A mean CIEDE2000 of 4.96 was calculated for the first sample set.

Since the mean color difference did not improve, but rather worsened, further methods were evaluated. Due to the non-linear processing of the display, evident through Figure 4.8, a profile was fit to the display, in an effort to complete a successful characterization.

4.1.2. Three-dimensional LUT

The measurements were, once again, taken under Movie/Warm2 as this setting provided a wide gamut, with a white point closest to D65. An 11x11x11 grid of RGB

values (Figure 4.10) were displayed and measured using the LMT-colorimeter, in order to establish the three-dimensional LUT (3DLUT).

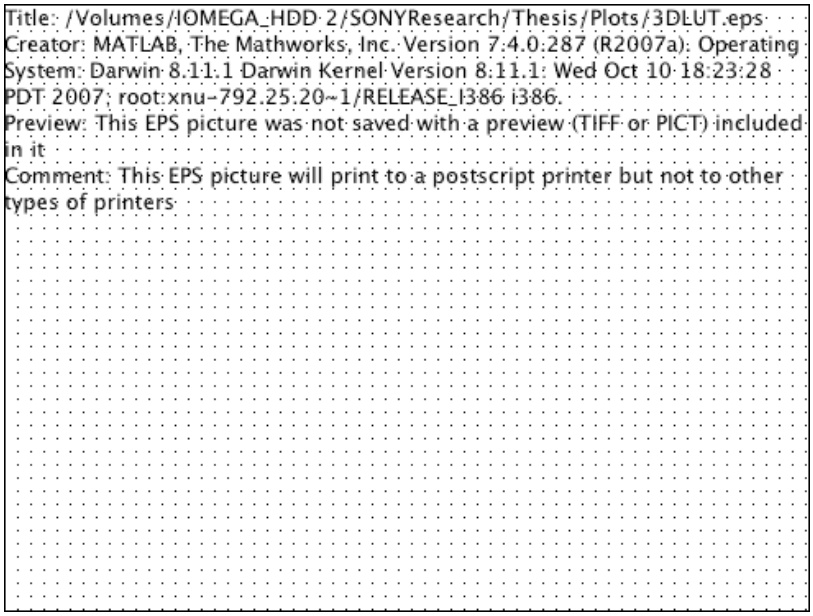

Figure 4.10. Three-dimensional scatter plot representing each measured digital count on the 11x11x11 set used to create the 3DLUT.

Upon measuring the tristimulus values that correspond to each data point within the 3D grid, a nearest neighbor interpolation was performed to relate RGB digital counts to tristimulus values. Therefore, evaluation of this method was enabled by comparing estimated tristimulus values for a given sample, to the measured tristimulus values for the same set of data. When this was conducted for 100 samples, the calculated color differences were as follows:

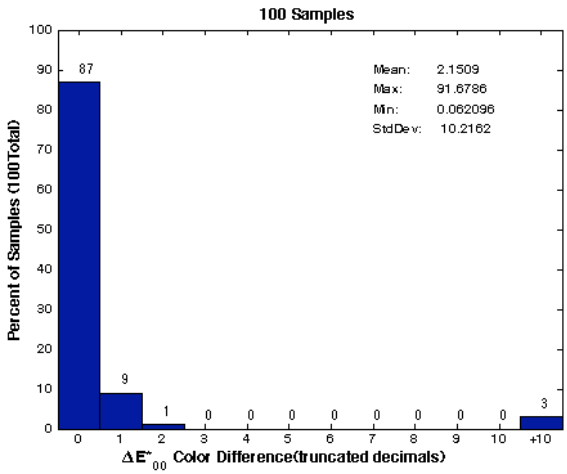

Figure 4.11. Color difference histogram representing 100 samples.

Evaluation of the 3DLUT required a color difference analysis performed on a randomly generated set of 100 RGB samples. The mean color difference of 2.15, in this case, is improved from the 1DLUT results of 4.65. However, the maximum color differences falls outside the realm of acceptable, at an outstanding 91.68. This color difference was an indication that the 3DLUT may be unable to characterize this display, in its entirety. The color difference vector plot, Figure 4.12, demonstrates the color regions and extent to which the 3DLUT fails.

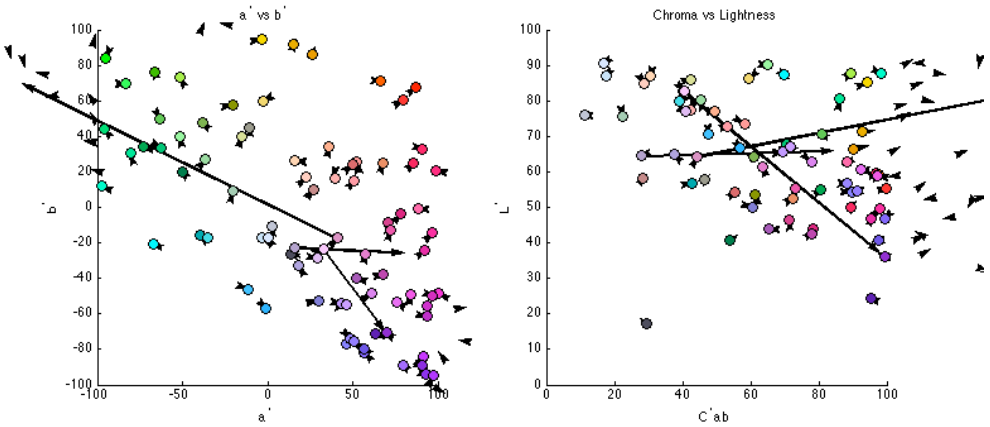

Figure 4.12. CIELAB vector plot representing each of the 100 samples, with color difference arrows representing the magnitude of CIEDE2000 and direction towards the estimated values.

The questionably large color differences were consistently extending from similar hues and chroma values. To better understand where the error was coming from, a histogram and vector plot of red, green, blue ramps and cyan, magenta and yellow color patches were analyzed for significant trends in error.

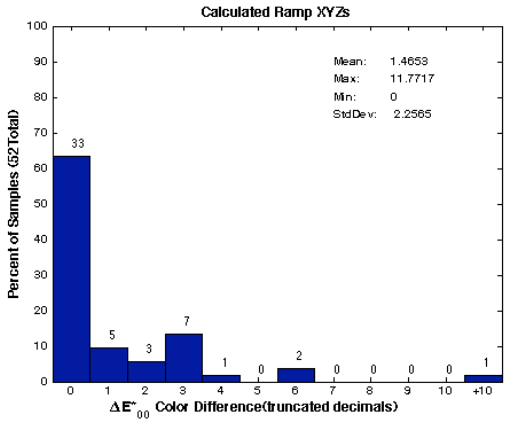

Figure 4.13. Color difference histogram of white, black, red, green, blue, yellow, cyan, and magenta color patches.

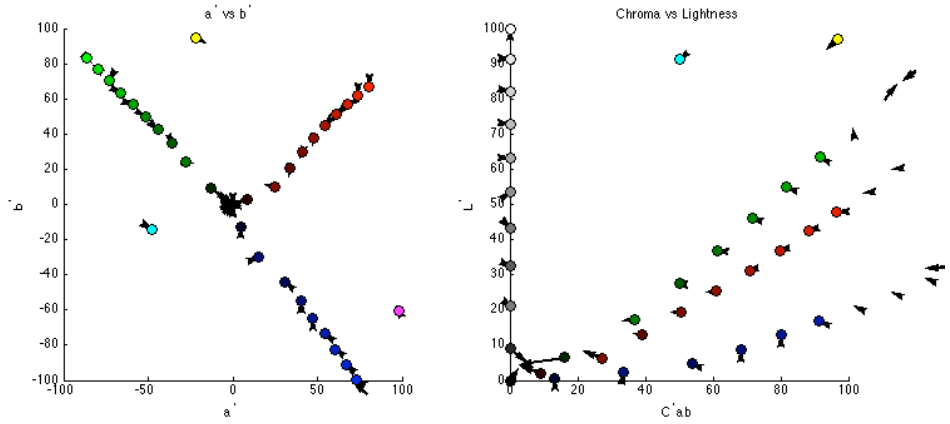

Figure 4.14. CIEDE2000 color differences for the gray, red, green blue generated ramps in addition to the white, black, red, green, blue, yellow, cyan and magenta colors.

Although the error was not a direct result of the measured ramps, further analysis proved this characterization method was insufficient in characterizing blue regions for this

Samsung display. A sample image demonstrates the result of using the 3DLUT as the characterization procedure.

Figure 4.15a. Original sRGB flower image

Figure 4.15b. Reproduction of flower image under 3DLUT characterization.

The gradations within Figure 4.15b were typical of the 3DLUT, and are independent of the mapping algorithm.

Considering the above analysis, the characterization procedure incorporated into the study, for the Samsung display, was the simple 1DLUT model. Therefore, both displays underwent this characterization procedure during the preparation of the images. Despite a higher mean color difference maintained by the Samsung display under this method, no artifacts in the images due to the characterization procedure were visually apparent, and thus, this did not affect the results.

4.2 Experimental Conditions: Dim Versus Dark Surround

The research directly preceding this gamut mapping algorithm study, evaluated the effects of ambient light, while addressing the effect of display gamut volume on image preference [Heckaman et al.; 2007]. The research conducted by Heckaman et al. entailed three different experiments, all designed to decipher the various effects of the

display color gamut volume. The first evaluated the effect of gamut volume on various perceptual attributes. The psychophysical results deemed colorfulness the attribute most dependent on the color gamut volume. Observer preference was evaluated in the second experiment, as a function of display color gamut volume. The results were encouraging in that many scenes benefited, in terms of observer preference, with a larger color gamut volume. However, there seemed to be a threshold at a color gamut ratio of 0.8 times the full, extended color gamut. The third experiment evaluated the effect of color gamut volume and display dynamic range on observer preference and perceived lightness contrast and colorfulness. The results proved changes in lightness contrast impact observer preference as much as change in color gamut volume.

These experiments all contributed to a better understanding of the effects of varying the display color gamut volume. However, in addition to the direct research questions examined in the above experiments, the effect of the experimental conditions also resulted from this research. Heckaman et al., 2007 performed the above experiments under dim surround, where the illumination off the wall was measured at 94 cd/m^2. In addition, the third experiment (denoted as Experiment III [Heckaman et al.;2007]) was repeated under dark surround (denoted as Experiment IIIb), measured by the Spectrascan PR650 Spectrophotometer at an illumination less than the device's sensitivity of $0.03cd/m^2$. Therefore, by including the research conducted prior to this gamut mapping evaluation, the experimental conditions for the mapping algorithm evaluation are substantiated.

4.2.1. The Effects of Dark Surround

Performing Experiment III for varying ambient lighting conditions enabled the effect of the surround to be established. Comparing the results provides sufficient argument for implementing the experimental conditions used in the gamut mapping algorithms evaluation.

4.2.1.1. Stimuli

The Munsell Color Science Laboratory (MCSL) at Rochester Institute of Technology (RIT) performed an experiment evaluating the effect of viewing conditions using the following three images:

Figure 4.16. a-c. (a) Coast Image, (b) Musicians Scene, (c) Flowers image.

The musician scene was chosen for its flesh tones, the flowers scene for its high degree of colorfulness over a full range of hue, and the coast for its high dynamic range. These scenes each represent one of the three key groups determined from the results of Experiment II [Heckaman et al.; 2007]: the flower scene is an image from the "highly colorful" group one, the coast from the scenic group (group two), and the musicians from the scenes containing flesh tones (group three).

4.2.1.2. Experimental Methods

The images were displayed on the Sony prototype described above in Section 3.2.1.1. All observers that participated in the evaluation ranged in age, ethnicity and experience (from young adults to the elderly and non-experts to Color Science/Imaging

Science experts, all representing multiple ethnicities). Seventeen observers judged preference, while eight evaluated perceived colorfulness and lightness contrast.

Again, the viewing conditions were identical to the conditions reported in Experiment III with one large exception: there was no ambient light. This experiment was performed in dark surround to highlight the effects of these viewing conditions on similar evaluations. For this experiment, the background behind the images was set to black (RGB digital counts equaled zero) rather than a mid-level gray, which enabled control of the adaptation level of the observers.

In accordance with the previous methodology for Experiment III, the same versions of the musicians, coast and flower scene were used for the dark room experiments. Thus, each version had a corresponding color gamut volume factor k, ranging from 1.00 to 0.40 times the display's actual color primaries in CIELAB a* and b*. In addition, lightness was similarly scaled in that, a dynamic range factor, k_{LC}, ranging from 1.00 to .0625 was also multiplied by the display's actual dynamic range to obtain the lightness contrast variations. By increasing the display's relative black point, or Y_{MIN}, of each of the display primaries, the range in lightness contrast for each successive version was obtained, and was scaled appropriate according to k_{LC}. The details on this process are explicitly described by Heckaman et al., 2007.

Observer preference was evaluated through a paired comparison experiment and colorfulness and lightness contrast through the method of Mean-Category-Value [Bartleson; 1984]. The preference experiment required the observers to:

"*Choose the image you like the best (prefer the most), and click directly on that image to select it*."

The instructions were the same for the perceived colorfulness (and lightness contrast) as

described in the preceding technical report, and entailed rating perceived colorfulness and lightness contrast on a scale ranging from one to nine. The analysis for the category scores from these evaluations is described there as well.

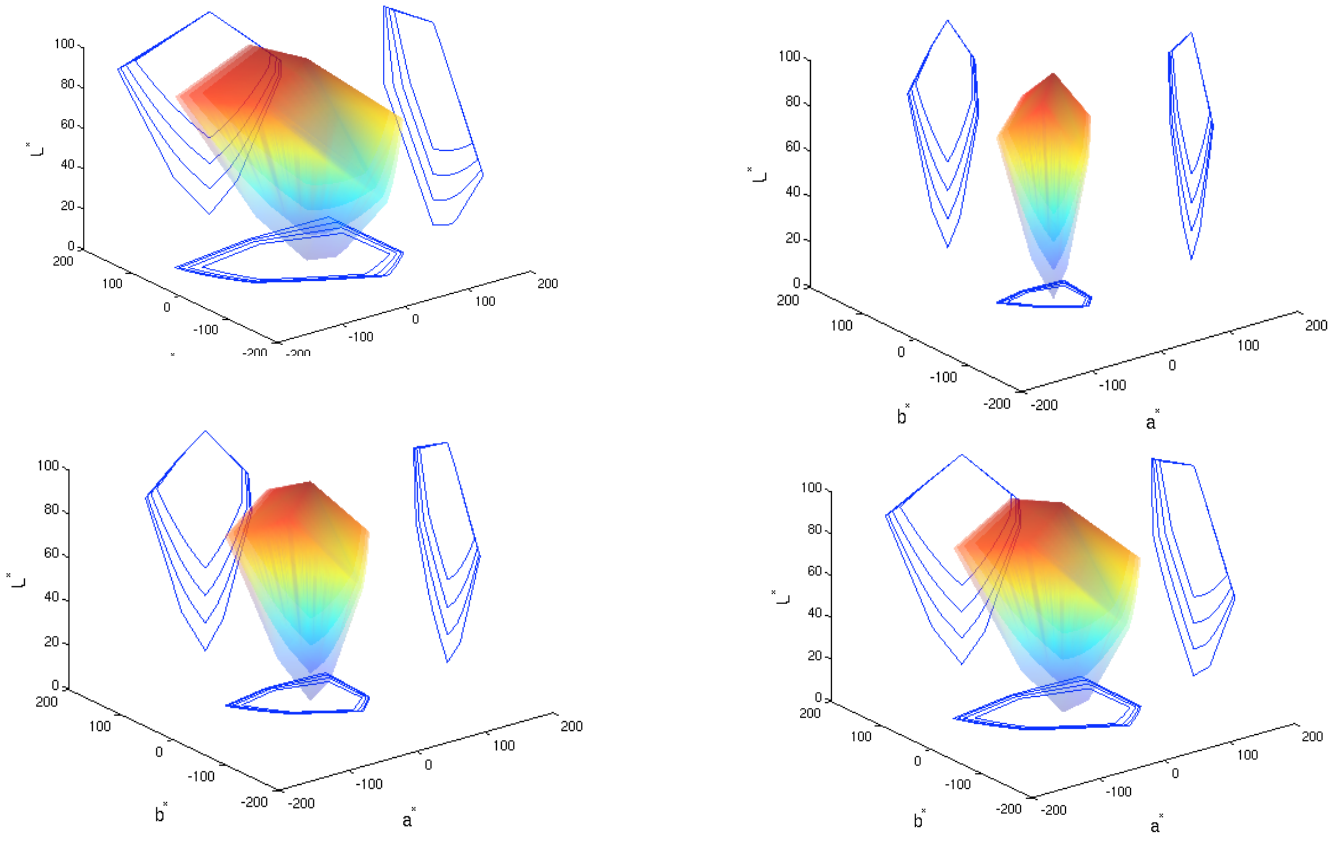

Figure 4.17. Simulated primaries in xy chromaticities for a color gamut volume factor of k=1.0(a), 0.8(b), 0.6(c), 0.4(d) and within each a lightness contrast factor kLC of 1.00, 0.875, 0.75, 0.625 times the full, extended gamut of the display.

The simulated set of sixteen primaries with their corresponding gamut volumes derived from variations in both colorfulness (k) and lightness contrast (k_{LC}) are displayed in Figure 4.17. These primaries were derived from the display's actual primaries and constrained in order to maintain hue and the display's white point.

4.2.1.3. Results and Discussion

For each of the three scenes evaluated, the scenes were analyzed independently. In Figure 4.18, the mean category scores for colorfulness as a function of the percentage of NTSC color gamut area in xy chromaticities, for each of the four levels of lightness contrast factor k_{LC}, or log contrast ratios, averaged across eight observers and the three scenes is plotted. Both Experiment III and the Experiment IIIb results are displayed for the flower scene.

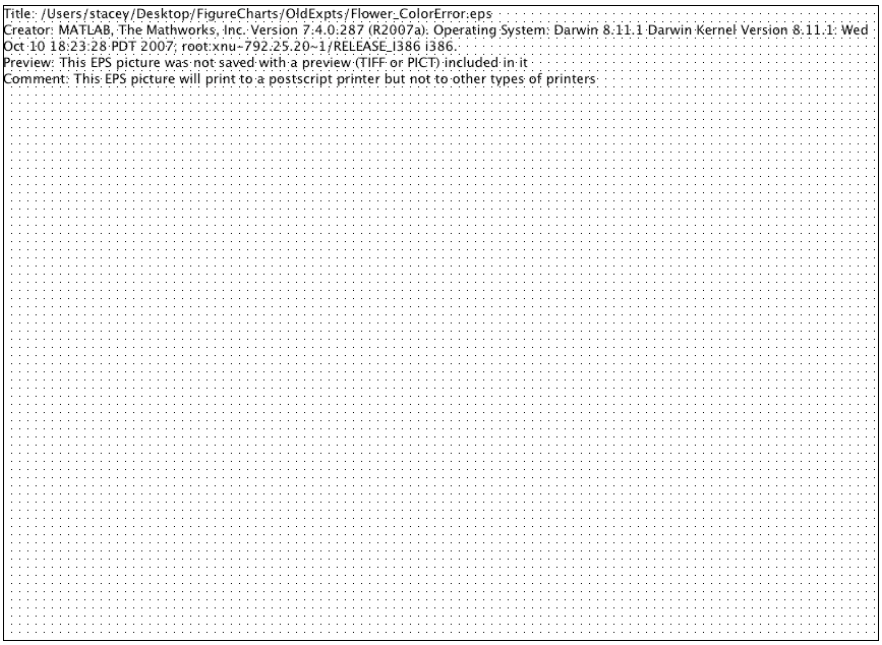

Figure 4.18: Perceived colorfulness as a function of the percentage of NTSC color gamut area in xy chromaticities for each log contrast ratio, for the flower scene averaged over eight observers for Experiment IIIb and six observers for Experiment III.

The 0.95 confidence intervals are displayed in Figure 4.18. Based on Figure 4.18, perceived colorfulness increases monotonically at each log contrast ratio. In addition, the dark room results are consistent with the previous report in that colorfulness is increasing at a decreasing rate with a larger color gamut. Therefore, as observed in Figure 4.18,

observers perceived colorfulness increases with larger chromaticity gamut areas, although the trend is non-linear. Also, there is no significant difference between the log contrast ratios, nor is there a significant difference between the two viewing conditions. The error is larger here, than reported in Experiment III, as this analysis is based on one scene, as compared with ten. The musician and coast scenes display similar results to that of the flower image.

Figure 4.19 represents the fitted contours of equal perceived colorfulness as a function of the percentage of the NTSC color gamut area in xy chromaticities and the log contrast ratio. The contours were once again based on multiple linear regression of the mean category scales for colorfulness. A correlation coefficient of above 0.97 was obtained for each scene. The flower scene contour plot, averaged over the eight observers, demonstrates similar results to that of the musician and coast scenes.

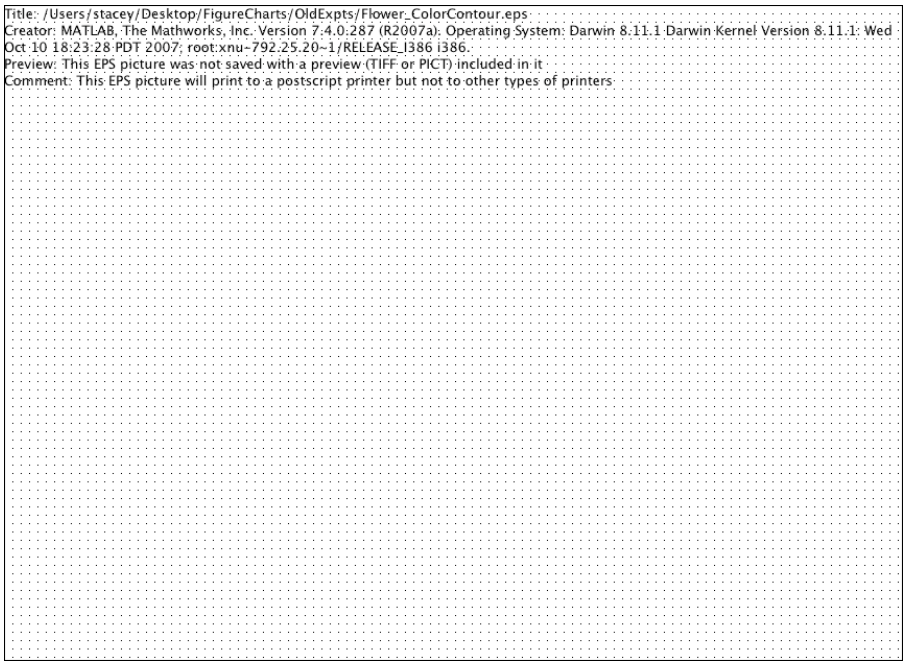

Figure 4.19: Contours of equal colorfulness, determined by multiple linear regression, as a function of percentage of NTSC color gamut area in xy chromaticities and log contrast ratio, for Experiment III (solid) and Experiment IIIb(dotted), averaged over observers, for the flower scene.

The numeric values on the plot in Figure 4.19 indicate a topographic-like comparison of equal, perceived colorfulness values. The contours reiterate the monotonically increasing characteristic of perceived colorfulness, at a diminishing rate, with an increased percentage of NTSC color gamut. In other words, perceived colorfulness increases steeply around ten through forty percent of NTSC color gamut, while increases more steadily for color gamut percentages greater than forty. In addition, lightness contrast remains insignificant to the response of perceived colorfulness. Figure 4.19 also demonstrates the similarities between the two experiments, in that once again, the results prove there is no significant difference between the two viewing conditions.

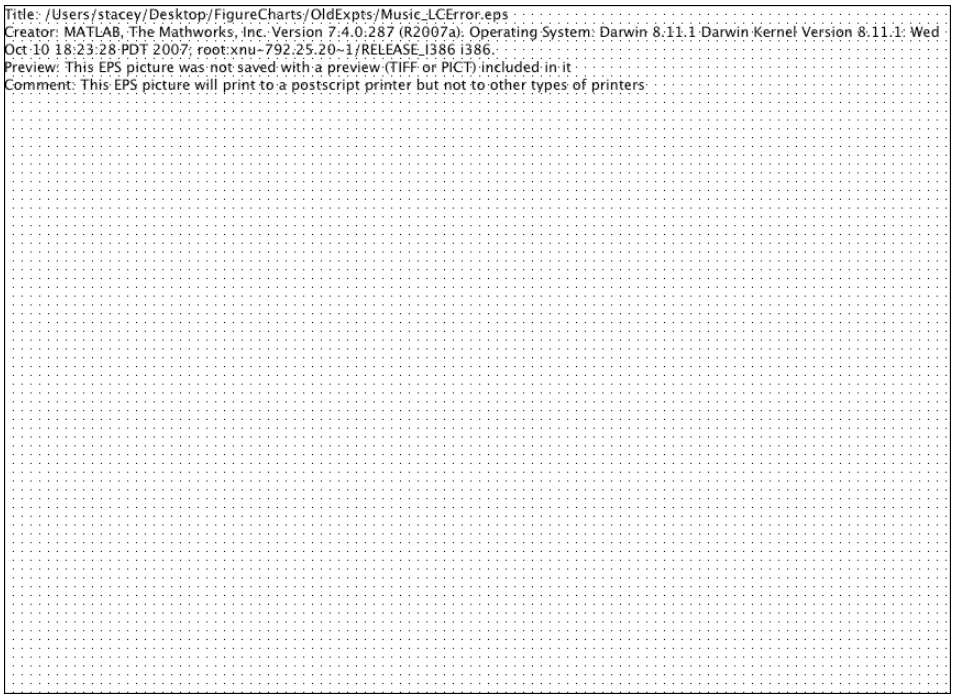

Figure 4.20: Lightness contrast interval scores as a function of the percentage of NTSC color gamut area in xy chromaticities for each log contrast ratio evaluated, for the musician scene from both Experiment III and the dark room experiment.

Since the flower and musician images resulted in similar lightness contrast responses, the musician image is displayed in Figure 4.20 for analysis. Due to the large error resulting from analyzing only one scene rather than the group, the conclusions are

limited. Lightness contrast appeared to a have linear relationship with the log contrast ratio evaluated: higher log contrast ratios resulted in an increased perceived lightness contrast.

The effect of the percent of color gamut is unclear based on Figure 4.20. In Experiment III a linear response of lightness contrast to the color gamut percentage was observed. Considering the error bars, this statement is difficult to make for the dark room experiment. However, the contribution of the percentage of color gamut on perceived lightness contrast is consistent with the Helmholtz-Kohlrausch effect, as was predicted [Fairchild; 2005].

Considering both Experiment III and IIIb, the Bartleson-Brennan Equations suggest that as the surround lighting conditions decrease, the perceived lightness contrast predictably would decrease as well [Fairchild; 2005]. Their research determined that viewing an image in a dark room causes dark areas of an image to appear lighter, with little effect on the light areas. However, it is not possible to discriminate between the two experiments, as seen in Figure 4.20, due to the limitations in the data.

Figure 4.21 represents the lightness contrast as a function of percentage of NTSC color gamut for the log contrast ratios for the coast scene. This scene exhibited a notably larger dynamic range than the flower and musician scenes.

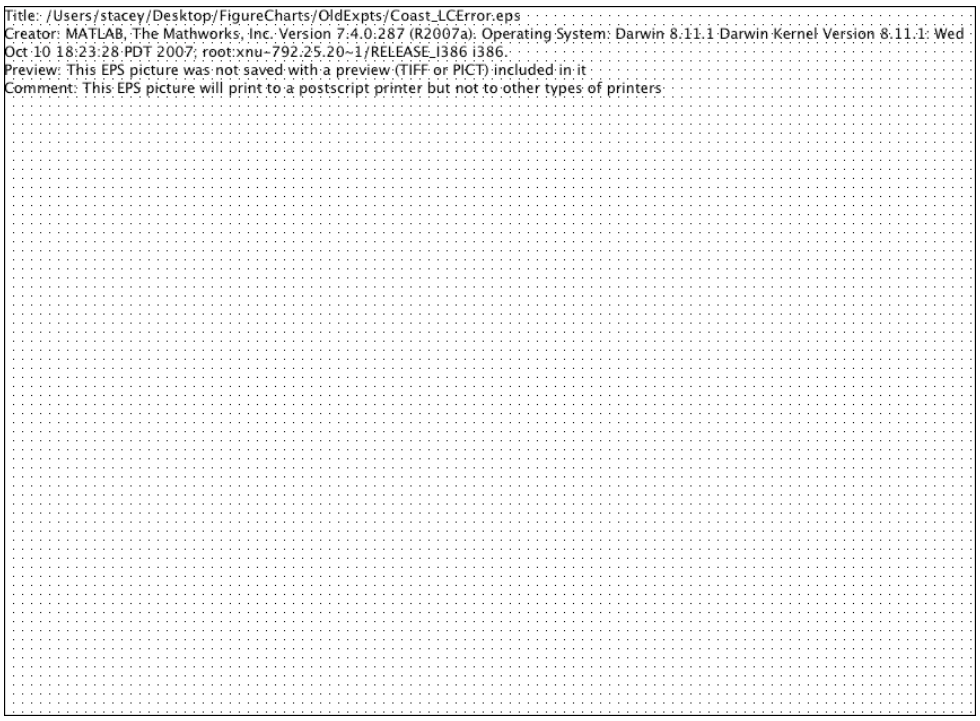

Figure 4.21: Lightness contrast in terms of category scores as a function of color gamut volume for each of the four log contrast ratios, for the coast scene.

The responses of lightness contrast in Figure 4.20 are more dispersed with respect to perceived lightness contrast. Therefore, the log contrast ratios had a greater effect on perceived lightness contrast in the coast scene than with the musician and flower scenes. The preceding effects all hold true for Figure 4.21 as well.

The fitted contours of equal lightness contrast for the coast scene, derived by multiple linear regression, are displayed in Figure 4.22. Once again, a correlation coefficient of 0.97 or higher was obtained for each scene evaluated.

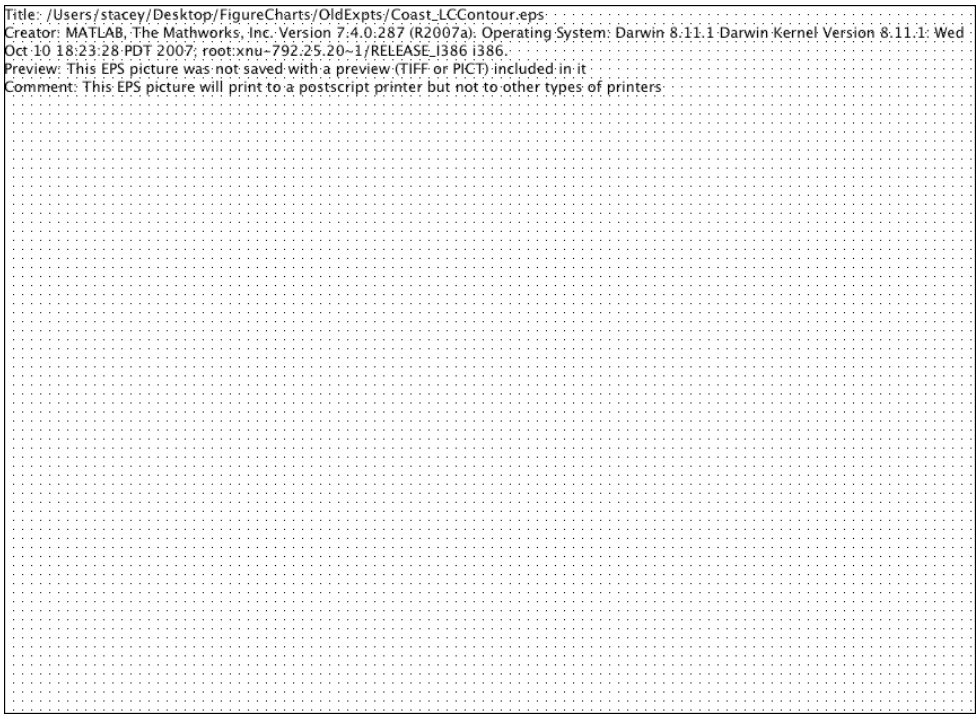

Figure 4.22: Fitted contours of equal lightness contrast as a function of percentage of NTSC color gamut area in xy chromaticites and log contrast ratio, for the coast scene.

Figure 4.22 demonstrated similar effects to those noted previously. The two experiments were not significantly different in any of the scenes with regards to lightness contrast. In addition, the variations among each scene were insignificant.

The preference results in terms of interval scores as a function of the percentage of NTSC color gamut in xy chromaticities and log contrast ratios for the musician scene is represented in Figure 4.23. The results from both experiments are displayed in Figure 4.23.

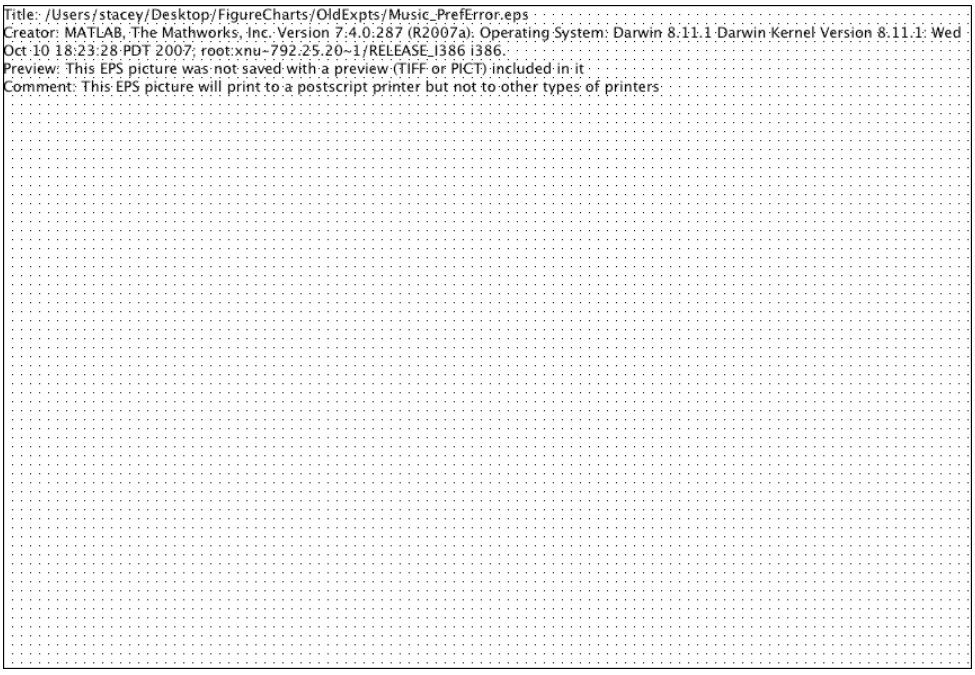

Figure 4.23: Both Experiment III and Experiment IIIb represented in an interval score plot for preference as a function of percentage of NTSC color gamut area in xy chromaticities and log contrast ratio, for the musician scene.

An increase in color gamut and log contrast ratios results in an increase in preference, as observed in Figure 4.23. Particularly for the dark room experiments, the increase in preference appears to be more pronounced, as well as have more obvious peaks in preference. The results from the coast scene illustrate similar effects to that of the musicians.

Figure 4.24 displays the preference in terms of interval scores, for the flower scene, as a function of the percentage of NTSC color gamut area and the four log contrast ratios.

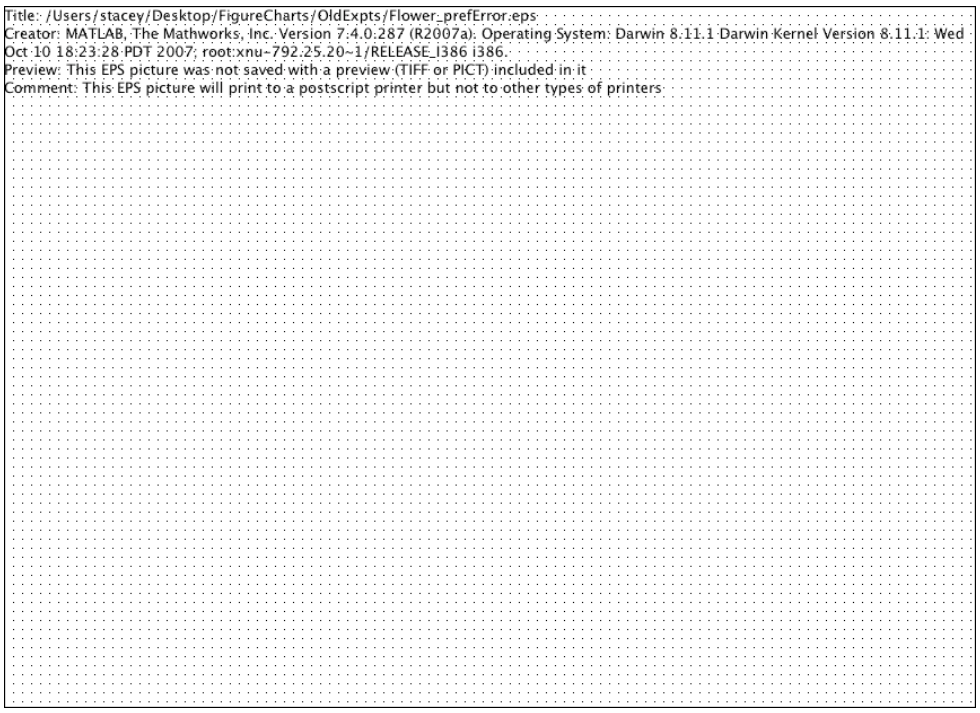

Figure 4.24. Preference interval scores, as a function of percentage NTSC color gamut area in xy chromaticities and log contrast ratios for the flower scene in both Experiments III and IIIb.

In Figure 4.24, the differentiation between log contrast ratios is not as clear as in Figure 4.22 for the musician scene. In addition, there appears to be a drop-off in preference for a higher percentage of NTSC color gamut area. This effect is more profound in Experiment IIIb.

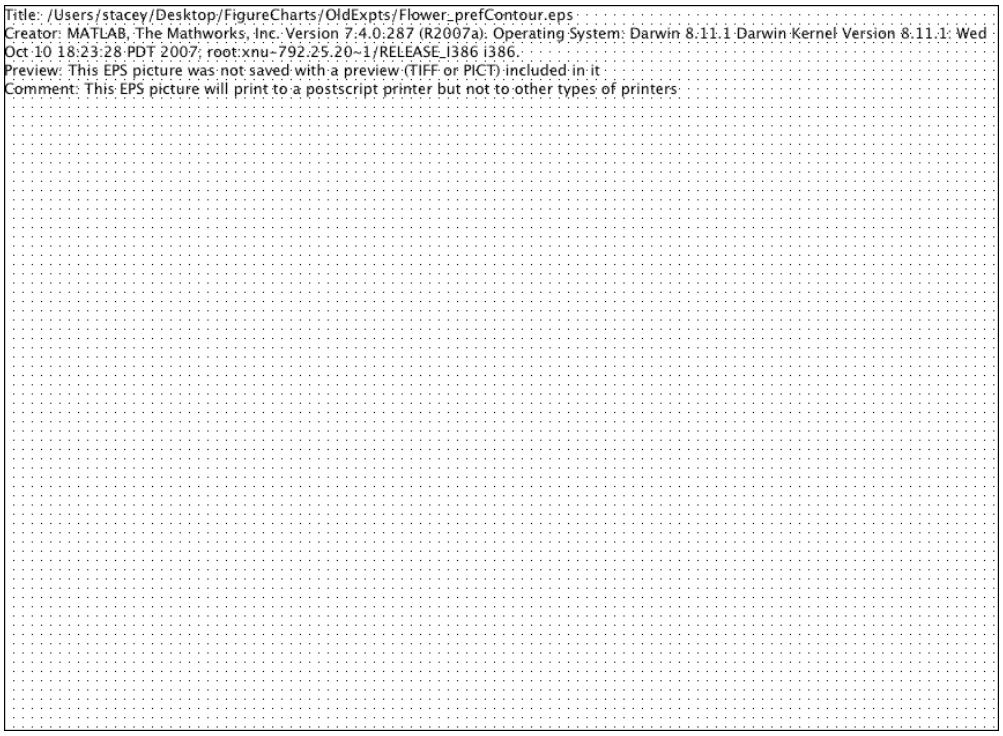

Figure 4.25: Fitted contours of equal preference interval scores as a function of percentage NTSC color gamut area in xy chromaticities and log contrast ratio, for the flower scene from Experiments III and IIIb.

The plots representing fitted contours, based on the multiple linear regression analysis, for each of the three scenes displayed similar results. In addition, similar effects to those mentioned above are observed in Figure 4.25 from the flower scene. There is a large range of interval scores correlating with the percentage of color gamut area. In addition, a few peaks are observed, as were discussed in Figure 4.24.

From Figures 4.23, 4.24 and 4.25, it is apparent that once again an optimal color gamut volume is obtained around 80 percent of the NTSC color gamut area, for the highest log contrast ratio. This suggests that similarly for Experiment IIIb, increases in lightness contrast are equally as significant as increases in color gamut volume. In addition, Experiment IIIb maintained notable preference peaks suggesting the dark room environment enables the observers to more easily choose which image they prefer. Because observers experience an increased sensitivity to differences in color and

lightness contrast in dark surround, this can translate to how feasibly the observers can decipher which image is more preferable.

Using the methodologies presented in the first technical report [Heckaman et al.; 2007] for Experiment III, the effects of color gamut volume and lightness contrast were evaluated over dark viewing conditions, on observer preference and perceived colorfulness and lightness contrast.

The results of Experiment IIIb correlated with those from Experiment III. In regards to colorfulness and lightness contrast, the results from each experiment were not significantly different. The effect of the dark surround on colorfulness was unknown, however, predictions had existed regarding lightness contrast. Although it was expected that lightness contrast would decrease in dark surround due to the Bartleson-Brennan Equations, this was not observed in the data for Experiment IIIb.

Colorfulness, however, was observed increasing monotonically with a larger color gamut volume, while lightness contrast linearly increased with gamut volume. Also, the Helmholtz-Kohlrausch effect was maintained for Experiment IIIb, given the contribution of color gamut volume is inherently related to the log contrast ratio.

In addition, while lightness contrast is an important contributor, colorfulness had an equally significant impact on preference. Both attributes were found to significantly influence observer preference, in regards to the three images evaluated. The results, while remaining consistent with Experiment III, suggest an optimal color gamut volume of approximately 80 percent of the NTSC color gamut area in xy chromaticities. This result is scene dependent, yet, again, consistent among all three scenes evaluated in Experiment IIIb.

Observer preference evaluated under dark surround suggest that observers more easily chose which version they preferred, as compared to completing the psychophysical experiment under ambient lighting conditions in Experiment III. The linear plots demonstrated that Experiment IIIb resulted in responses that "peaked" rather than smoothly transitioned. This indicates that the decision possibly was easier to make under dark room conditions because the observer was more sensitive to the color and lightness contrast differences in dark surround. However, since there were not dramatically different results between surround conditions, the experiments on gamut mapping algorithms were performed under dim surround. This enabled consistent procedures across experiments.

4.3 Methodology

The gamut mapping algorithm experiments were conducted at the Munsell Color Science Laboratory at Rochester Institute of Technology. There were two experiments, both performed under identical conditions in order to allow for a fair comparison between the two.

4.3.1. Viewing Conditions and Observations

There were twenty unique observers for each experiment, where the evaluation on each display represented an experiment. Although some observers participated in both experiments, this was not the case for everyone. The observers were both male and female, and ranged in age from 21 to 64. The observers ranged from non-experts to Imaging Scientists/Color Scientists, covering a diverse population, demographically and ethnically. The observers sat two meters from the display, which was placed in front of a

uniformly gray background, illuminated by two Buhlite 150 watt, diffuse studio lamps. Viewing flare was minimized as the only light source was placed behind the display. Using a Spectrascan PR650 Spectrophotometer, the illumination off the wall was measured to be 94cd/m^2 and at correlated color temperature of 3150˚K [Heckaman et al.; 2007]. The images were displayed on a uniform mid-gray background, separated by approximately 2˚ of visual angle. The experimental window is represented in Figure 4.26.

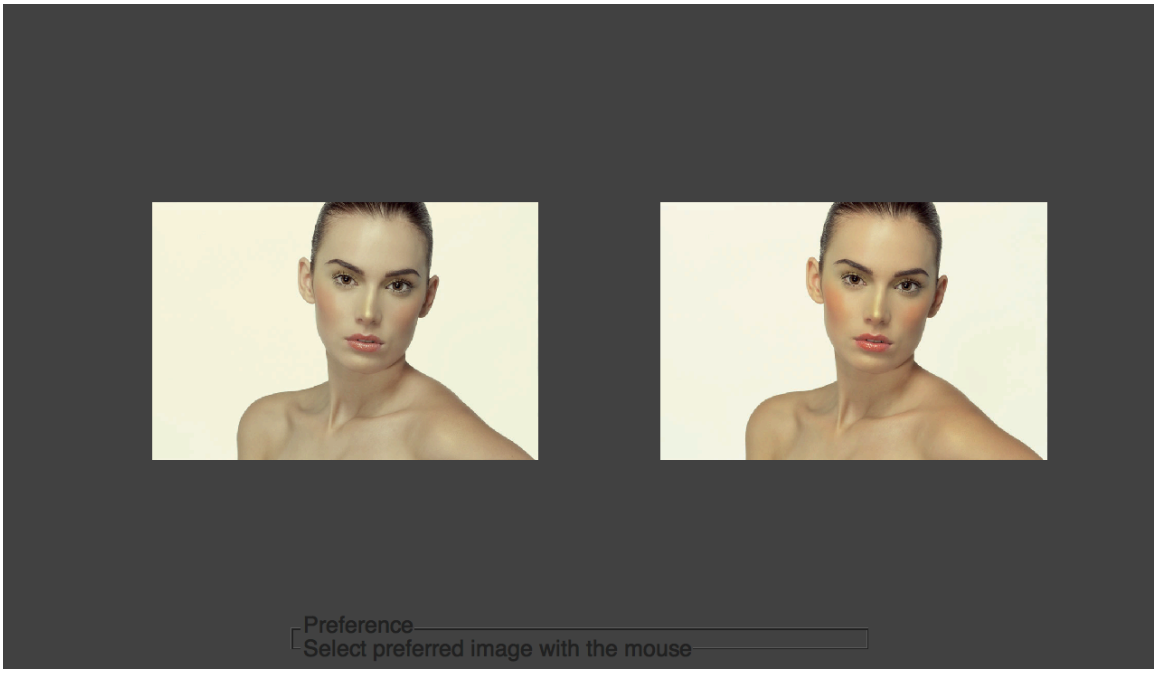

Figure 4.26. Experimental set-up for both displays.

The Sony display maintained 25˚ by 14˚ of visual angles, the Samsung maintained 32˚ by 22˚ visual angles; both were viewed perpendicularly.

4.3.2. Stimuli

There were ten standard scenes incorporated into the experiments, all of which were used in the experiments performed by Heckaman et al., 2007, and three of which were described previously for the viewing conditions experiment, Experiment IIIb. A range of scene content and complexity was achieved throughout the scenes.

There were two images selected for their flesh tone characteristics (Figures 4.27 and 4.28)

Figure 4.27. Lady image

Figure 4.28. Musician Scene

Figure 4.27 was incorporated into Experiment IIIb since it is largely comprised of flesh tones. Figure 4.28 also contains skin tones, however, in much smaller proportion compared to the remaining image attributes.

There were several images chosen for their natural content. Based on Fedorovskaya et al., naturalness appears to be a significant attribute responsible for guiding image preference. Therefore, incorporating scenes of natural context, and performing a cluster analysis on the results, will give a true indication of the significance of natural images in this evaluation.

Figure 4.29. Water image

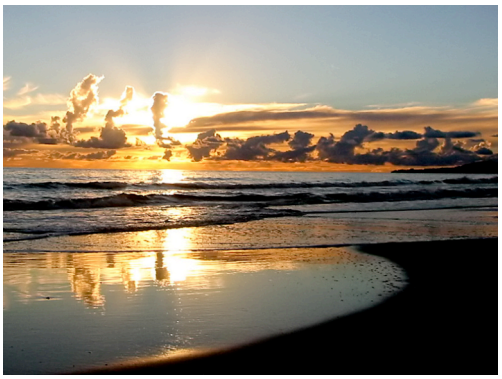

Figure 4.30. Coast scene

Figure 4.31. Fluorent Tetons image

In addition to natural context, however, the other attributes of Figure 4.30 and 4.31 were dually noted. The coast scene, Figure 4.30, was incorporated into the study both for its natural scene content, as well as its wide dynamic range. Given the mapping algorithms developed operated over a three-dimensional space, a variety of ranges of each attribute should be included in the scenes evaluated.

Similar to images with a wide range of lightness values, images were chosen for their high degree of colorfulness, or for their overall low saturation characteristics. Figure 4.31 was noted as a colorful image, however, not to the degree of the flower image.

Figure 4.32. Flower image

The flower image, Figure 4.32, was the most colorful image incorporated into the study. In addition, the barn image (Figure 4.33) and the pastel image (Figure 4.34) were also chosen for their color content.

Figure 4.33. Barn image

Figure 4.34. Pastel image

The fog image (Figure 4.35) represents the scene with the lowest overall saturation content. This scene served to aid in determining the algorithms' performance for low chroma values compared to the higher chromatic values prominent in the majority of the scenes.

Figure 4.35. Fog image

The last image was chosen based on its colorfulness in addition to it existing as the only target-type scene. The PW837_rgb image (Figure 4.36) represents varied red, green and blue values presented simultaneously as the target.

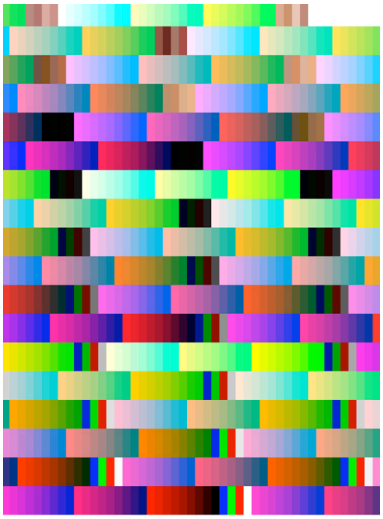

Figure 4.36. PW837_rgb

All of the scenes encompass a range of color and lightness attributes, across the full spectrum of hues, with varying scene content and complexity. The ten images

displayed above, were manipulated through a variety of GMAs and incorporated into both experiments using the characterization procedure above.

Overall, this research demonstrates the opportunity to display such highly colorful, largely dynamic images and the impact on observer preference. By improving the end-to-end color reproduction process (capturing, rendering and displaying the images) according to perceptual metrics, digital photography and television will both garner benefits.

4.4 Algorithms

In accordance with the purpose previously stated, multiple gamut expansion algorithms were evaluated in an effort to attain a single strategy that was statistically preferred over the other algorithms.

However, two baseline algorithms were incorporated into the evaluations, as suggested by Muijs et al., 2008, to ensure a specified mapping strategy was necessary. One baseline directly mapped the sRGB values to the display, bypassing the inherent expansion that occurs in the second baseline. In this manner, the original sRGB content is displayed correspondingly on the output device by accounting for the differences between display primaries. To obtain the digital counts necessary to properly display the sRGB image on the output device, the sRGB tristimulus values were calculated using the transformation matrix that converts digital counts to tristimulus values under sRGB conditions (Eqn. 4.7)

$$M_{sRGB} = \begin{bmatrix} 0.4124 & 0.3576 & 0.1805 \\ 0.2126 & 0.7152 & 0.0722 \\ 0.0193 & 0.1192 & 0.9505 \end{bmatrix} \quad (4.7)$$

Once the corresponding tristimulus values were calculated, the result was multiplied by the inverted output display (Eqns. 4.8 and 4.9) to obtain the digital counts that were sent to the display.

$$M_{Sony} = \begin{bmatrix} 147.524 & 43.019 & 37.382 \\ 61.729 & 152.744 & 21.633 \\ -0.190 & 23.235 & 219.957 \end{bmatrix}^{-1} \qquad (4.8)$$

$$M_{Samsung} = \begin{bmatrix} 51.528 & 15.803 & 17.948 \\ 23.967 & 59.217 & 5.910 \\ 0.714 & 9.194 & 105.571 \end{bmatrix}^{-1} \qquad (4.9)$$

The process is illustrated in Figure 4.37.

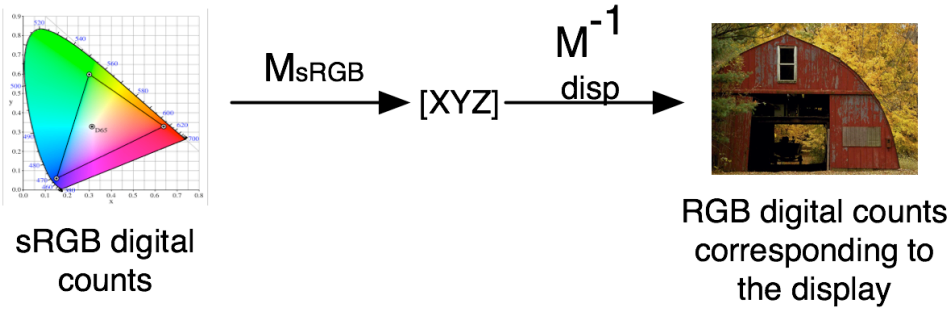

Figure 4.37 Flowchart converting digital counts under sRGB color space, to RGB digital counts corresponding to the display, representing the first baseline version.

Muijs et al., 2008, refer to this as a "true-color representation". To place emphasis on the baseline strategy, this method is referred to as "sRGB Original" throughout the remaining discussion.

The second baseline version, again described by Muijs et al., 2008, entailed directly mapping the digital counts under sRGB color space as though there were the digital counts corresponding to the display. Therefore, by sending the input digital counts directly to the output device (Figure 4.38), the counts are linearly stretched to fit

the destination display gamut, and thus, an inherent expansion of the data occurs. This baseline will be denoted, "sRGB Expanded" throughout this document.

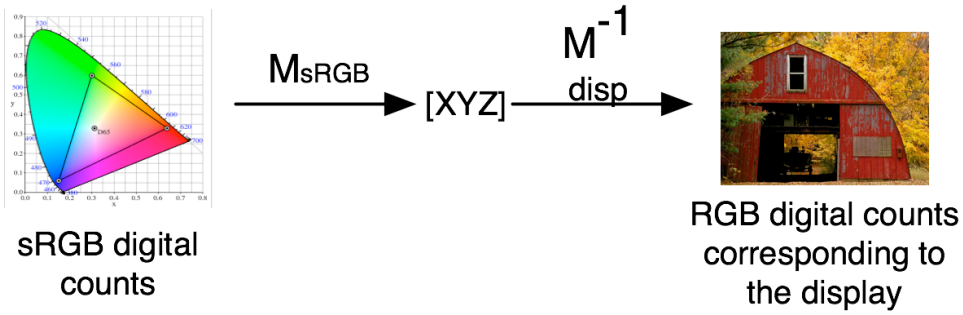

Figure 4.38. Flowchart representing the second baseline image, where the input digital counts were directly sent to the output device and displayed.

Although not as apparent on a standard gamut display, or as the output corresponding to the printer gamut, as it was on an extended gamut display, these two versions represent the extremes in terms of GEAs. Therefore, by setting the limits of gamut expansion algorithms, the preference ratings for the developed algorithms will be substantiated.

4.4.1. Background

Based on past research incorporating both linear and nonlinear algorithms into gamut expansion techniques, this evaluation implemented both linear and sigmoidal algorithms. The algorithms were performed in CIELAB, due to its ability to perform as a color appearance space, easy implementation, and widespread applicability [Montag and Fairchild 1996, Montag and Fairchild 1998, Kang et al. 2005, Hoshino 1994]. The mapping was applied to the lightness, chroma and hue dimensions of CIELAB's three-dimensional color space.

4.4.2. Linear Algorithms (LGEAs)

The general LGEA applied to the images was based on Eqn. 4.10, in terms of CIELAB values:

$$Lab_{out} = [1\ k_{a*}\ k_{b*}]*Lab_{in} \quad (4.10),$$

where k_a* and k_b* are equal. By multiplying a* and b* by the same scaling factor, hue was preserved. Therefore, this expansion did not result in undesireable hue shifts. Through Eqns. 4.11 and 4.12 the constant corresponding to the ratio between b* and a* was obtained and carried through the calculation of expanded a* and b* values to prevent hue shifts from occurring. Both equations,

$$k = \frac{b^*_{in}}{a^*_{in}}, or\ rearranging, {b^*_{in}}^2 = k^2 {a^*_{in}}^2 \quad (4.11), \text{ and}$$

$${C^*_{in}}^2 = {a^*_{in}}^2 + {b^*_{in}}^2, and, {C^*_{out}}^2 = {a^*_{out}}^2 + {b^*_{out}}^2 \quad (4.12),$$

are standard CIELAB equations.

When applying Eqn. 4.10 to multiple images, the scaling factor, k, was determined based on a ratio of the input gamut to the destination gamut, or based on the ratio of the output maximum chroma (Eqn. 4.12) to the input maximum chroma (Eqn. 4.12). Since it was not possible to measure the gamut of colors for the input or output devices, a 21x21x21 cube of red, green, and blue incremented digital counts was converted to CIELAB values, and from there, chroma and hue were calculated.

To avoid the effects of lightness and hue dependent maximum chromatic values, the ratio between the gamut boundary was calculated dependent upon the lightness and hue angle combination. For a series of ten lightness blocks, and seventy-two hue slices, each comprised of five degrees of hue angle, the corresponding maximum chroma was

obtained and used to form a LUT relating hue angle, lightness and maximum chroma. This type of algorithm was defined by Lee et al. as a parametric gamut-mapping algorithm [Lee et al. 2000], or an algorithm based on a user-defined parameter. For each hue slice, the maximum chroma was calculated for given ranges of lightness values. These data points were then linearly regressed to linearly relate chroma and lightness, and to exclude existing outliers that would later affect the results. This process was performed for both output displays (Figure 4.39). In this figure, the green data points represent the calculated maximum chroma values, and the red represent the theoretical maximum chroma at each lightness based on a linear regression between the achromatic axis and the overall maximum chromatic value.


Title: /Volumes/IOMEGA_HDD 2/SONYResearch/Strategies/MaxChromaFigures/combo_eps/hue0.eps
Creator: MATLAB, The Mathworks, Inc. Version 7.4.0.287 (R2007a). Operating System: Darwin 8.11.1 Darwin Kernel Version 8.11.1: Wed Oct 10 18:23:28 PDT 2007; root:xnu-792.25.20~1/RELEASE_I386 i386.
Preview: This EPS picture was not saved with a preview (TIFF or PICT) included in it
Comment: This EPS picture will print to a postscript printer but not to other types of printers
Title: /Volumes/IOMEGA_HDD 2/SONYResearch/Strategies/MaxChromaFigures/combo_eps/hue30.eps
Creator: MATLAB, The Mathworks, Inc. Version 7.4.0.287 (R2007a). Operating System: Darwin 8.11.1 Darwin Kernel Version 8.11.1: Wed Oct 10 18:23:28 PDT 2007; root:xnu-792.25.20~1/RELEASE_I386 i386.
Preview: This EPS picture was not saved with a preview (TIFF or PICT) included in it
Comment: This EPS picture will print to a postscript printer but not to other types of printers
Title: /Volumes/IOMEGA_HDD 2/SONYResearch/Strategies/MaxChromaFigures/combo_eps/hue60.eps
Creator: MATLAB, The Mathworks, Inc. Version 7.4.0.287 (R2007a). Operating System: Darwin 8.11.1 Darwin Kernel Version 8.11.1: Wed Oct 10 18:23:28 PDT 2007; root:xnu-792.25.20~1/RELEASE_I386 i386.
Preview: This EPS picture was not saved with a preview (TIFF or PICT) included in it
Comment: This EPS picture will print to a postscript printer but not to other types of printers
Title: /Volumes/IOMEGA_HDD 2/SONYResearch/Strategies/MaxChromaFigures/combo_eps/hue90.eps
Creator: MATLAB, The Mathworks, Inc. Version 7.4.0.287 (R2007a). Operating System: Darwin 8.11.1 Darwin Kernel Version 8.11.1: Wed Oct 10 18:23:28 PDT 2007; root:xnu-792.25.20~1/RELEASE_I386 i386.
Preview: This EPS picture was not saved with a preview (TIFF or PICT) included in it
Comment: This EPS picture will print to a postscript printer but not to other types of printers

Title: /Volumes/IOMEGA_HDD 2/SONYResearch/Strategies/MaxChromaFigures/combo_eps/hue120.eps
Creator: MATLAB, The Mathworks, Inc. Version 7.4.0.287 (R2007a). Operating System: Darwin 8.11.1 Darwin Kernel Version 8.11.1: Wed Oct 10 18:23:28 PDT 2007; root:xnu-792.25.20~1/RELEASE_I386 i386.
Preview: This EPS picture was not saved with a preview (TIFF or PICT) included in it
Comment: This EPS picture will print to a postscript printer but not to other types of printers

Title: /Volumes/IOMEGA_HDD 2/SONYResearch/Strategies/MaxChromaFigures/combo_eps/hue150.eps
Creator: MATLAB, The Mathworks, Inc. Version 7.4.0.287 (R2007a). Operating System: Darwin 8.11.1 Darwin Kernel Version 8.11.1: Wed Oct 10 18:23:28 PDT 2007; root:xnu-792.25.20~1/RELEASE_I386 i386.
Preview: This EPS picture was not saved with a preview (TIFF or PICT) included in it
Comment: This EPS picture will print to a postscript printer but not to other types of printers

Title: /Volumes/IOMEGA_HDD 2/SONYResearch/Strategies/MaxChromaFigures/combo_eps/hue180.eps
Creator: MATLAB, The Mathworks, Inc. Version 7.4.0.287 (R2007a). Operating System: Darwin 8.11.1 Darwin Kernel Version 8.11.1: Wed Oct 10 18:23:28 PDT 2007; root:xnu-792.25.20~1/RELEASE_I386 i386.
Preview: This EPS picture was not saved with a preview (TIFF or PICT) included in it
Comment: This EPS picture will print to a postscript printer but not to other types of printers

Title: /Volumes/IOMEGA_HDD 2/SONYResearch/Strategies/MaxChromaFigures/combo_eps/hue210.eps
Creator: MATLAB, The Mathworks, Inc. Version 7.4.0.287 (R2007a). Operating System: Darwin 8.11.1 Darwin Kernel Version 8.11.1: Wed Oct 10 18:23:28 PDT 2007; root:xnu-792.25.20~1/RELEASE_I386 i386.
Preview: This EPS picture was not saved with a preview (TIFF or PICT) included in it
Comment: This EPS picture will print to a postscript printer but not to other types of printers

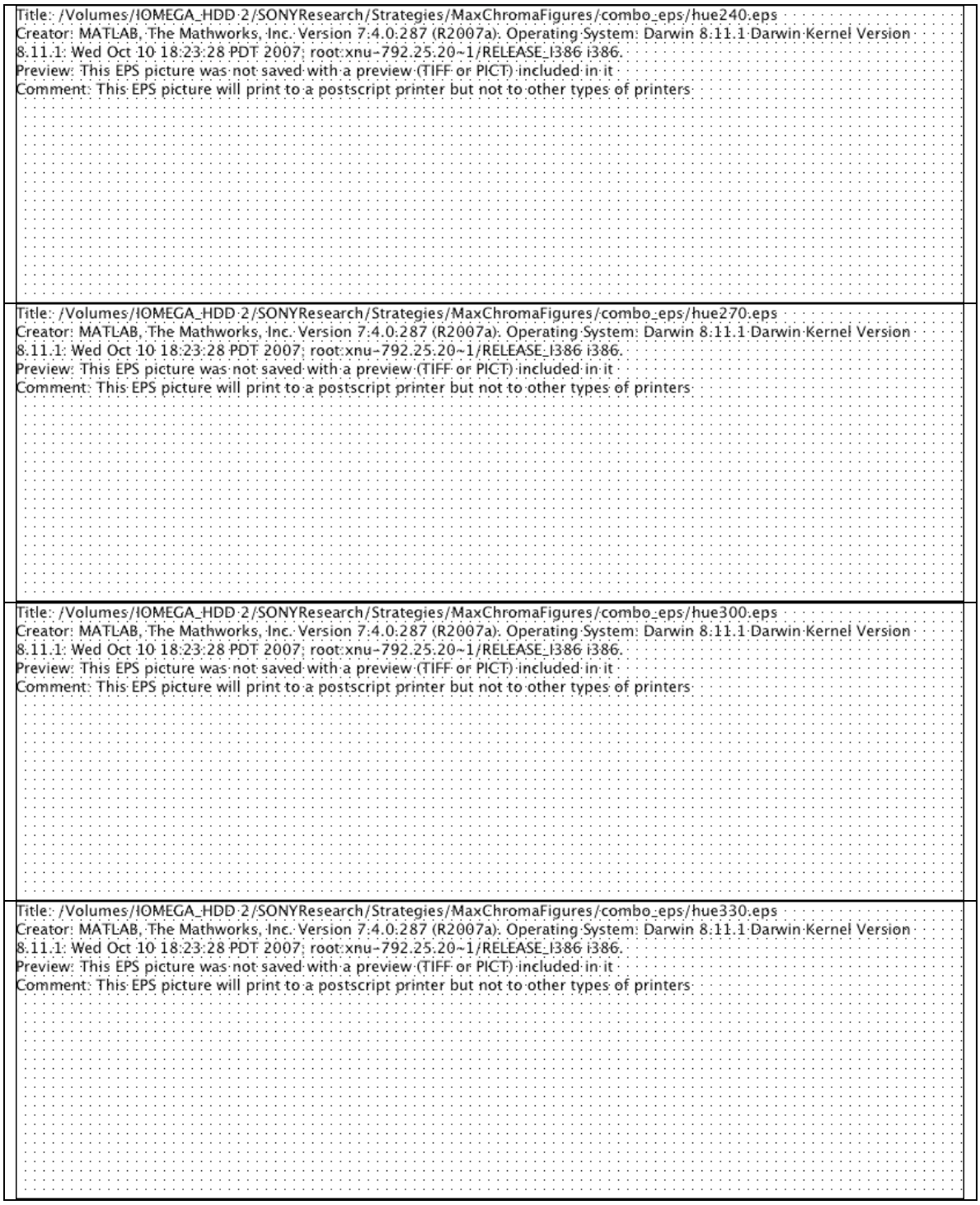

Figure 4.39. At multiple hue angles, the maximum chromatic values are computed for given lightness values for both the input (sRGB) gamut and destination (SONY and Samsung) gamuts.

Both destination gamuts are displayed in Figure 4.39; from left to right, sRGB, Sony and Samsung gamuts are represented, where the maximum chroma values for a given hue and lightness combination were calculated independently. Each plot within Figure 4.39 demonstrates the variability between devices, hue angles, and lightness values. Throughout the hue circle, however, both destination gamuts maintain higher maximum chroma points than sRGB does.

Using the linearly regressed data, a LUT was used to relate the three attributes of both gamuts, and hence, was used to establish the ratio between the two at every pixel of the image. This ratio defined the scaling factor used for each of the three LGEAs.

Three different scaling factors for each ratio, were incorporated into the chromatic extension. The distance between the ratio, at each hue, and the original image itself (or a value of one) was split into three equidistant sections, resulting in three extension constants for every pixel.

$$Ratio_i = \frac{C^*ab_{output,\max,i}}{C^*ab_{input,\max,i}} \qquad (4.13)$$

$$\left[SF1_i \quad SF2_i \quad SF3_i\right] = \left[\left(\frac{Ratio_i - 1}{3}\right) + 1 \quad \left(\frac{2(Ratio_i - 1)}{3}\right) + 1 \quad Ratio_i\right] \qquad (4.14)$$

The scaling factors (SF), at pixel i, were therefore, one-third, two-thirds and one times the calculated distance between the ratio of maximum chromatic values to the original input value (one). Equation 4.14 mathematically represents these constants.

An example is provided for clarity purposes.

$$Ratio_i = 1.2, \textit{therefore}$$
$$\left[SF1_i \quad SF2_i \quad SF3_i\right] = \left[\left(\frac{1.2 - 1}{3}\right) + 1 \quad \left(\frac{2(1.2 - 1)}{3}\right) + 1 \quad 1.2\right],$$
$$\textit{Thus, for pixel } i,$$
$$\left[SF1_i \quad SF2_i \quad SF3_i\right] = \left[1.067 \quad 1.133 \quad 1.2\right]$$

In the event that the maximum chroma of the output display was less than the corresponding maximum input chroma, all three scaling factors were constrained to one in order to prevent chromatic reduction from occurring at the applicable pixel.

Maintaining constant lightness, the chromatic values for each pixel of an image were expanded by each of the three scaling factors, totaling three unique LGEAs. The LGEAs are denoted LGEA1, LGEA2, LGEA3, where the numbers correspond to the degree of extension. LGEA1 represents the first scaling factor, or the most conservative extension. LGEA2 represents the second scaling factor, or two-thirds multiplied by the distance between the original and extended gamuts. LGEA3 corresponds to the most significant extension.

To demonstrate the various LGEAs, the same 21x21x21 cube of RGB digital counts was mapped according to these three LGEAs, and their corresponding transformations were plotted. Therefore, the number of data points for a given hue varies as the values were uniformly distributed in RGB digital counts. The transformations using the Sony display as the destination device are represented in Figure 4.40; the Samsung display transformations are in Figure 4.41.

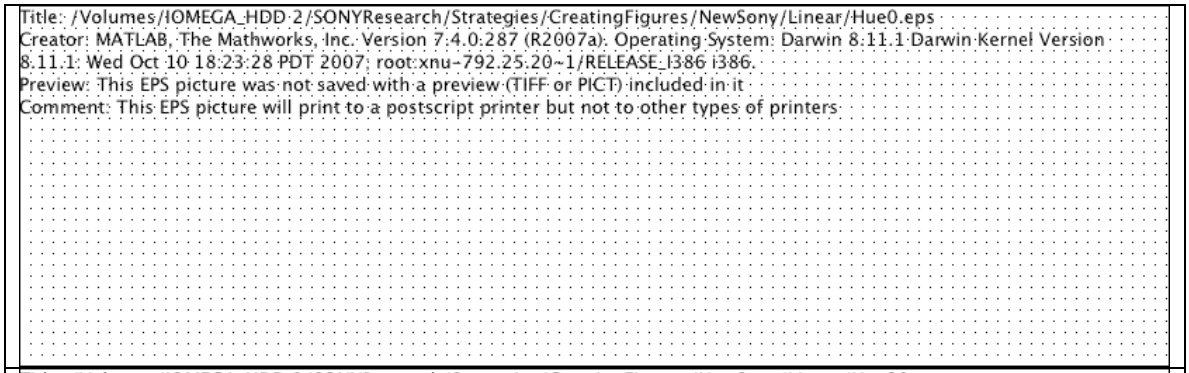
Title: /Volumes/IOMEGA_HDD 2/SONYResearch/Strategies/CreatingFigures/NewSony/Linear/Hue0.eps
Creator: MATLAB, The Mathworks, Inc. Version 7.4.0.287 (R2007a). Operating System: Darwin 8.11.1 Darwin Kernel Version 8.11.1: Wed Oct 10 18:23:28 PDT 2007; root:xnu-792.25.20~1/RELEASE_I386 i386.
Preview: This EPS picture was not saved with a preview (TIFF or PICT) included in it
Comment: This EPS picture will print to a postscript printer but not to other types of printers

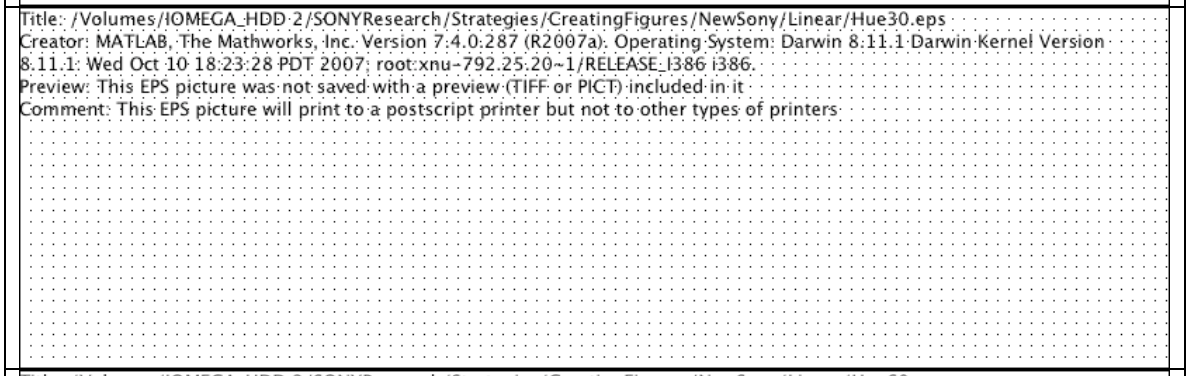
Title: /Volumes/IOMEGA_HDD 2/SONYResearch/Strategies/CreatingFigures/NewSony/Linear/Hue30.eps
Creator: MATLAB, The Mathworks, Inc. Version 7.4.0.287 (R2007a). Operating System: Darwin 8.11.1 Darwin Kernel Version 8.11.1: Wed Oct 10 18:23:28 PDT 2007; root:xnu-792.25.20~1/RELEASE_I386 i386.
Preview: This EPS picture was not saved with a preview (TIFF or PICT) included in it
Comment: This EPS picture will print to a postscript printer but not to other types of printers

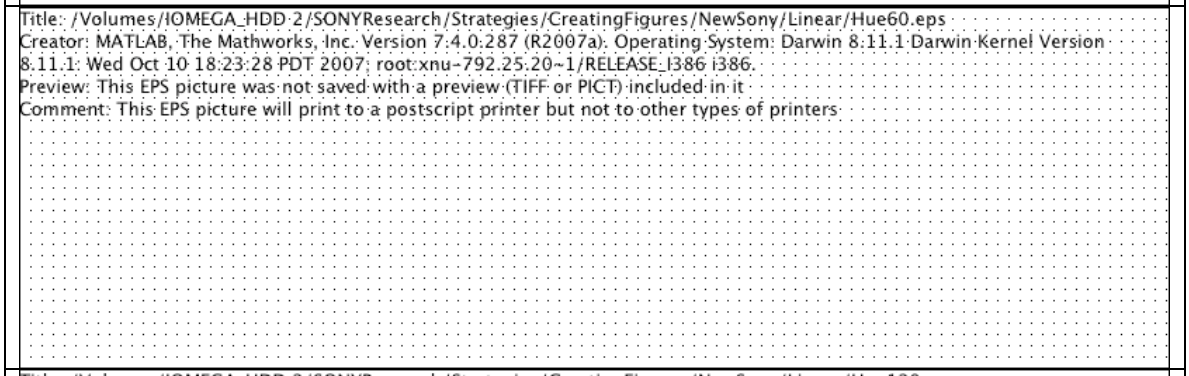
Title: /Volumes/IOMEGA_HDD 2/SONYResearch/Strategies/CreatingFigures/NewSony/Linear/Hue60.eps
Creator: MATLAB, The Mathworks, Inc. Version 7.4.0.287 (R2007a). Operating System: Darwin 8.11.1 Darwin Kernel Version 8.11.1: Wed Oct 10 18:23:28 PDT 2007; root:xnu-792.25.20~1/RELEASE_I386 i386.
Preview: This EPS picture was not saved with a preview (TIFF or PICT) included in it
Comment: This EPS picture will print to a postscript printer but not to other types of printers

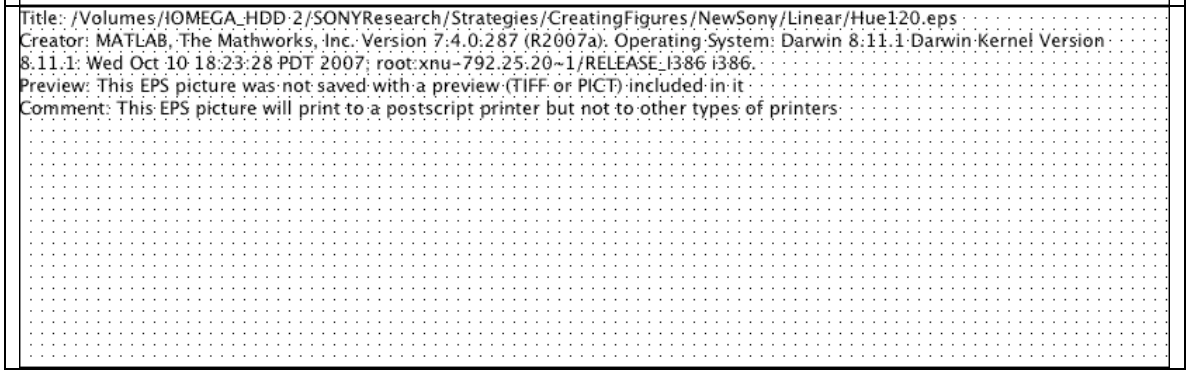
Title: /Volumes/IOMEGA_HDD 2/SONYResearch/Strategies/CreatingFigures/NewSony/Linear/Hue120.eps
Creator: MATLAB, The Mathworks, Inc. Version 7.4.0.287 (R2007a). Operating System: Darwin 8.11.1 Darwin Kernel Version 8.11.1: Wed Oct 10 18:23:28 PDT 2007; root:xnu-792.25.20~1/RELEASE_I386 i386.
Preview: This EPS picture was not saved with a preview (TIFF or PICT) included in it
Comment: This EPS picture will print to a postscript printer but not to other types of printers

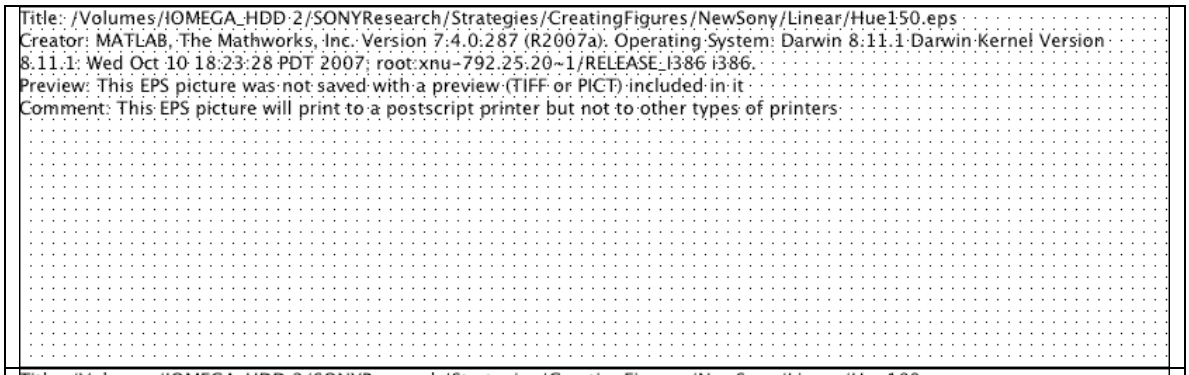
Title: /Volumes/IOMEGA_HDD 2/SONYResearch/Strategies/CreatingFigures/NewSony/Linear/Hue150.eps
Creator: MATLAB, The Mathworks, Inc. Version 7.4.0.287 (R2007a). Operating System: Darwin 8.11.1 Darwin Kernel Version 8.11.1: Wed Oct 10 18:23:28 PDT 2007; root:xnu-792.25.20~1/RELEASE_I386 i386.
Preview: This EPS picture was not saved with a preview (TIFF or PICT) included in it
Comment: This EPS picture will print to a postscript printer but not to other types of printers

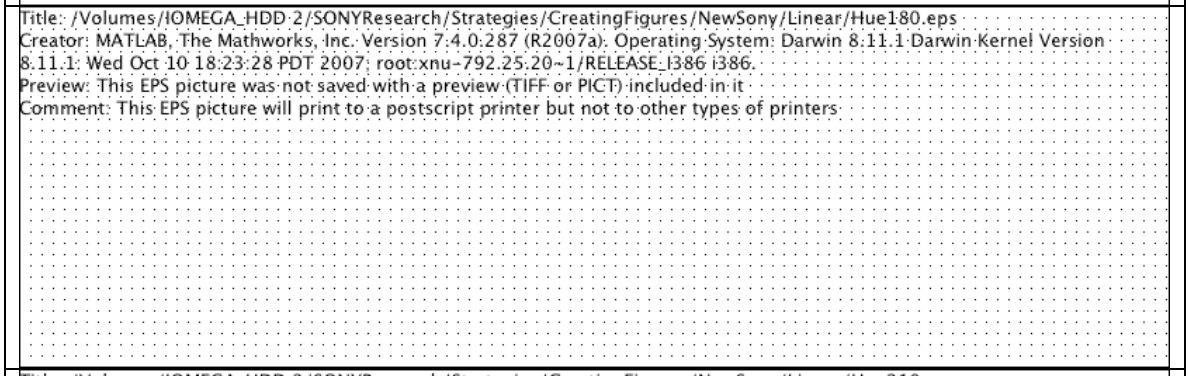
Title: /Volumes/IOMEGA_HDD 2/SONYResearch/Strategies/CreatingFigures/NewSony/Linear/Hue180.eps
Creator: MATLAB, The Mathworks, Inc. Version 7.4.0.287 (R2007a). Operating System: Darwin 8.11.1 Darwin Kernel Version 8.11.1: Wed Oct 10 18:23:28 PDT 2007; root:xnu-792.25.20~1/RELEASE_I386 i386.
Preview: This EPS picture was not saved with a preview (TIFF or PICT) included in it
Comment: This EPS picture will print to a postscript printer but not to other types of printers

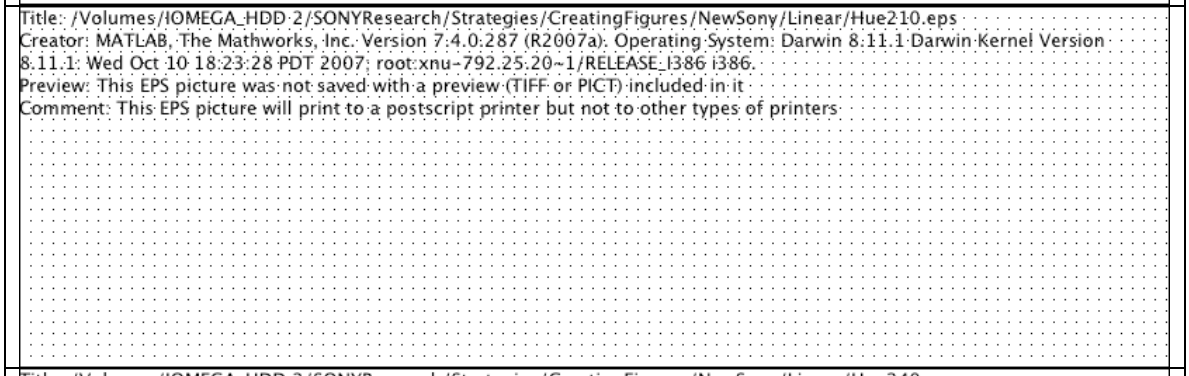
Title: /Volumes/IOMEGA_HDD 2/SONYResearch/Strategies/CreatingFigures/NewSony/Linear/Hue210.eps
Creator: MATLAB, The Mathworks, Inc. Version 7.4.0.287 (R2007a). Operating System: Darwin 8.11.1 Darwin Kernel Version 8.11.1: Wed Oct 10 18:23:28 PDT 2007; root:xnu-792.25.20~1/RELEASE_I386 i386.
Preview: This EPS picture was not saved with a preview (TIFF or PICT) included in it
Comment: This EPS picture will print to a postscript printer but not to other types of printers

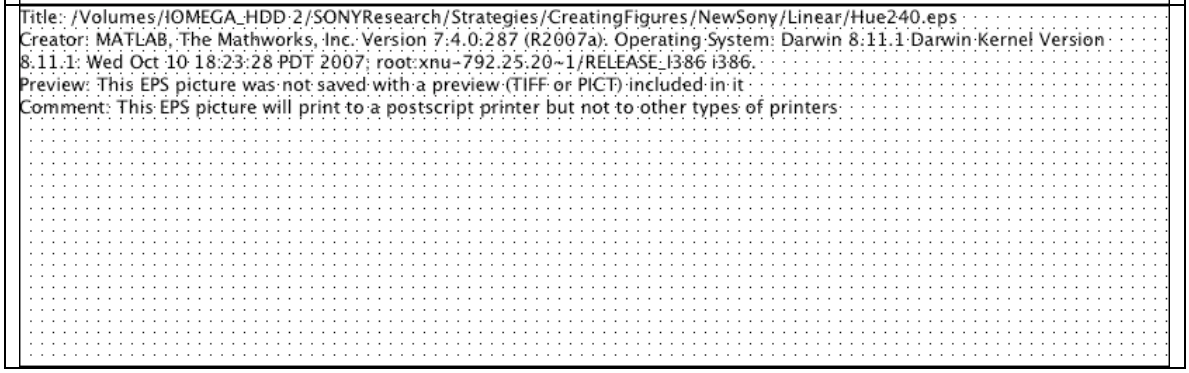
Title: /Volumes/IOMEGA_HDD 2/SONYResearch/Strategies/CreatingFigures/NewSony/Linear/Hue240.eps
Creator: MATLAB, The Mathworks, Inc. Version 7.4.0.287 (R2007a). Operating System: Darwin 8.11.1 Darwin Kernel Version 8.11.1: Wed Oct 10 18:23:28 PDT 2007; root:xnu-792.25.20~1/RELEASE_I386 i386.
Preview: This EPS picture was not saved with a preview (TIFF or PICT) included in it
Comment: This EPS picture will print to a postscript printer but not to other types of printers

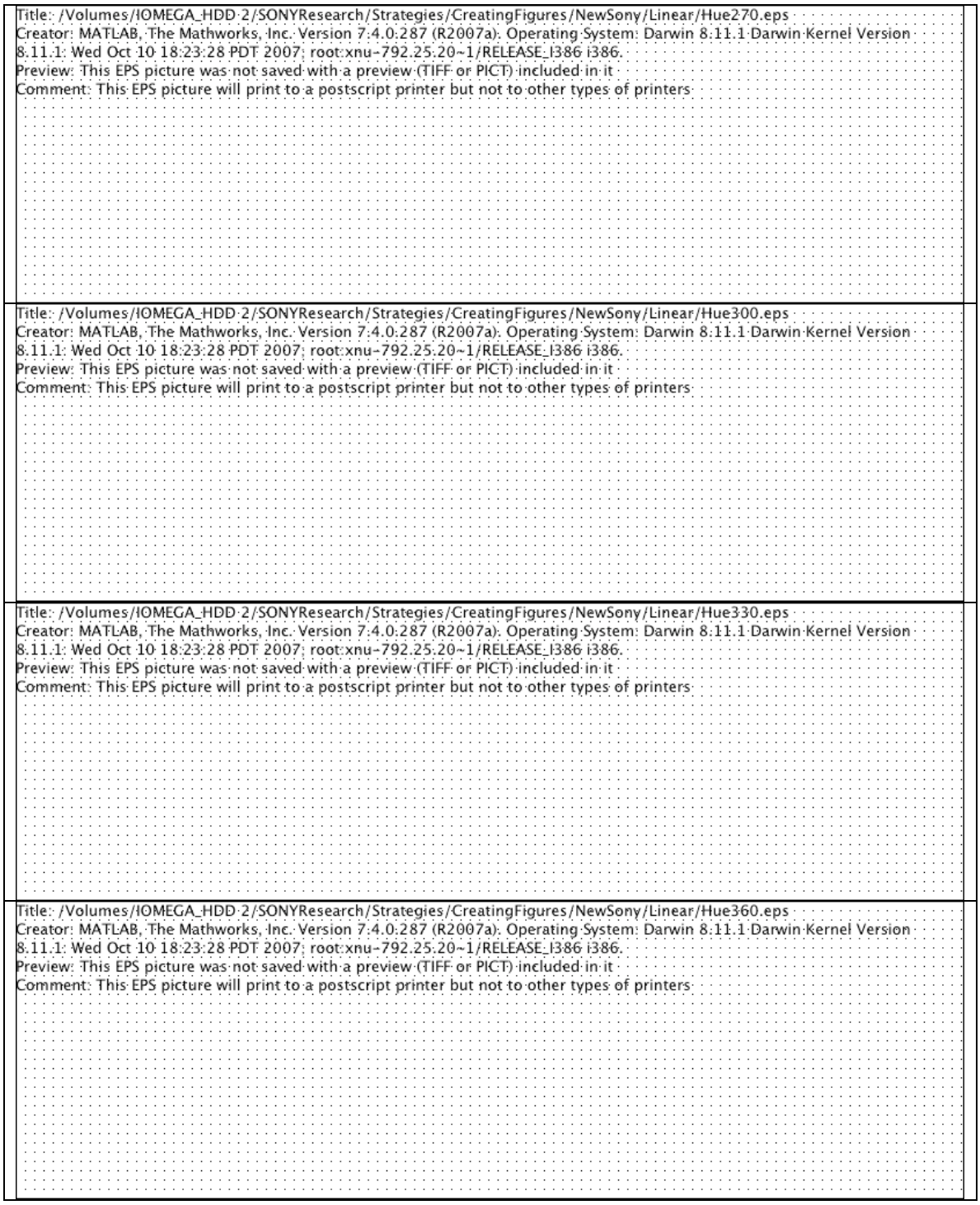

Figure 4.40. The transformations of all three LGEAs for the Sony display at various hue angles. The lines extend from sRGB chroma values to expanded chroma. Note: the color of the data corresponds to the appropriate hue angle.


Title: /Volumes/IOMEGA_HDD 2/SONYResearch/Strategiesw1DLUT/CreatingFigures/NewSamsung/Linear/Hue0.eps
Creator: MATLAB, The Mathworks, Inc. Version 7.4.0.287 (R2007a). Operating System: Darwin 8.11.1 Darwin Kernel Version 8.11.1: Wed Oct 10 18:23:28 PDT 2007; root:xnu-792.25.20~1/RELEASE_I386 i386.
Preview: This EPS picture was not saved with a preview (TIFF or PICT) included in it
Comment: This EPS picture will print to a postscript printer but not to other types of printers
Title: /Volumes/IOMEGA_HDD 2/SONYResearch/Strategiesw1DLUT/CreatingFigures/NewSamsung/Linear/Hue30.eps
Creator: MATLAB, The Mathworks, Inc. Version 7.4.0.287 (R2007a). Operating System: Darwin 8.11.1 Darwin Kernel Version 8.11.1: Wed Oct 10 18:23:28 PDT 2007; root:xnu-792.25.20~1/RELEASE_I386 i386.
Preview: This EPS picture was not saved with a preview (TIFF or PICT) included in it
Comment: This EPS picture will print to a postscript printer but not to other types of printers
Title: /Volumes/IOMEGA_HDD 2/SONYResearch/Strategiesw1DLUT/CreatingFigures/NewSamsung/Linear/Hue60.eps
Creator: MATLAB, The Mathworks, Inc. Version 7.4.0.287 (R2007a). Operating System: Darwin 8.11.1 Darwin Kernel Version 8.11.1: Wed Oct 10 18:23:28 PDT 2007; root:xnu-792.25.20~1/RELEASE_I386 i386.
Preview: This EPS picture was not saved with a preview (TIFF or PICT) included in it
Comment: This EPS picture will print to a postscript printer but not to other types of printers
Title: /Volumes/IOMEGA_HDD 2/SONYResearch/Strategiesw1DLUT/CreatingFigures/NewSamsung/Linear/Hue90.eps
Creator: MATLAB, The Mathworks, Inc. Version 7.4.0.287 (R2007a). Operating System: Darwin 8.11.1 Darwin Kernel Version 8.11.1: Wed Oct 10 18:23:28 PDT 2007; root:xnu-792.25.20~1/RELEASE_I386 i386.
Preview: This EPS picture was not saved with a preview (TIFF or PICT) included in it
Comment: This EPS picture will print to a postscript printer but not to other types of printers

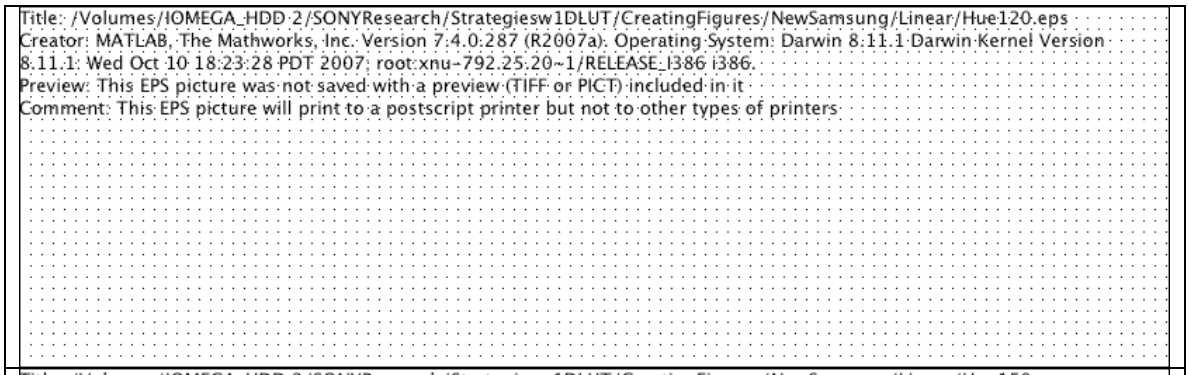
Title: /Volumes/IOMEGA_HDD 2/SONYResearch/Strategiesw1DLUT/CreatingFigures/NewSamsung/Linear/Hue120.eps
Creator: MATLAB, The Mathworks, Inc. Version 7.4.0.287 (R2007a). Operating System: Darwin 8.11.1 Darwin Kernel Version 8.11.1: Wed Oct 10 18:23:28 PDT 2007; root:xnu-792.25.20~1/RELEASE_I386 i386.
Preview: This EPS picture was not saved with a preview (TIFF or PICT) included in it
Comment: This EPS picture will print to a postscript printer but not to other types of printers

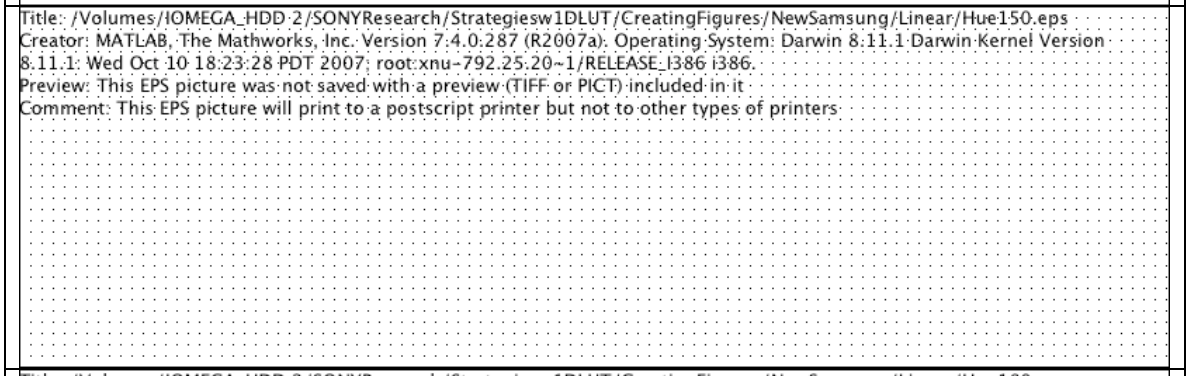
Title: /Volumes/IOMEGA_HDD 2/SONYResearch/Strategiesw1DLUT/CreatingFigures/NewSamsung/Linear/Hue150.eps
Creator: MATLAB, The Mathworks, Inc. Version 7.4.0.287 (R2007a). Operating System: Darwin 8.11.1 Darwin Kernel Version 8.11.1: Wed Oct 10 18:23:28 PDT 2007; root:xnu-792.25.20~1/RELEASE_I386 i386.
Preview: This EPS picture was not saved with a preview (TIFF or PICT) included in it
Comment: This EPS picture will print to a postscript printer but not to other types of printers

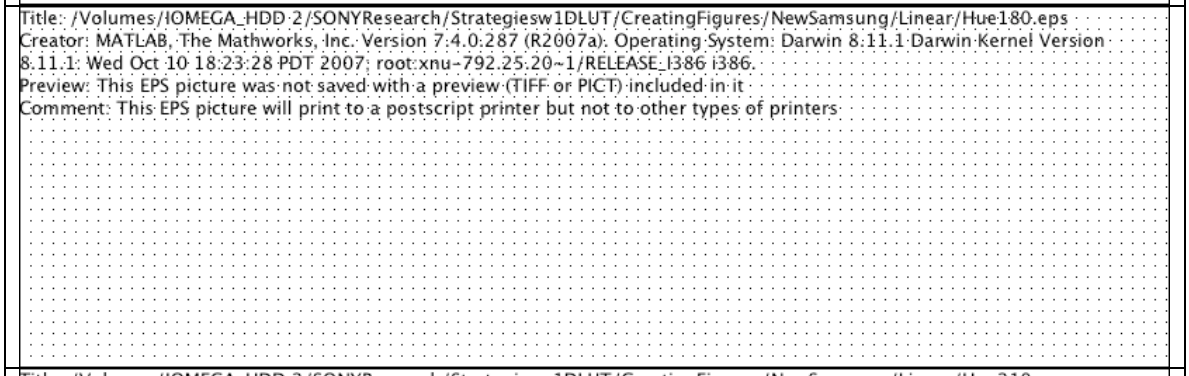
Title: /Volumes/IOMEGA_HDD 2/SONYResearch/Strategiesw1DLUT/CreatingFigures/NewSamsung/Linear/Hue180.eps
Creator: MATLAB, The Mathworks, Inc. Version 7.4.0.287 (R2007a). Operating System: Darwin 8.11.1 Darwin Kernel Version 8.11.1: Wed Oct 10 18:23:28 PDT 2007; root:xnu-792.25.20~1/RELEASE_I386 i386.
Preview: This EPS picture was not saved with a preview (TIFF or PICT) included in it
Comment: This EPS picture will print to a postscript printer but not to other types of printers

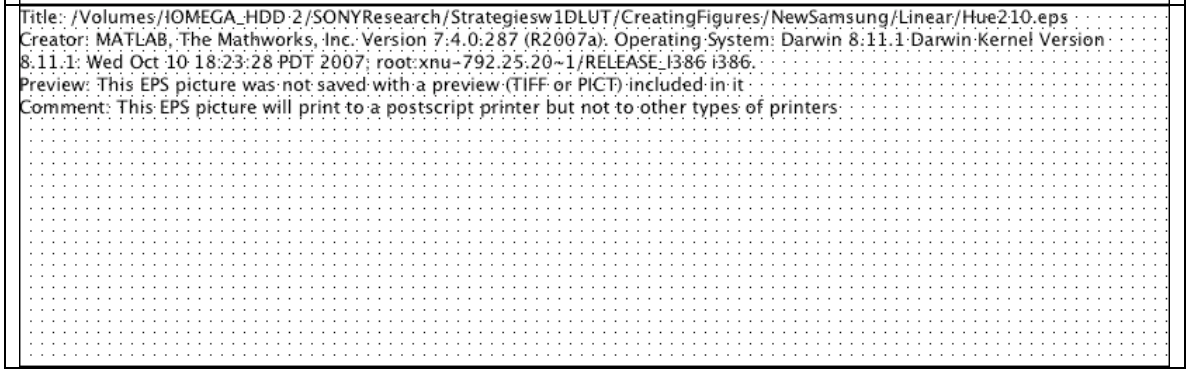
Title: /Volumes/IOMEGA_HDD 2/SONYResearch/Strategiesw1DLUT/CreatingFigures/NewSamsung/Linear/Hue210.eps
Creator: MATLAB, The Mathworks, Inc. Version 7.4.0.287 (R2007a). Operating System: Darwin 8.11.1 Darwin Kernel Version 8.11.1: Wed Oct 10 18:23:28 PDT 2007; root:xnu-792.25.20~1/RELEASE_I386 i386.
Preview: This EPS picture was not saved with a preview (TIFF or PICT) included in it
Comment: This EPS picture will print to a postscript printer but not to other types of printers

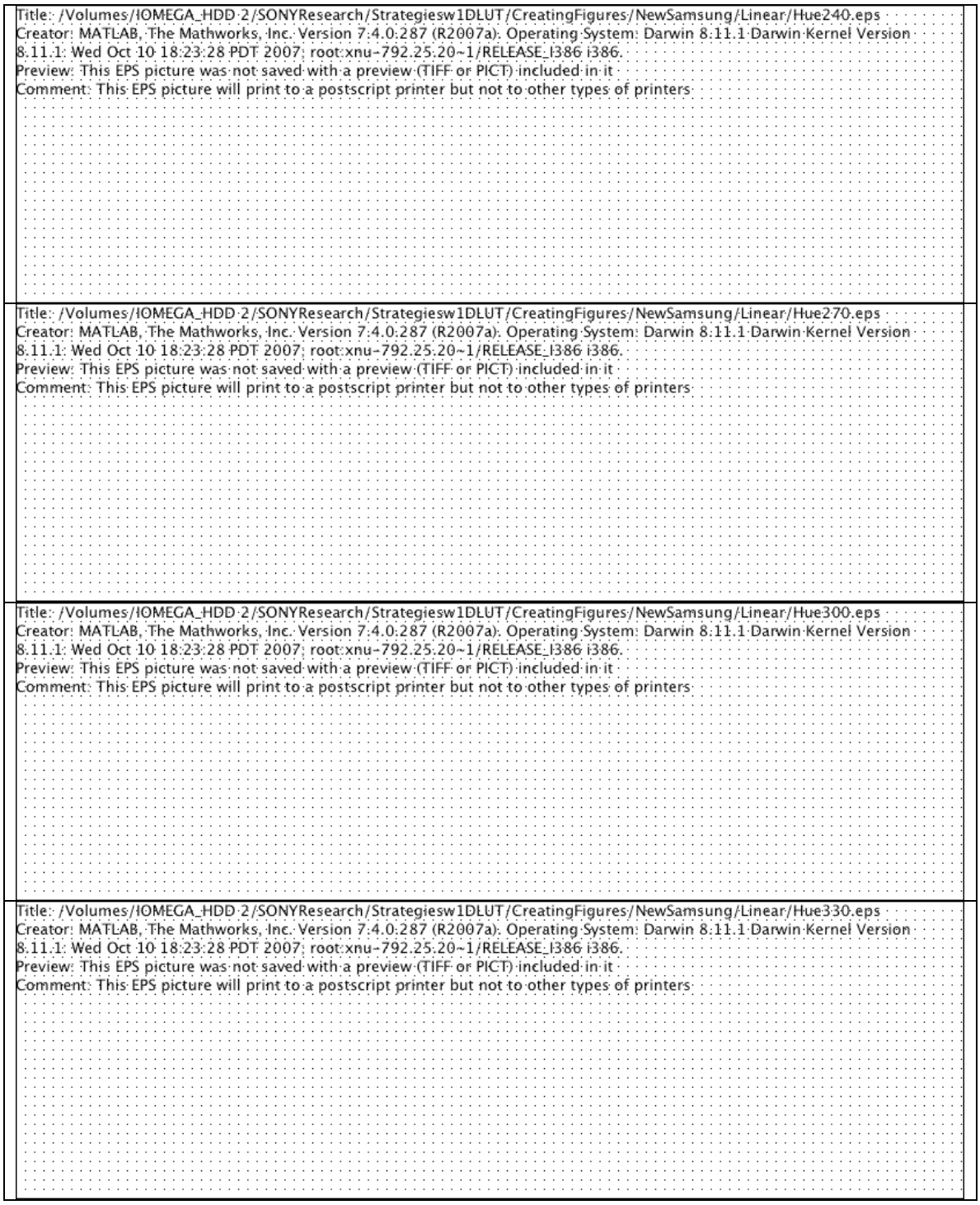

Figure 4.41. The transformations of all three LGEAs for the Samsung display at various hue angles. The lines extend from sRGB chroma values to expanded chroma. Note: the color of the data corresponds to the appropriate hue angle.

The effects of the three scaling factors, where LGEA1, 2 and 3, are each comprised of the corresponding scaling factor, are apparent in both Figures 4.40 and 4.41. The most left plot, LGEA1, represents the lowest expansion and the most right plot, LGEA3, represents the greatest expansion. Again, the transformation heavily depends on both the device, hue angle and lightness value.

The differences between the sRGB gamut and destination gamut govern the degree of extension possible. For both destination displays, hue angles corresponding to approximately 60˚ through 120˚ display very little extension. This is a result of the gamut shapes for both input and output devices, in that, the output devices are not significantly larger than the input, for this range in hue. Therefore, very little extension occurs in these areas. This will become particularly important for the nonlinear mapping algorithms.

After the transformations, the expanded chroma value is converted back to a*,b* via Eqns. 4.15 through 4.18. Rearranging Eqns. 4.15 and 4.16, output chroma was calculated in terms of a*.

$$C^*_{out}{}^2 = a^*_{out}{}^2 + k^2 a^*_{out}{}^2 \quad (4.15).$$

By rearranging Eqn. 5.10, output a* values were obtained.

$$a^*_{out}{}^2 = \frac{C^*_{out}{}^2}{1+k^2} \qquad (4.16)$$

The same process can be repeated, solving for chroma in terms of b*.

$$C^*_{out}{}^2 = \frac{b^*_{out}{}^2}{k^2} + b^*_{out}{}^2 \qquad (4.17),$$

and again, rearranging results in b* output values.

$$b^{*}_{out}{}^{2} = \frac{C^{*}_{out}{}^{2}}{\left(\frac{1}{k^{2}} + 1\right)} \qquad (4.18)$$

Maintaining lightness, L* is combined with the calculated a*, b* from Eqns. 4.16 and 4.18 respectively, where these expanded CIELAB values were then converted to display digital counts using the inverse transformation matrix, and incorporated into the psychophysical experiments.

4.4.3. Sigmoidal (Nonlinear) Algorithms (SGEAs)

In addition to linearly expanding the chrominance of multiple scenes, a sigmoidal transfer function was incorporated into the mapping strategies, as an attempt to minimize any negative results of the linear expansion (expanding near neutrals more than observers deem pleasing). It has been found that colors of low chroma should not necessarily be manipulated as those of high chroma [MacDonald et al.; 2001]. As mentioned previously, MacDonald et al. depict the values of low chroma as a core gamut, in that within the core gamut a one-to-one mapping exists but outside of that core, expansion will occur in accordance to the sigmoidal transfer function at hand.

The sigmoidal transfer functions incorporated into this study were based on the cumulative normal distribution [Braun and Fairchild, 1999]

$$S = \frac{1}{\sigma\sqrt{2\pi}} \int_{-\infty}^{x} e^{\frac{-(t-u)^{2}}{2\sigma^{2}}} dt \qquad (4.19)$$

Eqn. 4.19 represents the general equation form, where only the positive values of the function were incorporated into the study.

The chromatic expansion for the SGEA required once again, linearly interpolating the maximum chromatic input and output data at each hue slice, for given lightness values, at each pixel in the image. After obtaining the maximum chroma values for every pixel,

three cumulative normal distributions (Figure 4.42) of varying standard deviations (Table 4.2) were applied to the data to form the sigmoidal transfer functions.

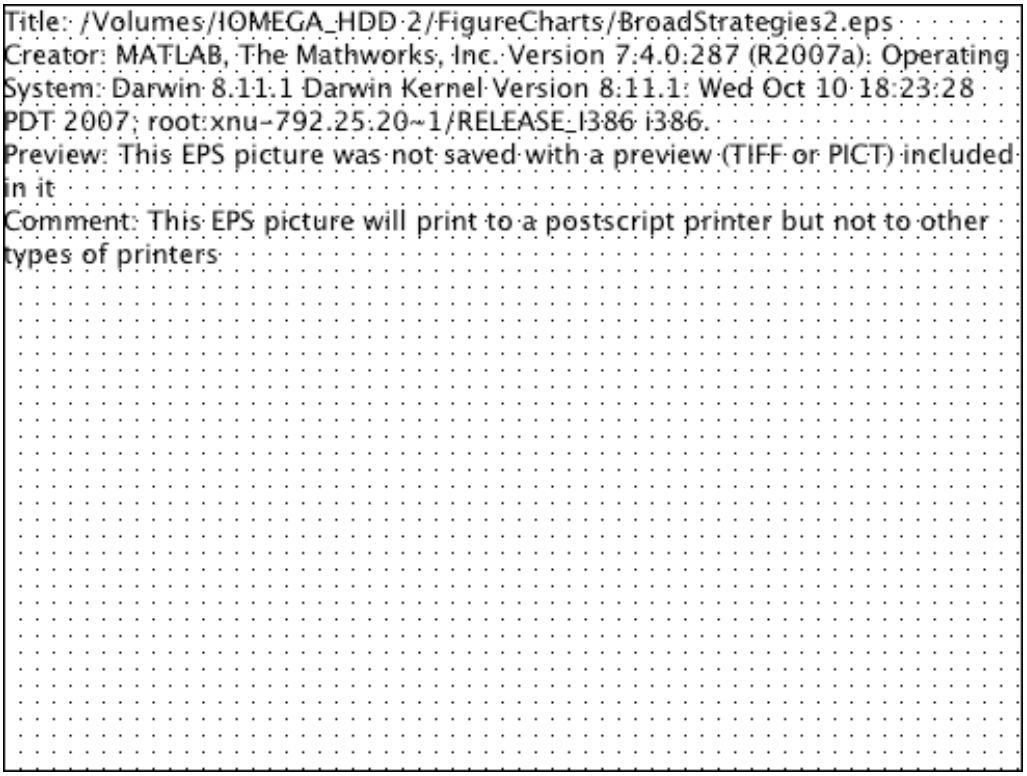

Figure 4.42. The three sigmoidal curves applied to this study are based on Eqn. 4.11. The red curve represents SGEA1, the blue curve represents SGEA2 and the cyan curve represents the third SGEA.

Table 4.1. Curve characteristics of the sigmoidal functions represented in Figure 4.42.

Algorithm	Corresponding to Curve (Fig4.15)	Mean	Std Dev	Over Interval
SGEA1	Red	0	1.5	[0:3]
SGEA2	Blue	0	1.6	[0:3]
SGEA3	Cyan	0	1.5	[0:2]
		0	1.2	[2:3]

As stated in Table 4.1, the red and blue curves are unique functions, whereas the cyan curve is a combination of two sigmoidal functions. This combination results in a steeper expansion at lower input chromas. After applying these three curves to the input sRGB digital counts, the resulting chromatic expansions corresponding to both the Sony and

Samsung displays, at multiple hue angles, are represented in Figures 4.43 and 4.44, respectively.

The plots within Figures 4.43 and 4.44 demonstrate the closeness between the three sigmoidal algorithms. In addition, the resulting transformations depended on the hue and lightness. Any variation among plots was a factor of the dependent attributes, the devices, as well as the specific SGEA applied.

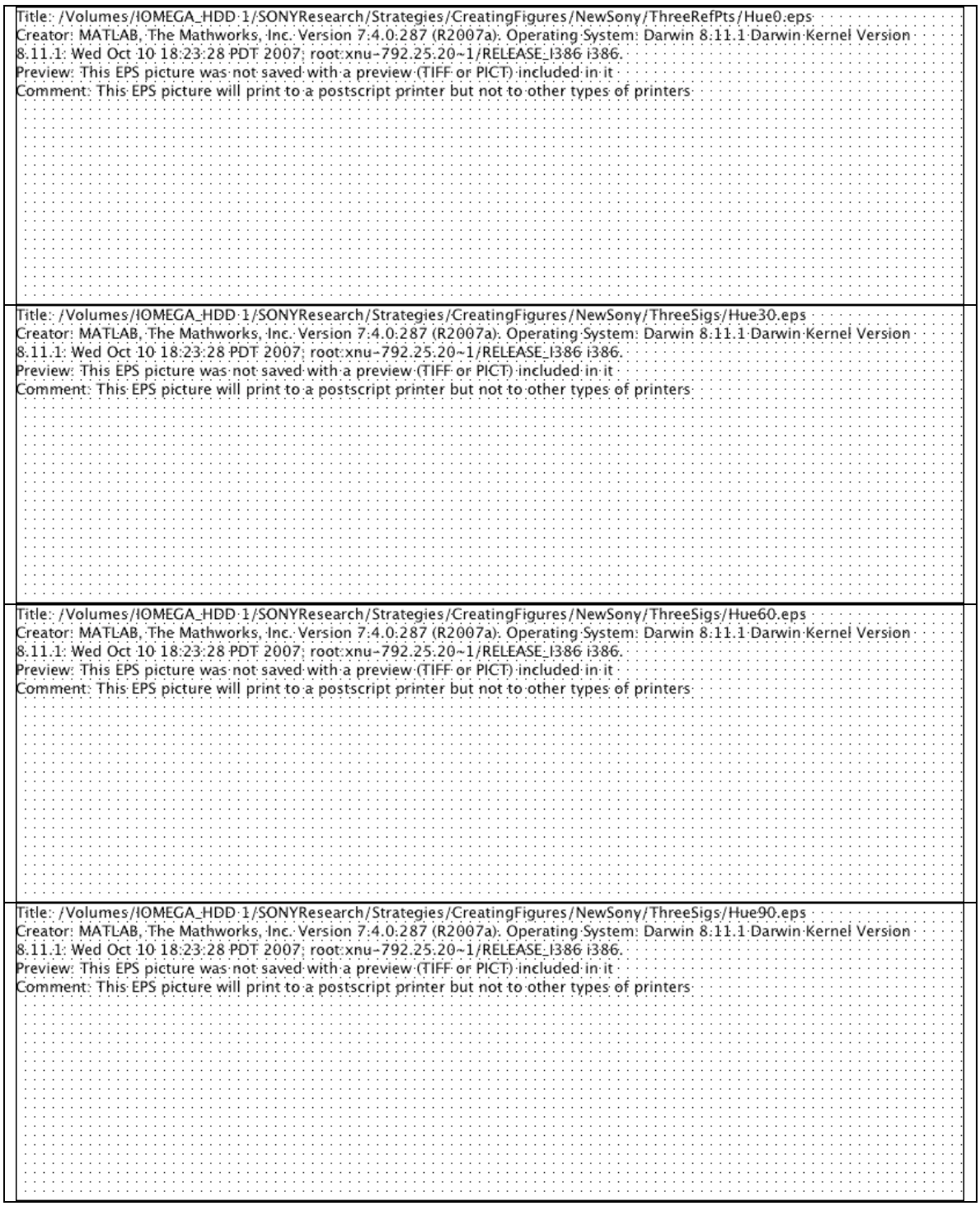
Title: /Volumes/IOMEGA_HDD 1/SONYResearch/Strategies/CreatingFigures/NewSony/ThreeRefPts/Hue0.eps
Creator: MATLAB, The Mathworks, Inc. Version 7.4.0.287 (R2007a). Operating System: Darwin 8.11.1 Darwin Kernel Version 8.11.1: Wed Oct 10 18:23:28 PDT 2007; root:xnu-792.25.20~1/RELEASE_I386 i386.
Preview: This EPS picture was not saved with a preview (TIFF or PICT) included in it
Comment: This EPS picture will print to a postscript printer but not to other types of printers
Title: /Volumes/IOMEGA_HDD 1/SONYResearch/Strategies/CreatingFigures/NewSony/ThreeSigs/Hue30.eps
Creator: MATLAB, The Mathworks, Inc. Version 7.4.0.287 (R2007a). Operating System: Darwin 8.11.1 Darwin Kernel Version 8.11.1: Wed Oct 10 18:23:28 PDT 2007; root:xnu-792.25.20~1/RELEASE_I386 i386.
Preview: This EPS picture was not saved with a preview (TIFF or PICT) included in it
Comment: This EPS picture will print to a postscript printer but not to other types of printers
Title: /Volumes/IOMEGA_HDD 1/SONYResearch/Strategies/CreatingFigures/NewSony/ThreeSigs/Hue60.eps
Creator: MATLAB, The Mathworks, Inc. Version 7.4.0.287 (R2007a). Operating System: Darwin 8.11.1 Darwin Kernel Version 8.11.1: Wed Oct 10 18:23:28 PDT 2007; root:xnu-792.25.20~1/RELEASE_I386 i386.
Preview: This EPS picture was not saved with a preview (TIFF or PICT) included in it
Comment: This EPS picture will print to a postscript printer but not to other types of printers
Title: /Volumes/IOMEGA_HDD 1/SONYResearch/Strategies/CreatingFigures/NewSony/ThreeSigs/Hue90.eps
Creator: MATLAB, The Mathworks, Inc. Version 7.4.0.287 (R2007a). Operating System: Darwin 8.11.1 Darwin Kernel Version 8.11.1: Wed Oct 10 18:23:28 PDT 2007; root:xnu-792.25.20~1/RELEASE_I386 i386.
Preview: This EPS picture was not saved with a preview (TIFF or PICT) included in it
Comment: This EPS picture will print to a postscript printer but not to other types of printers

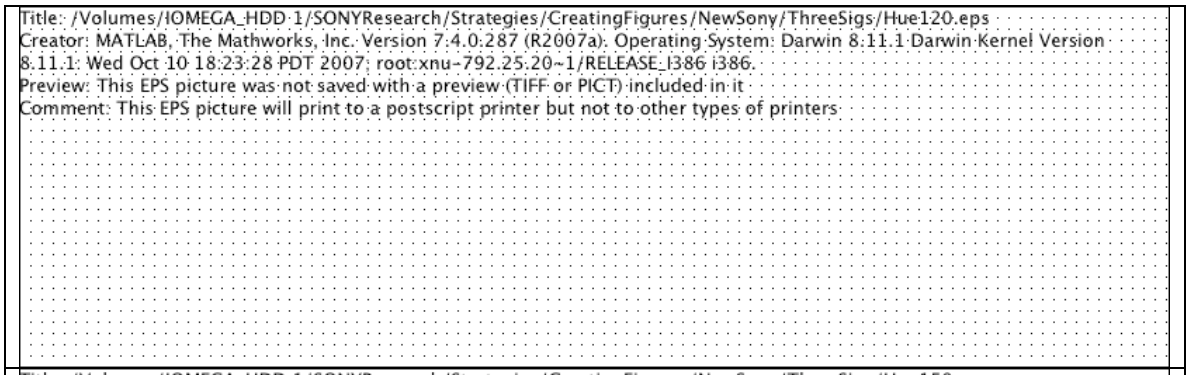
Title: /Volumes/IOMEGA_HDD 1/SONYResearch/Strategies/CreatingFigures/NewSony/ThreeSigs/Hue120.eps
Creator: MATLAB, The Mathworks, Inc. Version 7.4.0.287 (R2007a). Operating System: Darwin 8.11.1 Darwin Kernel Version 8.11.1: Wed Oct 10 18:23:28 PDT 2007; root:xnu-792.25.20~1/RELEASE_I386 i386.
Preview: This EPS picture was not saved with a preview (TIFF or PICT) included in it
Comment: This EPS picture will print to a postscript printer but not to other types of printers

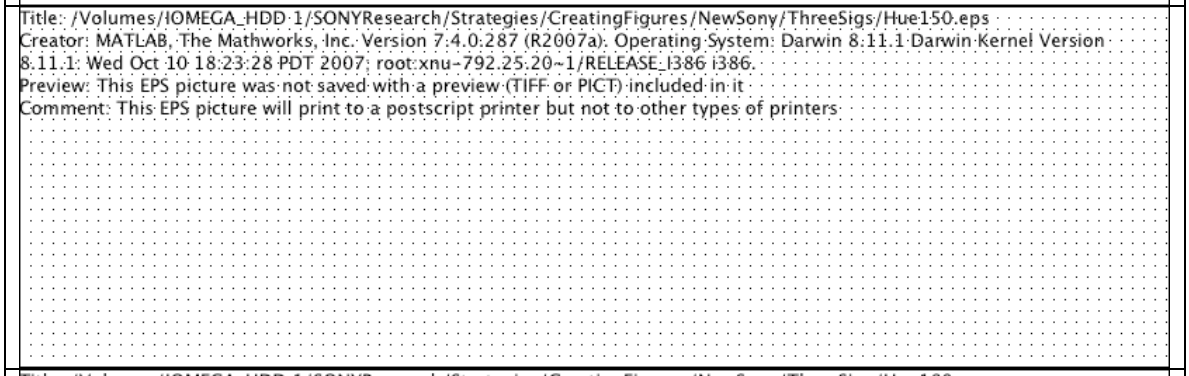
Title: /Volumes/IOMEGA_HDD 1/SONYResearch/Strategies/CreatingFigures/NewSony/ThreeSigs/Hue150.eps
Creator: MATLAB, The Mathworks, Inc. Version 7.4.0.287 (R2007a). Operating System: Darwin 8.11.1 Darwin Kernel Version 8.11.1: Wed Oct 10 18:23:28 PDT 2007; root:xnu-792.25.20~1/RELEASE_I386 i386.
Preview: This EPS picture was not saved with a preview (TIFF or PICT) included in it
Comment: This EPS picture will print to a postscript printer but not to other types of printers

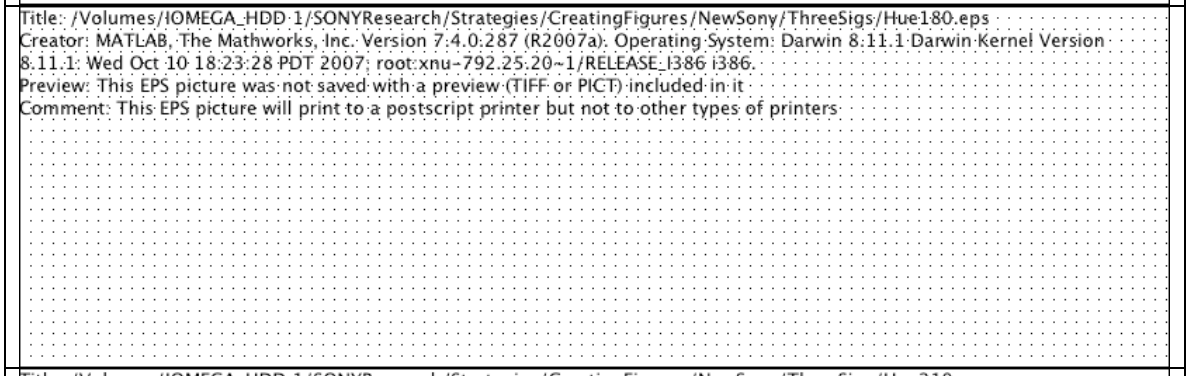
Title: /Volumes/IOMEGA_HDD 1/SONYResearch/Strategies/CreatingFigures/NewSony/ThreeSigs/Hue180.eps
Creator: MATLAB, The Mathworks, Inc. Version 7.4.0.287 (R2007a). Operating System: Darwin 8.11.1 Darwin Kernel Version 8.11.1: Wed Oct 10 18:23:28 PDT 2007; root:xnu-792.25.20~1/RELEASE_I386 i386.
Preview: This EPS picture was not saved with a preview (TIFF or PICT) included in it
Comment: This EPS picture will print to a postscript printer but not to other types of printers

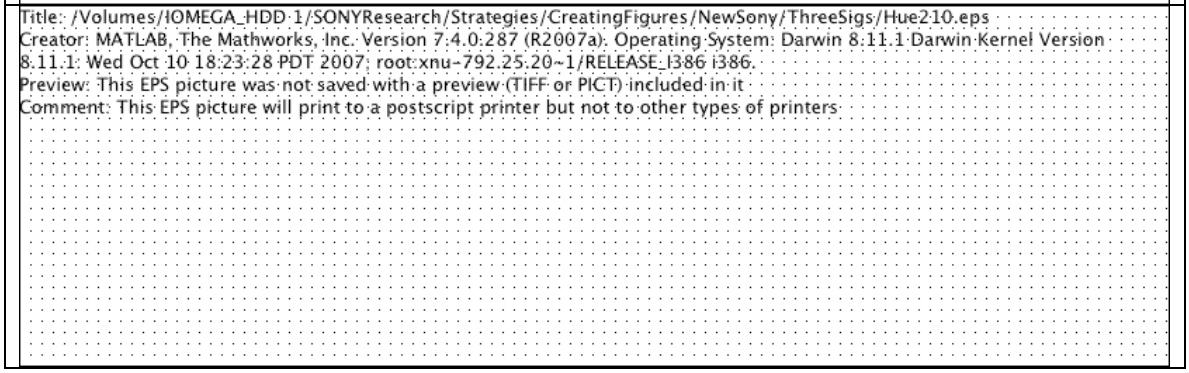
Title: /Volumes/IOMEGA_HDD 1/SONYResearch/Strategies/CreatingFigures/NewSony/ThreeSigs/Hue210.eps
Creator: MATLAB, The Mathworks, Inc. Version 7.4.0.287 (R2007a). Operating System: Darwin 8.11.1 Darwin Kernel Version 8.11.1: Wed Oct 10 18:23:28 PDT 2007; root:xnu-792.25.20~1/RELEASE_I386 i386.
Preview: This EPS picture was not saved with a preview (TIFF or PICT) included in it
Comment: This EPS picture will print to a postscript printer but not to other types of printers

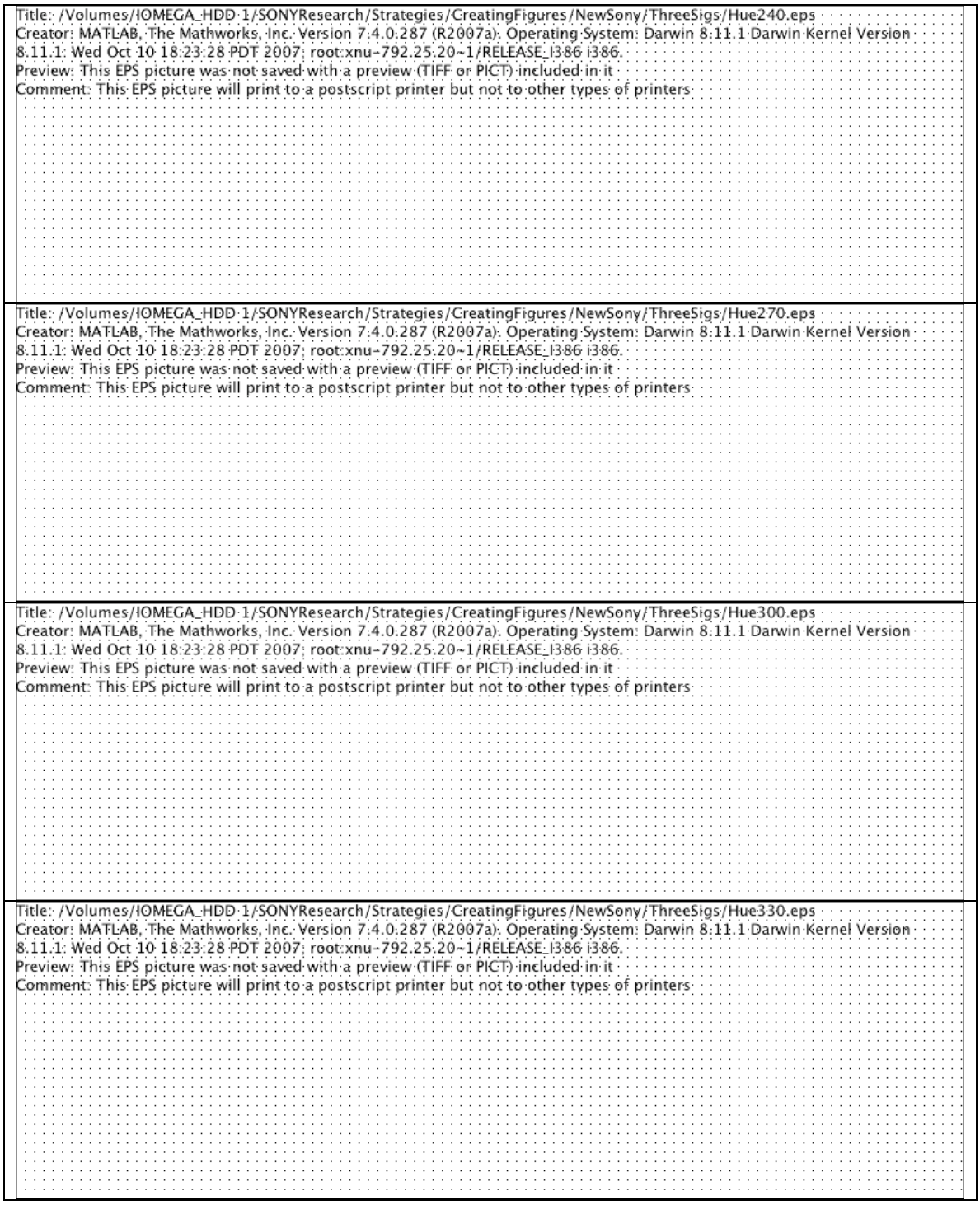

Figure 4.43. The chroma transformations of the three sigmoidal transfer functions (SGEA1-left, SGEA2-center, SGEA3-right. The lines extend from the original sRGB chroma values to the Sony expanded. Note: the color of the data corresponds to the appropriate hue angle.

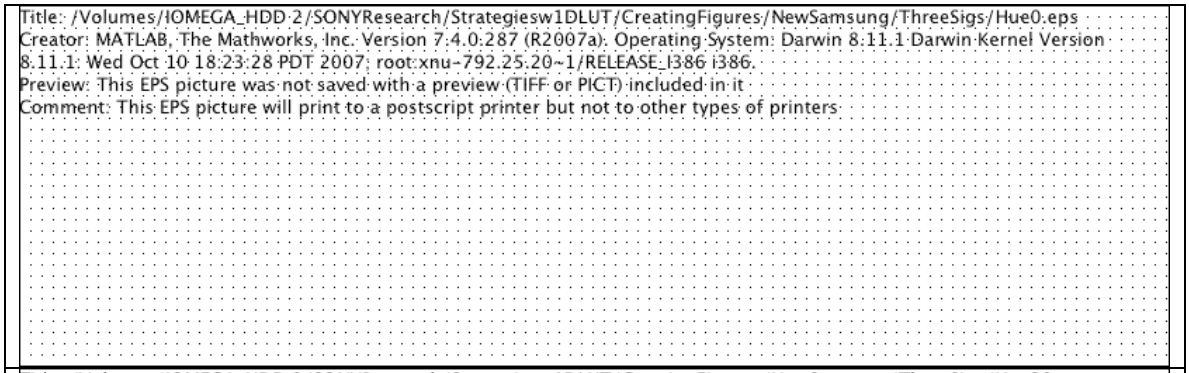
Title: /Volumes/IOMEGA_HDD 2/SONYResearch/Strategiesw1DLUT/CreatingFigures/NewSamsung/ThreeSigs/Hue0.eps
Creator: MATLAB, The Mathworks, Inc. Version 7.4.0.287 (R2007a). Operating System: Darwin 8.11.1 Darwin Kernel Version 8.11.1: Wed Oct 10 18:23:28 PDT 2007; root:xnu-792.25.20~1/RELEASE_I386 i386.
Preview: This EPS picture was not saved with a preview (TIFF or PICT) included in it
Comment: This EPS picture will print to a postscript printer but not to other types of printers

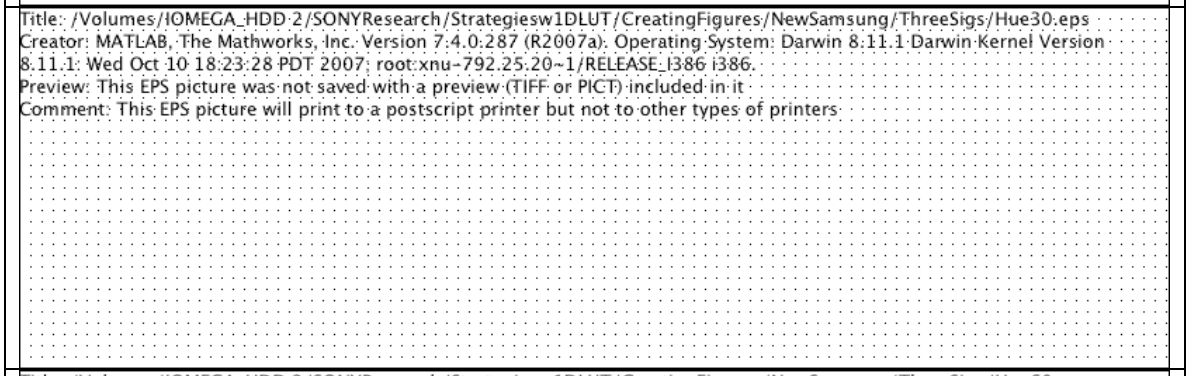
Title: /Volumes/IOMEGA_HDD 2/SONYResearch/Strategiesw1DLUT/CreatingFigures/NewSamsung/ThreeSigs/Hue30.eps
Creator: MATLAB, The Mathworks, Inc. Version 7.4.0.287 (R2007a). Operating System: Darwin 8.11.1 Darwin Kernel Version 8.11.1: Wed Oct 10 18:23:28 PDT 2007; root:xnu-792.25.20~1/RELEASE_I386 i386.
Preview: This EPS picture was not saved with a preview (TIFF or PICT) included in it
Comment: This EPS picture will print to a postscript printer but not to other types of printers

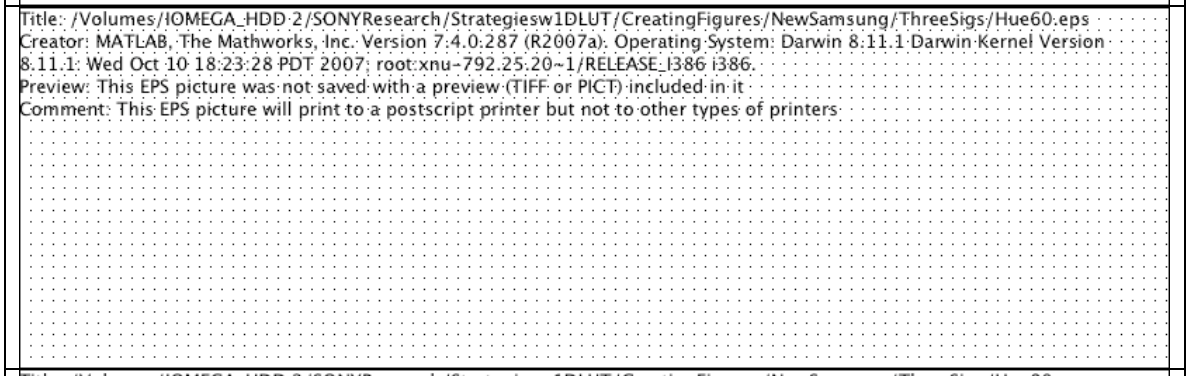
Title: /Volumes/IOMEGA_HDD 2/SONYResearch/Strategiesw1DLUT/CreatingFigures/NewSamsung/ThreeSigs/Hue60.eps
Creator: MATLAB, The Mathworks, Inc. Version 7.4.0.287 (R2007a). Operating System: Darwin 8.11.1 Darwin Kernel Version 8.11.1: Wed Oct 10 18:23:28 PDT 2007; root:xnu-792.25.20~1/RELEASE_I386 i386.
Preview: This EPS picture was not saved with a preview (TIFF or PICT) included in it
Comment: This EPS picture will print to a postscript printer but not to other types of printers

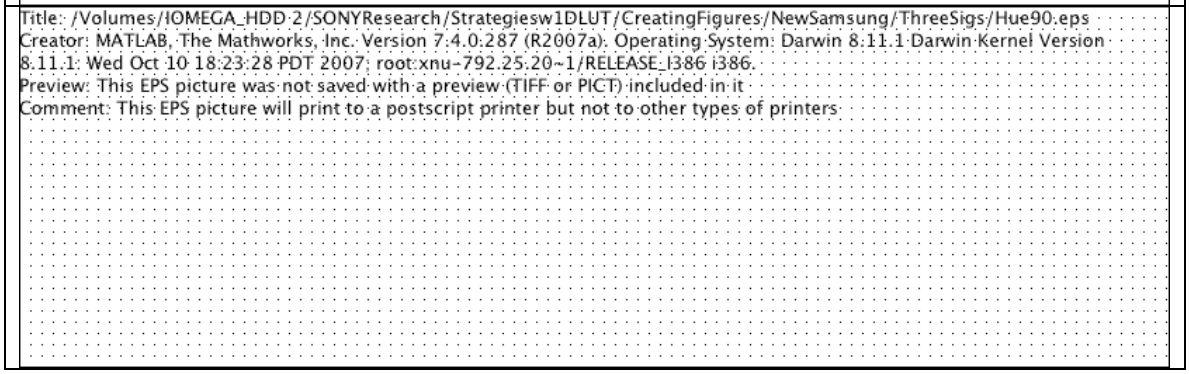
Title: /Volumes/IOMEGA_HDD 2/SONYResearch/Strategiesw1DLUT/CreatingFigures/NewSamsung/ThreeSigs/Hue90.eps
Creator: MATLAB, The Mathworks, Inc. Version 7.4.0.287 (R2007a). Operating System: Darwin 8.11.1 Darwin Kernel Version 8.11.1: Wed Oct 10 18:23:28 PDT 2007; root:xnu-792.25.20~1/RELEASE_I386 i386.
Preview: This EPS picture was not saved with a preview (TIFF or PICT) included in it
Comment: This EPS picture will print to a postscript printer but not to other types of printers

Title: /Volumes/IOMEGA_HDD 2/SONYResearch/Strategiesw1DLUT/CreatingFigures/NewSamsung/ThreeSigs/Hue120.eps
Creator: MATLAB, The Mathworks, Inc. Version 7.4.0.287 (R2007a). Operating System: Darwin 8.11.1 Darwin Kernel Version 8.11.1: Wed Oct 10 18:23:28 PDT 2007; root:xnu-792.25.20~1/RELEASE_I386 i386.
Preview: This EPS picture was not saved with a preview (TIFF or PICT) included in it
Comment: This EPS picture will print to a postscript printer but not to other types of printers

Title: /Volumes/IOMEGA_HDD 2/SONYResearch/Strategiesw1DLUT/CreatingFigures/NewSamsung/ThreeSigs/Hue150.eps
Creator: MATLAB, The Mathworks, Inc. Version 7.4.0.287 (R2007a). Operating System: Darwin 8.11.1 Darwin Kernel Version 8.11.1: Wed Oct 10 18:23:28 PDT 2007; root:xnu-792.25.20~1/RELEASE_I386 i386.
Preview: This EPS picture was not saved with a preview (TIFF or PICT) included in it
Comment: This EPS picture will print to a postscript printer but not to other types of printers

Title: /Volumes/IOMEGA_HDD 2/SONYResearch/Strategiesw1DLUT/CreatingFigures/NewSamsung/ThreeSigs/Hue180.eps
Creator: MATLAB, The Mathworks, Inc. Version 7.4.0.287 (R2007a). Operating System: Darwin 8.11.1 Darwin Kernel Version 8.11.1: Wed Oct 10 18:23:28 PDT 2007; root:xnu-792.25.20~1/RELEASE_I386 i386.
Preview: This EPS picture was not saved with a preview (TIFF or PICT) included in it
Comment: This EPS picture will print to a postscript printer but not to other types of printers

Title: /Volumes/IOMEGA_HDD 2/SONYResearch/Strategiesw1DLUT/CreatingFigures/NewSamsung/ThreeSigs/Hue210.eps
Creator: MATLAB, The Mathworks, Inc. Version 7.4.0.287 (R2007a). Operating System: Darwin 8.11.1 Darwin Kernel Version 8.11.1: Wed Oct 10 18:23:28 PDT 2007; root:xnu-792.25.20~1/RELEASE_I386 i386.
Preview: This EPS picture was not saved with a preview (TIFF or PICT) included in it
Comment: This EPS picture will print to a postscript printer but not to other types of printers

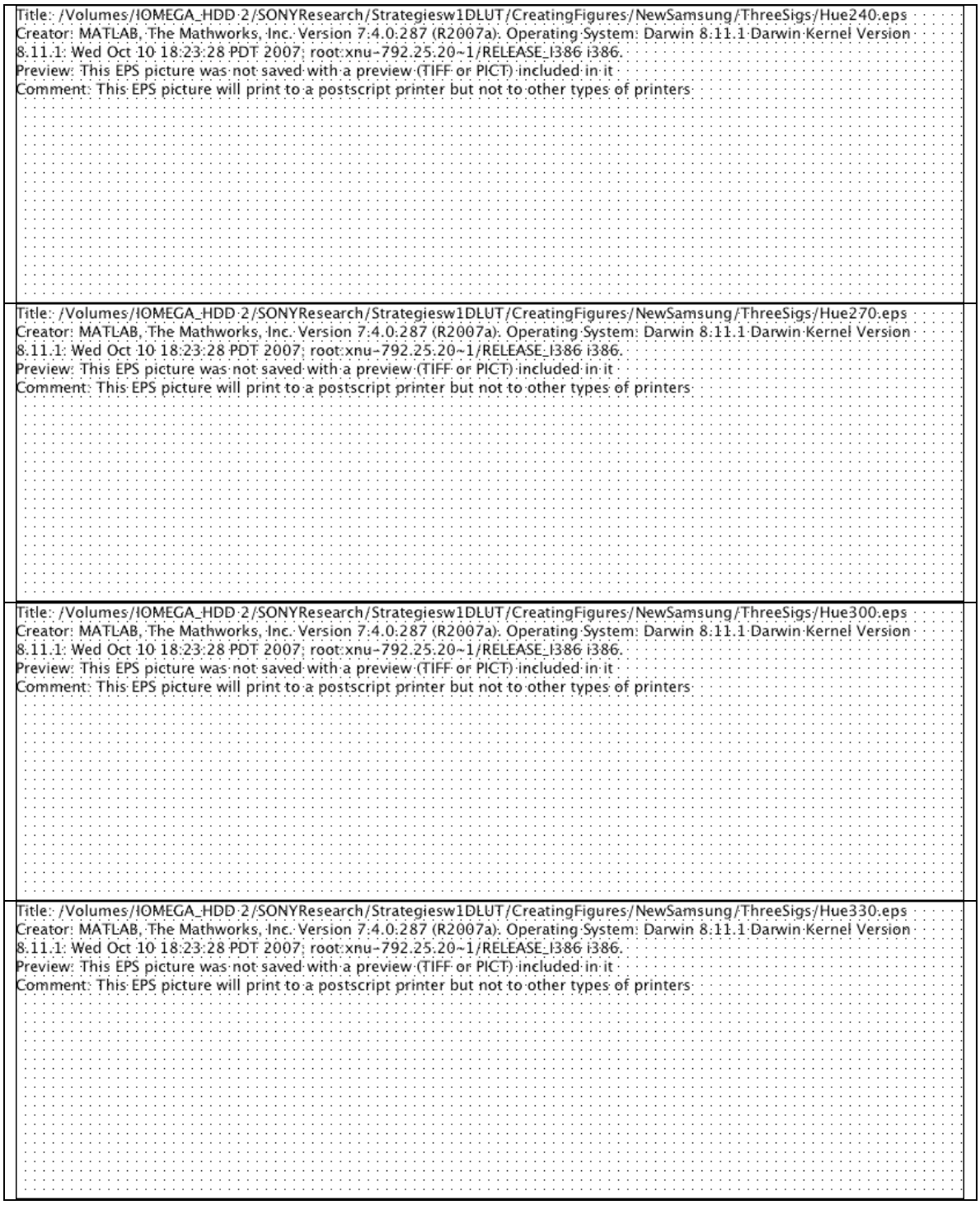

Figure 4.44. The chroma transformations of the three sigmoidal transfer functions (SGEA1-left, SGEA2-center, SGEA3-right. The lines extend from the original sRGB chroma values to the Samsung expanded values. Note: the color of the data corresponds to the appropriate hue angle.

The degree of extension for both output devices, as a result of the various SGEAs (Figure 4.43 and 4.44) depends, once again, on the hue angle and lightness combination. The transformations for each hue angle represented in these figures are not visually distinguishable across each of the three SGEAs. However, each SGEA was evaluated by the observers to determine whether the SGEAs are distinguishable when image content is mapped under the algorithms.

4.4.3.1. Reference Point Extension

In addition, to the mapping function described through the SGEAs above, each SGEA curve was varied based on the direction of extension by incorporating multiple reference points. Lee et al. utilized various anchor points in their gamut compression algorithms, and concluded mapping errors could be reduced when anchor points are incorporated [Lee et al., 2000]. Therefore, in accordance with their anchor points, where the center of gravity was on the lightness axis, lightness values of both 50 and 0 units were proposed for this evaluation, in addition to maintaining a constant lightness.

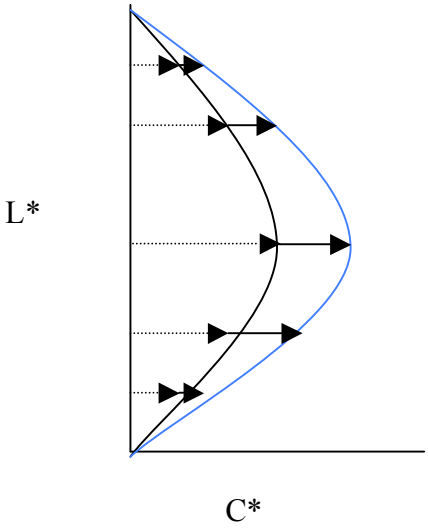

Figure 4.45. Constant Lightness with sigmoidal gamut expansion.

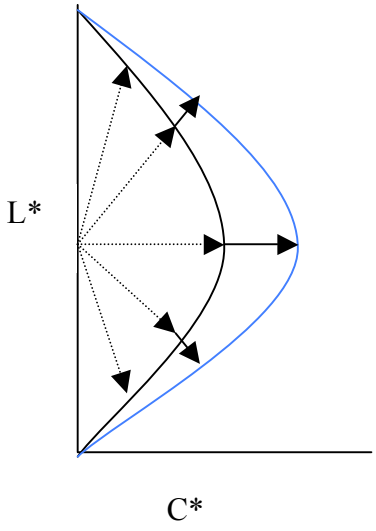

Figure 4.46. Sigmoidal gamut expansion away from L=50, or mid-gray.*

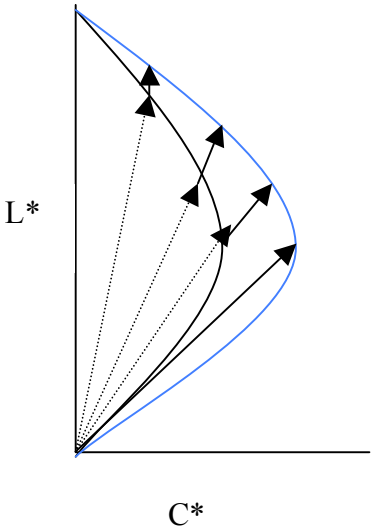

Figure 4.47. Sigmoidal gamut expansion away from L=0, or black.*

There were three different SGEA reference points evaluated (Figures 4.45, 4.46, 4.47). Figure 4.45 represents SGEA, while maintaining constant lightness. Thus, once the expanded chromatic values were obtained, the CIELAB image was converted to tristimulus values, and then to display digital counts. Figures 4.46 and 4.47 involve a lightness conversion, extending from a lightness value of 50, or mid-gray, and 0, or black. Using geometric relationships, the angle between lightness and chroma was calculated and held constant throughout the expansion.

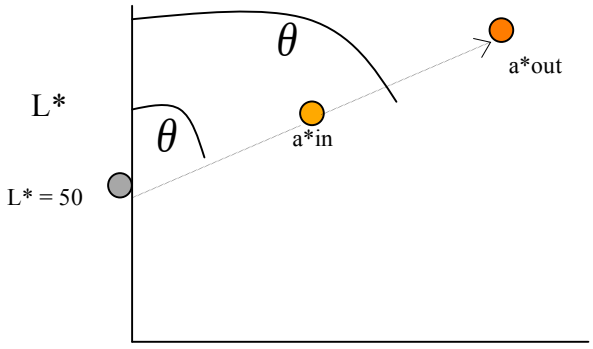

Figure 4.48. The expansion of one specific pixel, where the expansion is extending from L=50*

The expansion from mid-gray is represented in Figure 4.48. A similar image can be created in which the reference point is at L*=0. However, the common denominator is a constant angle theta. By maintaining a constant theta, the SGEA can ensure the entire gamut expansion extends from the same reference point, and therefore, results in mapping transformations much like the theoretical depiction in Figures 4.46 and 4.47. (Actual transformations are displayed in Figures 4.50 and 4.51).

Equations 4.20, 4.21, and 4.22 represent the calculations performed to obtain the angle, theta, and the corresponding lightness value for every pixel in the image, derived through geometry relationships.

$$\theta_{L^*_r} = \tan\left(\frac{a^*}{|L^* - L^*_r|}\right) \qquad (4.20),$$

where L^*_r represents the reference lightness value, either fifty or zero for these research purposes.

$$L^*_{out_{50}} = \frac{a^*_{out} - 50\tan^{-1}(\theta_{50})}{\tan^{-1}(\theta_{50})} \quad (4.21),$$

or for a reference point of L* equal to zero,

$$L^*_{out_0} = \frac{a^*_{out}}{\tan^{-1}(\theta_0)} \qquad (4.22).$$

Once L^*_{out} was calculated, linear regression was performed to form the line illustrated in Figure 4.21, extending from C* equals zero, L* equals 50 towards the original (C*, L*) coordinates, through to the point (C^*_{out}, L^*_{out}), where L^*_{out} equals that from Eqn. 4.22. Therefore, through linear regression, the output maximum chroma value was obtained. A LUT was then formed between the input maximum chroma, and output maximum chroma, according to the cumulative normal distributions described in Table 4.2 and Figure 4.15. This process was repeated for the reference point of L* equal to zero.

Theoretically, the transformations were depicted in Figures 4.45 through 4.47. However, the actual transformations indicated that mapping direction extending from L* equal to zero introduced a few artifacts too significant to ignore.

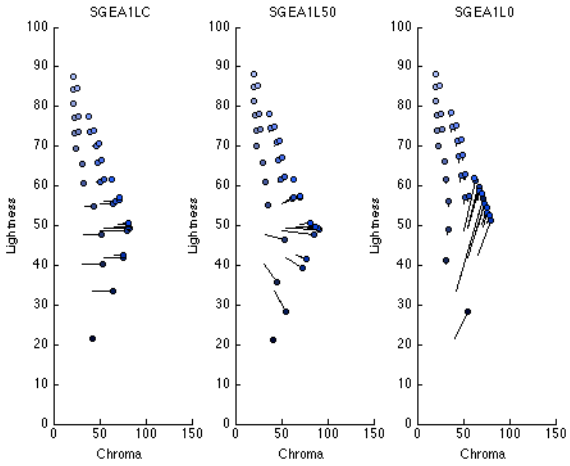

Figure 4.49. The transformations of sRGB values, corresponding to the Sony display output values, for hue angles between 270 and 275. The most left plot is constant lightness, the center extends from L=50 and the right plot extends from L*=0.*

The reference points are denoted as LC, L50 and L0, which refer to the anchor point in which the expansion is extending from. LC represents expansion while maintaining constant chroma, and L50 or L0 represent expansion extending from either a lightness value of fifty or zero units.

Figure 4.49 serves to demonstrate the possible sigmoidal expansions under a specified mapping direction. The potential effect the SGEAs with expansion from a lightness of zero is evident in this figure, as a few low lightness, low chromatic values were extended to dramatically higher lightness values with only relatively higher chromatic values. Therefore, the resulting appearance at these points is substantially desaturated. After examining the scenes visually and observing the significant artifacts as a result of this algorithm, the reference point of L* equal to zero was removed from the psychophysical analysis. Figures 4.50 and 4.51 represent the transformations for a range of hue angles, when mapping to the Sony and Samsung gamuts, respectively, according to SGEA1LC and SGEA1L50.

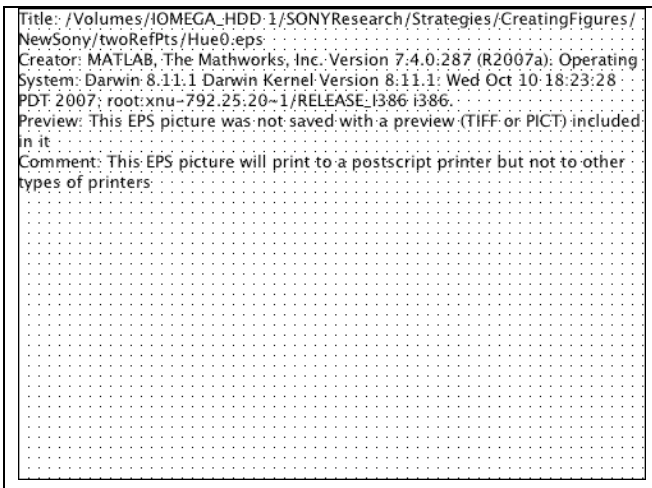
Title: /Volumes/IOMEGA_HDD 1/SONYResearch/Strategies/CreatingFigures/NewSony/twoRefPts/Hue0.eps
Creator: MATLAB, The Mathworks, Inc. Version 7.4.0.287 (R2007a). Operating System: Darwin 8.11.1 Darwin Kernel Version 8.11.1: Wed Oct 10 18:23:28 PDT 2007; root:xnu-792.25.20~1/RELEASE_I386 i386.
Preview: This EPS picture was not saved with a preview (TIFF or PICT) included in it
Comment: This EPS picture will print to a postscript printer but not to other types of printers

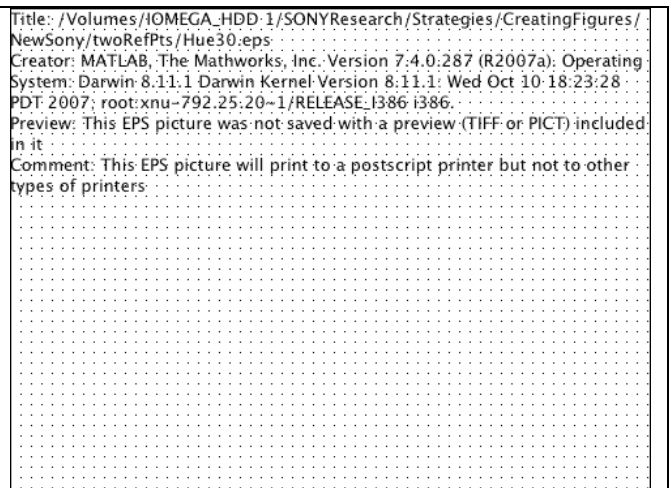
Title: /Volumes/IOMEGA_HDD 1/SONYResearch/Strategies/CreatingFigures/NewSony/twoRefPts/Hue30.eps
Creator: MATLAB, The Mathworks, Inc. Version 7.4.0.287 (R2007a). Operating System: Darwin 8.11.1 Darwin Kernel Version 8.11.1: Wed Oct 10 18:23:28 PDT 2007; root:xnu-792.25.20~1/RELEASE_I386 i386.
Preview: This EPS picture was not saved with a preview (TIFF or PICT) included in it
Comment: This EPS picture will print to a postscript printer but not to other types of printers

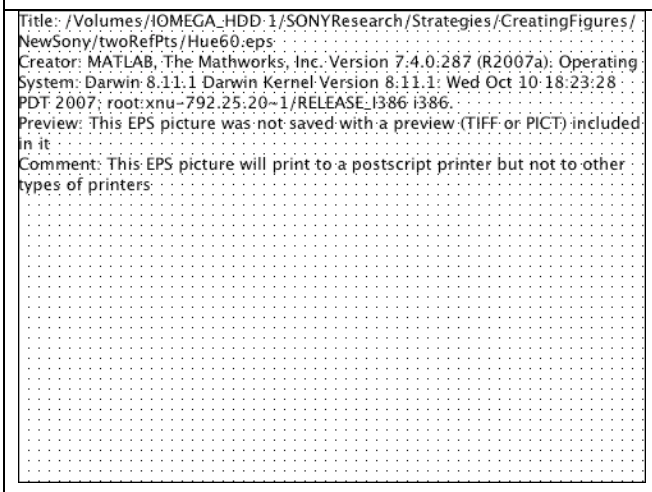
Title: /Volumes/IOMEGA_HDD 1/SONYResearch/Strategies/CreatingFigures/NewSony/twoRefPts/Hue60.eps
Creator: MATLAB, The Mathworks, Inc. Version 7.4.0.287 (R2007a). Operating System: Darwin 8.11.1 Darwin Kernel Version 8.11.1: Wed Oct 10 18:23:28 PDT 2007; root:xnu-792.25.20~1/RELEASE_I386 i386.
Preview: This EPS picture was not saved with a preview (TIFF or PICT) included in it
Comment: This EPS picture will print to a postscript printer but not to other types of printers

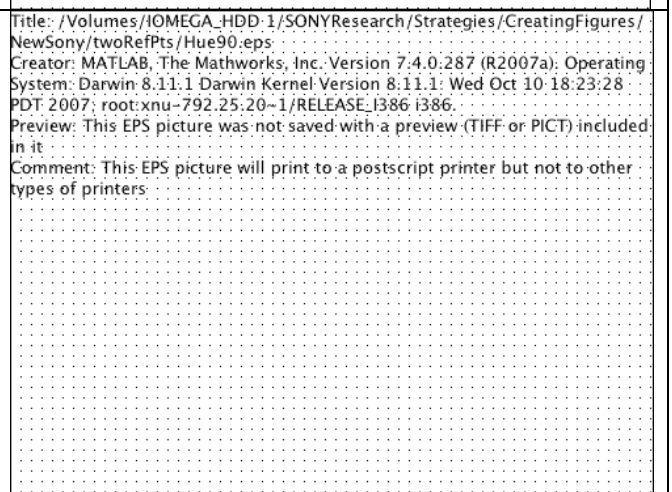
Title: /Volumes/IOMEGA_HDD 1/SONYResearch/Strategies/CreatingFigures/NewSony/twoRefPts/Hue90.eps
Creator: MATLAB, The Mathworks, Inc. Version 7.4.0.287 (R2007a). Operating System: Darwin 8.11.1 Darwin Kernel Version 8.11.1: Wed Oct 10 18:23:28 PDT 2007; root:xnu-792.25.20~1/RELEASE_I386 i386.
Preview: This EPS picture was not saved with a preview (TIFF or PICT) included in it
Comment: This EPS picture will print to a postscript printer but not to other types of printers

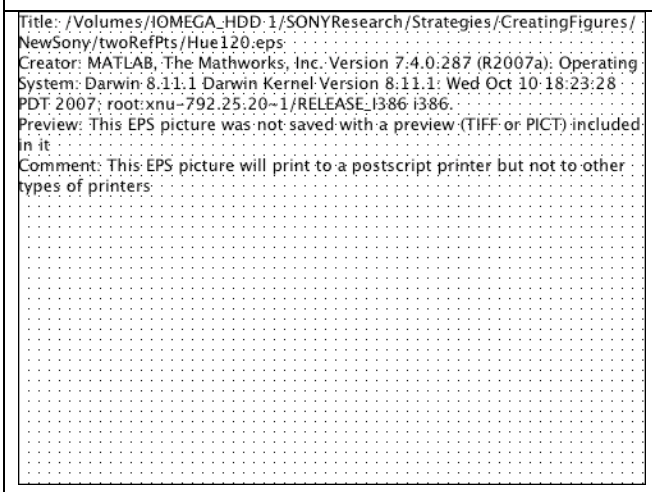
Title: /Volumes/IOMEGA_HDD 1/SONYResearch/Strategies/CreatingFigures/NewSony/twoRefPts/Hue120.eps
Creator: MATLAB, The Mathworks, Inc. Version 7.4.0.287 (R2007a). Operating System: Darwin 8.11.1 Darwin Kernel Version 8.11.1: Wed Oct 10 18:23:28 PDT 2007; root:xnu-792.25.20~1/RELEASE_I386 i386.
Preview: This EPS picture was not saved with a preview (TIFF or PICT) included in it
Comment: This EPS picture will print to a postscript printer but not to other types of printers

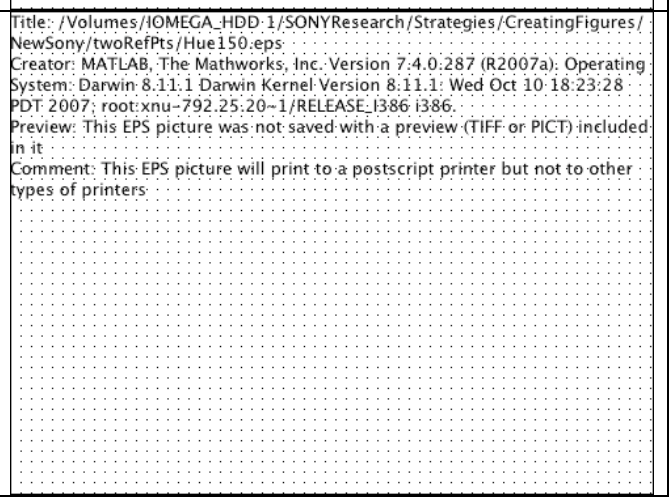
Title: /Volumes/IOMEGA_HDD 1/SONYResearch/Strategies/CreatingFigures/NewSony/twoRefPts/Hue150.eps
Creator: MATLAB, The Mathworks, Inc. Version 7.4.0.287 (R2007a). Operating System: Darwin 8.11.1 Darwin Kernel Version 8.11.1: Wed Oct 10 18:23:28 PDT 2007; root:xnu-792.25.20~1/RELEASE_I386 i386.
Preview: This EPS picture was not saved with a preview (TIFF or PICT) included in it
Comment: This EPS picture will print to a postscript printer but not to other types of printers

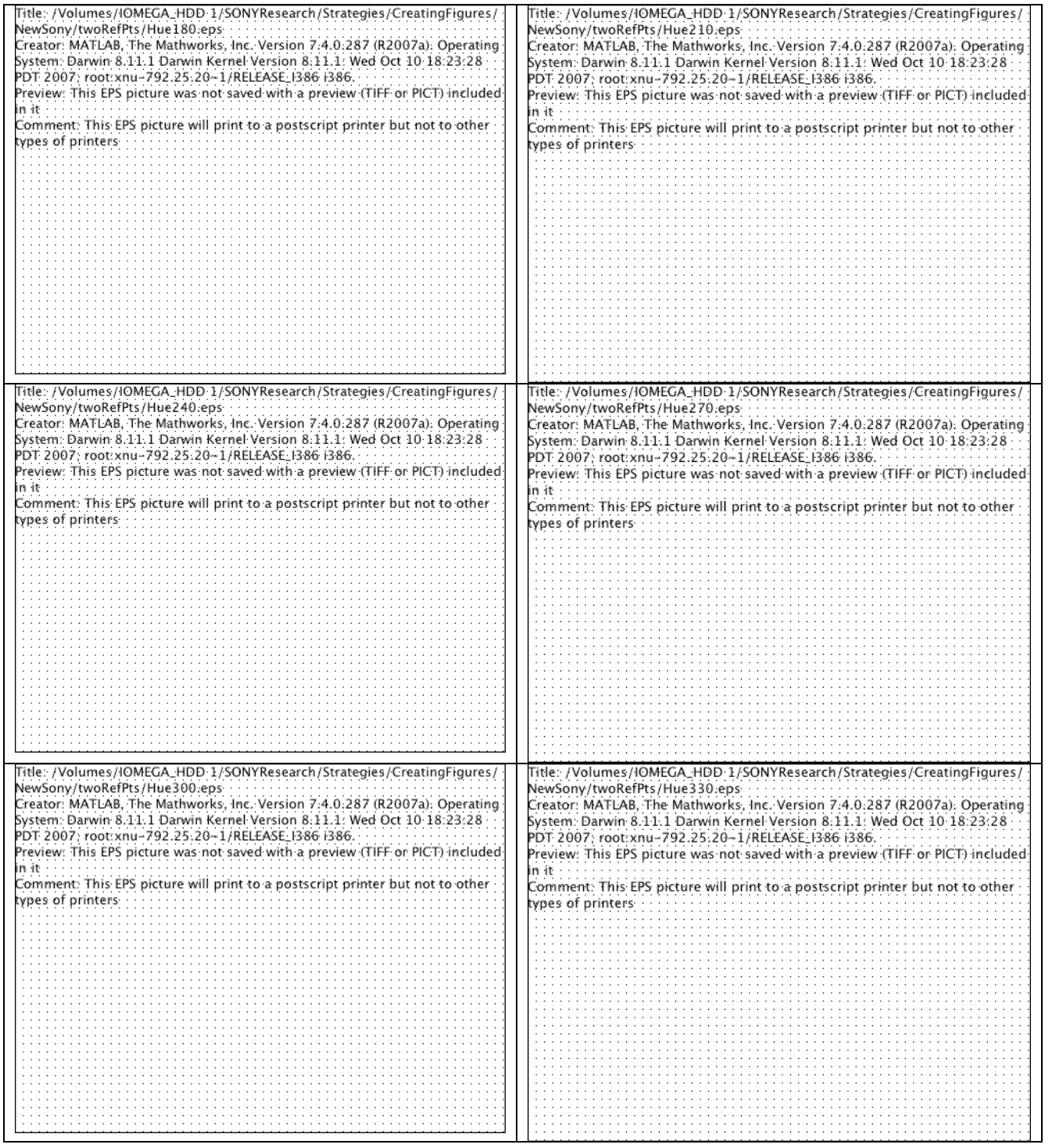

Figure 4.50. The transformations as a result of SGEA1LC andSGEA1L50, corresponding to the Sony display, for a range of hue angle (the color of the data corresponds to the applicable hue angle).

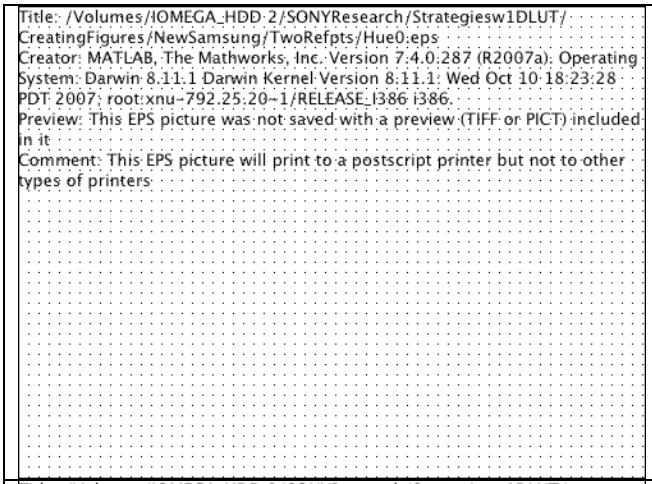
Title: /Volumes/IOMEGA_HDD 2/SONYResearch/Strategiesw1DLUT/CreatingFigures/NewSamsung/TwoRefpts/Hue0.eps
Creator: MATLAB, The Mathworks, Inc. Version 7.4.0.287 (R2007a). Operating System: Darwin 8.11.1 Darwin Kernel Version 8.11.1: Wed Oct 10 18:23:28 PDT 2007; root:xnu-792.25.20~1/RELEASE_I386 i386.
Preview: This EPS picture was not saved with a preview (TIFF or PICT) included in it
Comment: This EPS picture will print to a postscript printer but not to other types of printers

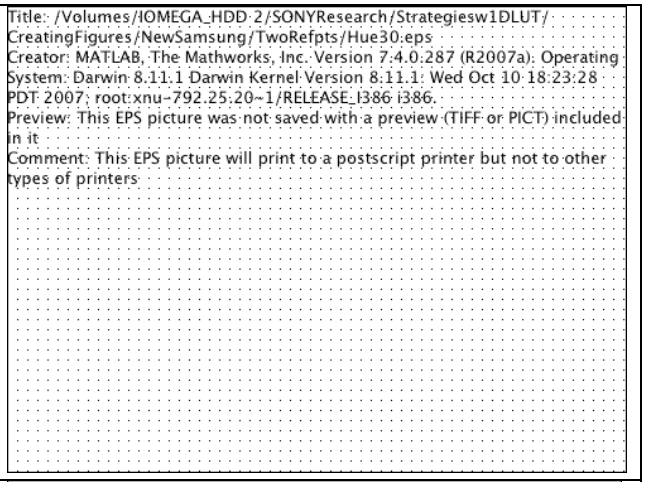
Title: /Volumes/IOMEGA_HDD 2/SONYResearch/Strategiesw1DLUT/CreatingFigures/NewSamsung/TwoRefpts/Hue30.eps
Creator: MATLAB, The Mathworks, Inc. Version 7.4.0.287 (R2007a). Operating System: Darwin 8.11.1 Darwin Kernel Version 8.11.1: Wed Oct 10 18:23:28 PDT 2007; root:xnu-792.25.20~1/RELEASE_I386 i386.
Preview: This EPS picture was not saved with a preview (TIFF or PICT) included in it
Comment: This EPS picture will print to a postscript printer but not to other types of printers

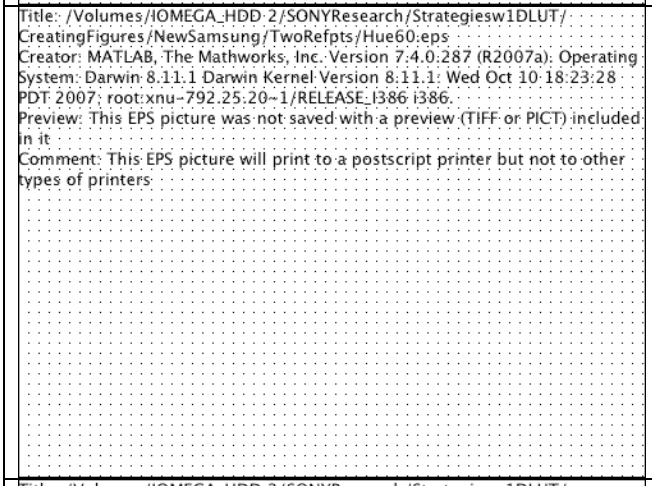
Title: /Volumes/IOMEGA_HDD 2/SONYResearch/Strategiesw1DLUT/CreatingFigures/NewSamsung/TwoRefpts/Hue60.eps
Creator: MATLAB, The Mathworks, Inc. Version 7.4.0.287 (R2007a). Operating System: Darwin 8.11.1 Darwin Kernel Version 8.11.1: Wed Oct 10 18:23:28 PDT 2007; root:xnu-792.25.20~1/RELEASE_I386 i386.
Preview: This EPS picture was not saved with a preview (TIFF or PICT) included in it
Comment: This EPS picture will print to a postscript printer but not to other types of printers

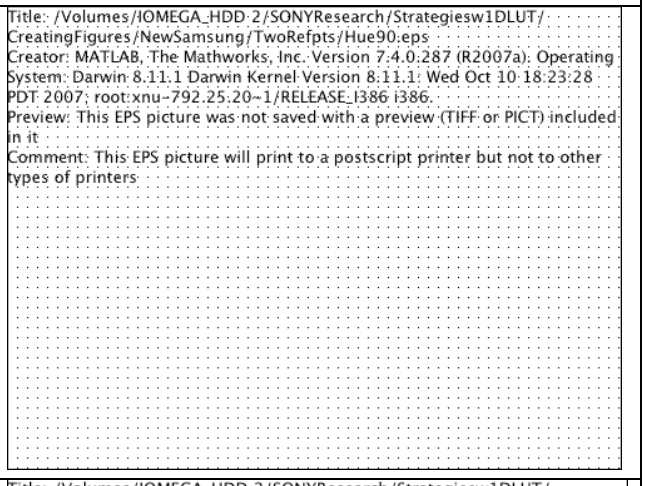
Title: /Volumes/IOMEGA_HDD 2/SONYResearch/Strategiesw1DLUT/CreatingFigures/NewSamsung/TwoRefpts/Hue90.eps
Creator: MATLAB, The Mathworks, Inc. Version 7.4.0.287 (R2007a). Operating System: Darwin 8.11.1 Darwin Kernel Version 8.11.1: Wed Oct 10 18:23:28 PDT 2007; root:xnu-792.25.20~1/RELEASE_I386 i386.
Preview: This EPS picture was not saved with a preview (TIFF or PICT) included in it
Comment: This EPS picture will print to a postscript printer but not to other types of printers

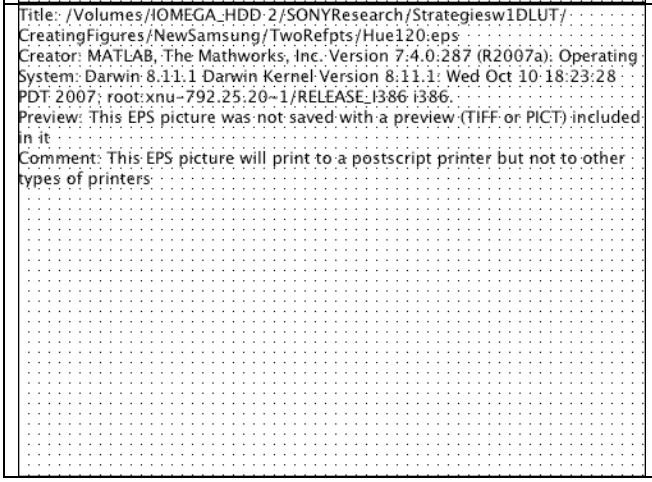
Title: /Volumes/IOMEGA_HDD 2/SONYResearch/Strategiesw1DLUT/CreatingFigures/NewSamsung/TwoRefpts/Hue120.eps
Creator: MATLAB, The Mathworks, Inc. Version 7.4.0.287 (R2007a). Operating System: Darwin 8.11.1 Darwin Kernel Version 8.11.1: Wed Oct 10 18:23:28 PDT 2007; root:xnu-792.25.20~1/RELEASE_I386 i386.
Preview: This EPS picture was not saved with a preview (TIFF or PICT) included in it
Comment: This EPS picture will print to a postscript printer but not to other types of printers

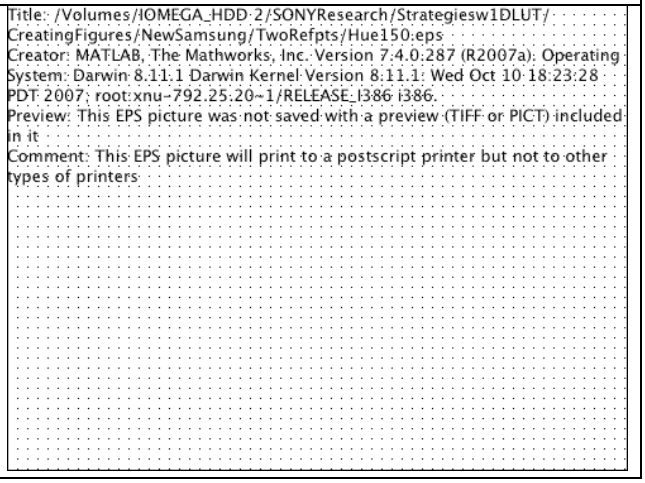
Title: /Volumes/IOMEGA_HDD 2/SONYResearch/Strategiesw1DLUT/CreatingFigures/NewSamsung/TwoRefpts/Hue150.eps
Creator: MATLAB, The Mathworks, Inc. Version 7.4.0.287 (R2007a). Operating System: Darwin 8.11.1 Darwin Kernel Version 8.11.1: Wed Oct 10 18:23:28 PDT 2007; root:xnu-792.25.20~1/RELEASE_I386 i386.
Preview: This EPS picture was not saved with a preview (TIFF or PICT) included in it
Comment: This EPS picture will print to a postscript printer but not to other types of printers

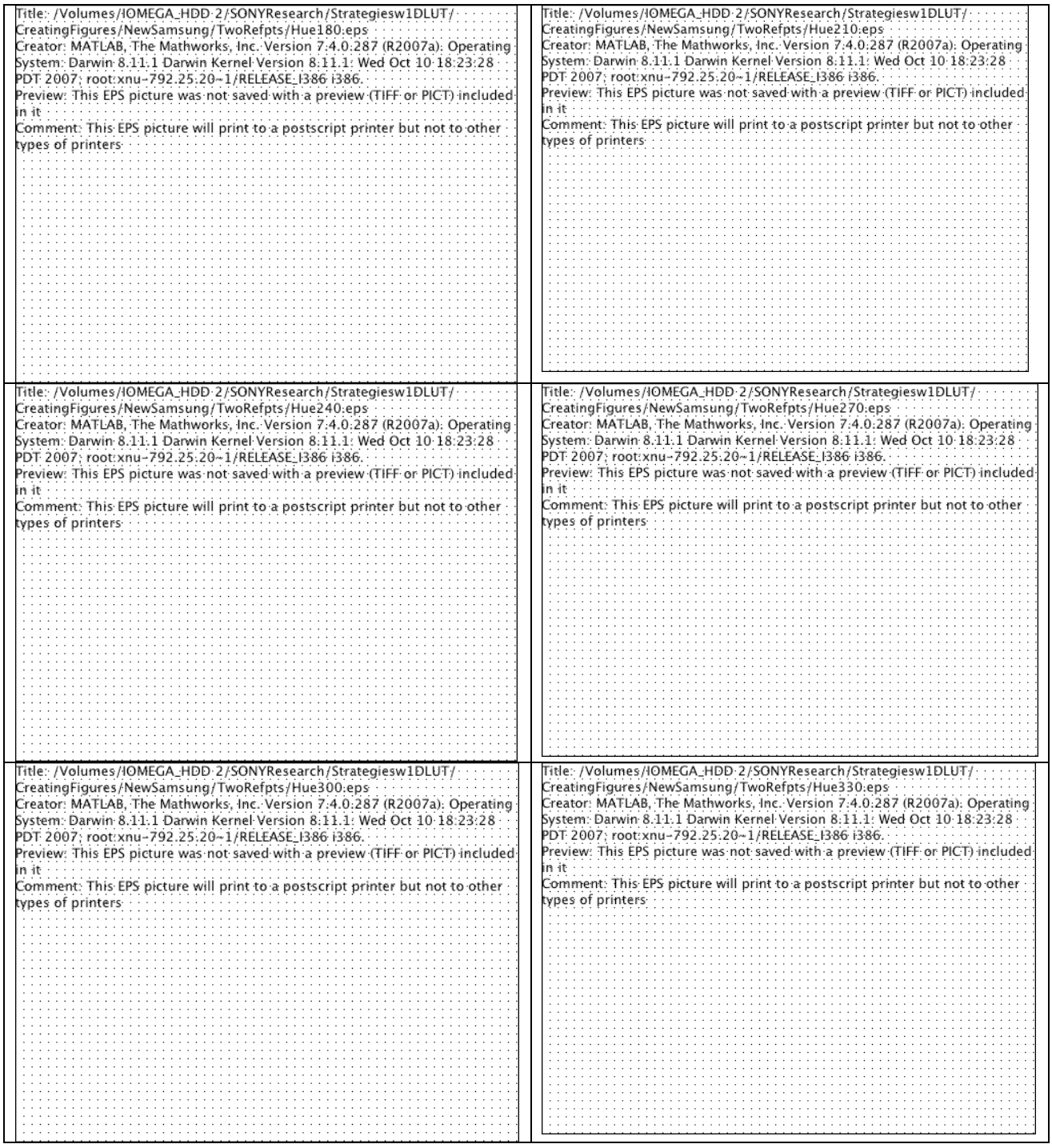

Figure 4.51. The transformations as a result of SGEA1LC and SGEA1L50, corresponding to the Samsung display, for a range of hue angles (the color of the data corresponds to the applicable hue angle).

In Figures 4.50 and 4.51, the influence of the mapping direction is well illustrated. Therefore, any differences in preference between mapping directions will be easily explained via both of these figures.

Overall there were six different sigmoidal algorithms psychophysically analyzed, SGEA1, 2, and 3, all evaluated at both constant lightness, and extending from a lightness value of 50.

5. Data Analysis

The evaluation entailed a forced-choice, paired comparison based on Thurstone's Law of Comparitive Judgement (Case V), where observers were instructed to choose the image they preferred overall. There are several factors that influenced the observers' preference, some of which include: color rendering, tone reproduction, sharpness and contrast of image. Given an ideal mapping strategy preferred by the average observer was evaluated, the observer was not given any further instructions than to choose the , "overall" preferred image. The order of image presentation was randomized for each observer, in addition to the position relative to image placement on the screen. There were 550 total observations for each observer (ten scenes and 11 versions per scene).

An interval scale of preference ratings was generated from the paired-comparison evaluations via Gulliksen's regression for unanimous decisions [Johnson; 2004]. The psychophysical experiments were performed for twenty observers on each display, where the mean standard deviation for each image, across all observers, was 0.09 interval scores. This confidence interval was calculated based on Ethan Montag's definitions [Johnson; 2004]. The results portrayed clear trends among observers, however, scene dependency was still evident as in past research.

With great variation in the image content, image dependencies became clear. A cluster analysis was performed on the images to define any relationships among image sets, however, no explainable clusters resulted (unlike the results from Experiment III by Heckman et al.). Therefore, by evaluating the overall results, for each individual image, the importance of each attribute became clear. These results are displayed in Figure 5.1 for the Sony display, Figure 5.2 for the Samsung display.

The most profound result, quite evident in Figure 5.1, was degree to which the sRGB expanded (or the method that linearly stretched the data to the display) was disliked. This effect is clearest for the Sony display, although this method did not perform well for the Samsung either. When evaluating the baseline images, both mapped to the display's gamut versus the original content unexpanded, the tone reproduction curve is inconsistent between the two reproductions. Both images undergo slightly different processing. By converting sRGB values to tristimulus values using the display's matrix versus the sRGB matrix respectively, the inherent tone reproduction curves for each corresponding gamut are applied to the images. Therefore, the expanded sRGB image is reproduced under the Sony's tone reproduction curve, whereas the unexpanded sRGB version is reproduced under sRGB's tone reproduction curve. This could in part, explain why observer preference for these two versions varied significantly in some cases. However, across the majority of scene content, neither version was preferred over the developed algorithms. Therefore, these results confirm that the development of a GEA is pertinent to the success of extended gamut displays.

The significant image dependencies become very apparent through Figure 5.1. This was expected, as the images are comprised of different primary attributes, since it was important to incorporate a variety of images during the image selection phase. Still, some trends are stable across images. One of the baselines, or the expanded sRGB version, represented by the cyan-colored bar at the most left position for each image, was least preferred across the images. In addition, the original sRGB version never performed significantly better than any other version.

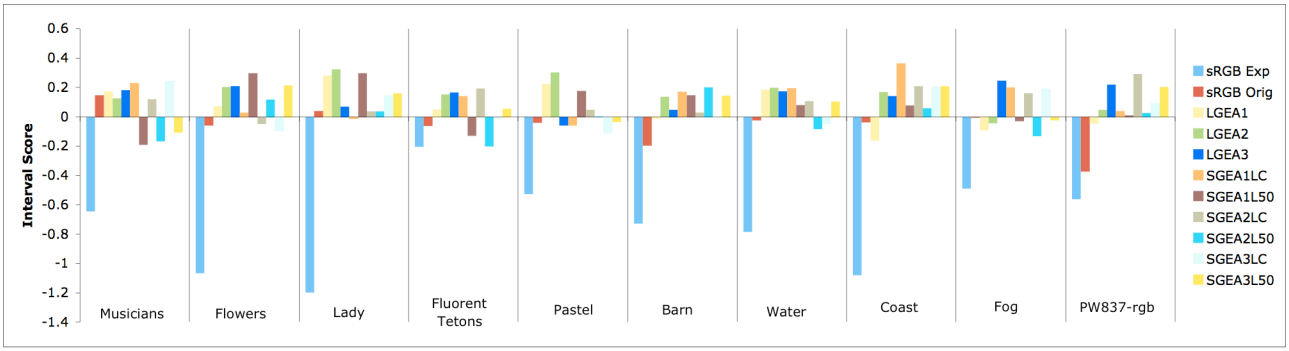

Figure 5.1. Sony display results for all of the images. The interval scores are represented for each algorithm as a separate bar, where the legend describes the color each algorithm corresponds to.

In Figure 5.1, image dependencies become very evident. Although some algorithms are preferred for multiple images, there is not a definitive answer for which algorithm performed best, based on this bar plot. The evaluation performed on the Samsung display resulted in similar conclusions.

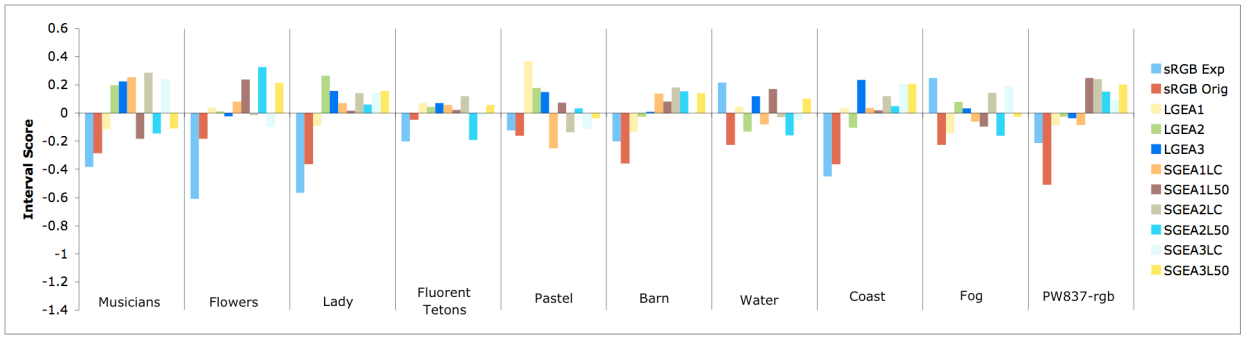

Figure 5.2. The result from the Samsung evaluation, for all of the images. The interval scores are represented for each algorithm as a separate bar, where the legend describes the color each algorithm corresponds to.

Both Figures 5.1, 5.2 are based on the interval scale calculations, which are displayed in Tables 5.1 and 5.2.

Table 5.1 Interval Score calculations for Sony evaluation

	Music.	Flower	Lady	F.Tetons	Pastel	Barn	Water	Coast	Fog	RGB	AVG
sRGBexp	-0.644	-1.064	-1.195	-0.203	-0.525	-0.725	-0.781	-1.078	-0.487	-0.559	-0.73
sRGBorig	0.147	-0.058	0.039	-0.061	-0.038	-0.196	-0.022	-0.035	-0.004	-0.371	-0.06
LGEA1	0.174	0.071	0.280	0.051	0.224	-0.011	0.185	-0.159	-0.091	-0.045	0.07
LGEA2	0.124	0.202	0.324	0.152	0.302	0.136	0.196	0.167	-0.043	0.047	0.16
LGEA3	0.182	0.207	0.069	0.164	-0.059	0.048	0.173	0.140	0.246	0.218	0.14
SGEA1LC	0.230	0.027	-0.011	0.141	-0.059	0.171	0.196	0.363	0.199	0.038	0.13
SGEA1L50	-0.190	0.297	0.296	-0.129	0.175	0.146	0.078	0.077	-0.029	0.010	0.07
SGEA2LC	0.119	-0.046	0.036	0.191	0.047	0.028	0.107	0.207	0.160	0.292	0.11
SGEA2L50	-0.164	0.118	0.037	-0.201	0.003	0.200	-0.083	0.057	-0.130	0.026	-0.01
SGEA3LC	0.260	0.032	0.047	-0.026	-0.092	0.069	-0.053	0.251	0.357	0.133	0.10
SGEA3L50	-0.240	0.292	0.185	-0.079	0.023	0.199	0.004	0.093	-0.179	0.211	0.05

Table 5.2 Interval Score calculations for Samsung evaluation

	Music.	Flower	Lady	F.Tetons	Pastel	Barn	Water	Coast	Fog	RGB	AVG
sRGBexp	-0.381	-0.605	-0.564	-0.198	-0.119	-0.198	0.215	-0.448	0.250	-0.211	-0.23
sRGBorig	-0.284	-0.181	-0.362	-0.044	-0.159	-0.354	-0.223	-0.361	-0.224	-0.506	-0.27
LGEA1	-0.113	0.038	-0.087	0.072	0.368	-0.130	0.046	0.037	-0.141	-0.083	0.00
LGEA2	0.197	0.013	0.266	0.045	0.180	-0.024	-0.127	-0.102	0.080	-0.024	0.05
LGEA3	0.226	-0.020	0.157	0.071	0.149	0.008	0.120	0.235	0.033	-0.035	0.09
SGEA1LC	0.255	0.082	0.071	0.057	-0.248	0.140	-0.078	0.036	-0.058	-0.082	0.02
SGEA1L50	-0.179	0.239	0.017	0.023	0.073	0.082	0.171	0.020	-0.094	0.249	0.06
SGEA2LC	0.287	-0.012	0.140	0.119	-0.133	0.181	-0.026	0.120	0.145	0.241	0.11
SGEA2L50	-0.143	0.326	0.059	-0.188	0.035	0.153	-0.155	0.050	-0.157	0.152	0.01
SGEA3LC	0.242	-0.094	0.144	-0.013	-0.111	0.000	-0.047	0.205	0.188	0.093	0.06
SGEA3L50	-0.107	0.215	0.159	0.056	-0.034	0.142	0.103	0.208	-0.023	0.204	0.09

Using these interval scores, the respective rank orderings were calculated and displayed in Tables 5.3 and 5.4 as a better means for comparison amongst algorithms than Table 5.1 and 5.2 provide.

Table 5.3 Rank order for Sony evaluation

Rank	Music.	Flower	Lady	F.Tetons	Pastel	Barn	Water	Coast	Fog	RGB	MeanRank
sRGBexp	11	11	11	11	11	11	11	11	11	11	11
sRGBorig	5	10	7	7	7	10	8	9	5	10	10
LGEA1	4	6	3	5	2	9	3	9	7	9	7
LGEA2	4	4	1	3	1	5	1	4	6	5	1
LGEA3	3	3	3	2	5	6	2	4	2	2	1
SGEA1LC	2	5	6	2	5	3	1	1	2	4	1
SGEA1L50	4	1	1	4	1	3	2	4	3	5	3
SGEA2LC	2	4	4	1	1	4	1	2	2	1	1
SGEA2L50	2	2	3	3	2	1	3	3	2	3	3
SGEA3LC	1	2	2	1	2	2	2	1	1	2	1
SGEA3L50	1	1	1	1	1	1	1	1	1	1	1

Table 5.4 Rank order for Samsung evaluation

Rank	Music.	Flower	Lady	F.Tetons	Pastel	Barn	Water	Coast	Fog	RGB	MeanRank
sRGBexp	11	11	11	11	8	10	1	11	1	10	10
sRGBorig	10	10	10	9	9	10	10	10	10	10	10
LGEA1	7	5	9	2	1	9	4	6	8	9	9
LGEA2	5	5	1	5	1	8	7	8	3	6	6
LGEA3	4	6	2	2	1	6	2	1	3	6	2
SGEA1LC	2	4	4	2	7	4	6	5	5	6	5
SGEA1L50	7	2	7	4	2	4	2	5	6	1	5
SGEA2LC	1	5	5	2	7	1	5	4	2	1	2
SGEA2L50	7	1	6	7	3	1	7	5	7	3	6
SGEA3LC	1	7	4	6	7	5	7	3	3	3	6
SGEA3L50	6	2	4	4	4	3	5	2	4	2	4

In order to evaluate the algorithms performance, the rank orderings were used in addition to the individual plots below as a gauge for the overall observer preference scores.

Through Tables 5.3 and 5.4, the performance of both of the baselines is reiterated. Overall, across all ten images, the baselines performed the worst under both destination gamuts. However, the best-performing algorithm is not as definitive. Particularly for the Sony display, there were several algorithms that returned a number one rank in the rank ordering table, Table 5.3. The Samsung narrowed it down slightly from the Sony results, as LGEA3 and SGEA2LC appeared to perform the best, across all images and observers.

The general categories denoted by Heckaman et al., 2007, were specifically analyzed to detect any apparent trends within those groups. Therefore, scenes of high colorfulness (mainly the flower scene), flesh tones (including both the musician and lady images) and natural scenes with a large range in lightness contrast (the coast scene) will be individually evaluated for trends within these categories. In regard to the specific images and preferred algorithms, Figures 5.3 through 5.10 display the results for individual images evaluated. The error bars represent the 0.09 standard deviation as a confidence interval.

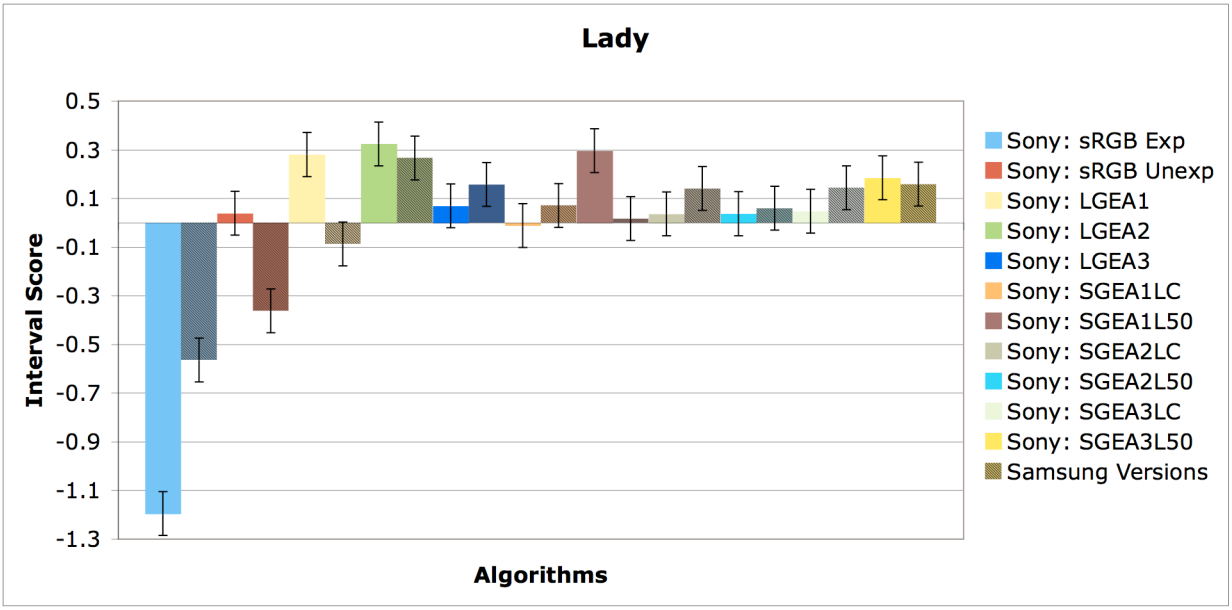

Figure 5.3. The Lady bar plot in interval scores, which directly correlate to overall observer preference. These data are representative of the average observer's response.

For the lady scene, which was comprised predominantly of flesh tones, LGEA1 and LGEA2 performed well on the Sony display, while observers preferred LGEA2 significantly more on the Samsung display. In addition, the SGEA1L50 method performed well on the Sony, which did not occur on the Samsung. Therefore, this image

brings out the preference differences for each display. This image, for both displays, resulted in clearer trends than the Musicians scene, as is apparent in Figure 5.4.

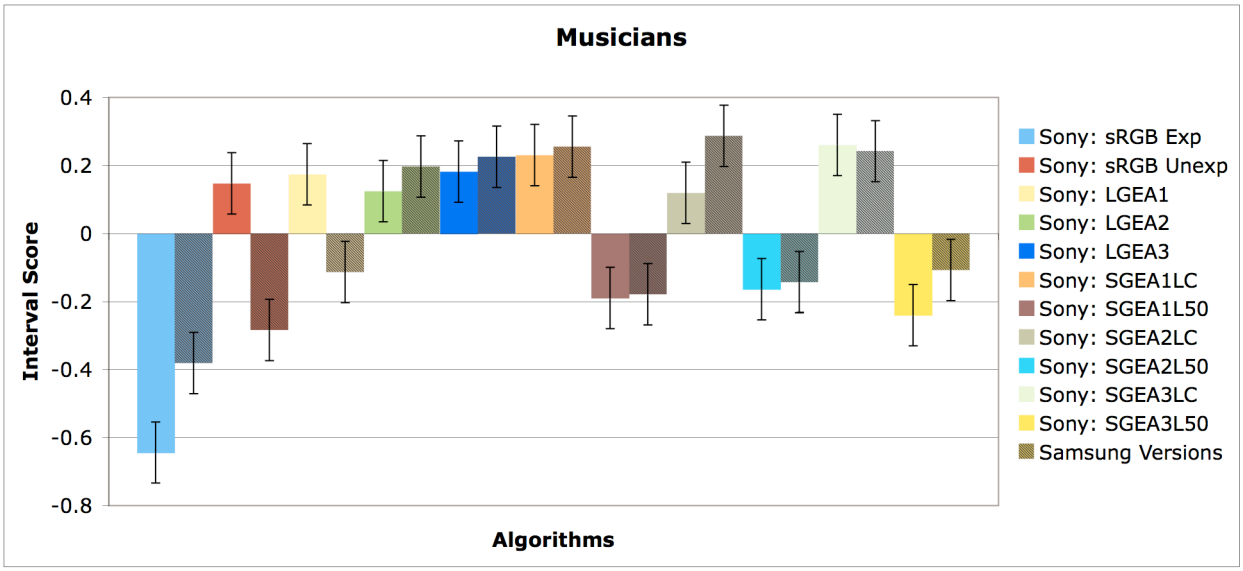

Figure 5.4. The musician image results represented as interval scores for the average observer.

Across both flesh tone scenes, and both displays, the LGEAs performed better than the SGEAs. The scales on Figure 5.3 and 5.4 are different, however, when evaluating the interval score values it becomes apparent the differences between these two scenes. Despite Experiment II linking them in the same "flesh tone" category, they performed uniquely in response to the evaluated algorithms. Observers preferred a more conservative approach to linear gamut mapping for the lady scene, whereas LGEA3 performed the best out of the LGEAs for the musician scene. Also, observers opposed the gamut mapping strategies extending from L* equal to 50, whereas there was not this clear distinction for the lady image.

The observed trends in the SGEAs could be a result of the expansion calculation, as hue and lightness dependencies were accounted for. In other words, as demonstrated

in Figures 4.43-4.51, it was possible for values of low chromatic content to be drastically expanded, or not expanded at all, provided the corresponding hue and lightness combination allowed for either situation. In the former case, although the sigmoidal functions were designed to maintain chroma values for flesh tones, in actuality it did not appear they were expanded at all (Figure 4.42). Since the ratio between output maximum chroma and input maximum chroma for the hue ranges encompassing flesh tones, the resulting transformations were limited.

Therefore, possibly the reasoning the SGEAs were not significantly preferred over the LGEAs was because they were almost performing the same transformations (Figures 4.43, 4.44, 4.50, 4.51). Therefore, in scenes where flesh tones are prevalent, the resulting output chromatic values were lower than the observer's threshold for colorfulness of flesh tones, which explains the near zero, or negative interval scores. Although flesh tones needed to remain true to the observer's memory, if there was truly no expansion, these regions potentially perform similarly to the sRGB unexpanded version.

The SGEA function, SGEA2LC performed much better for a more colorful image.

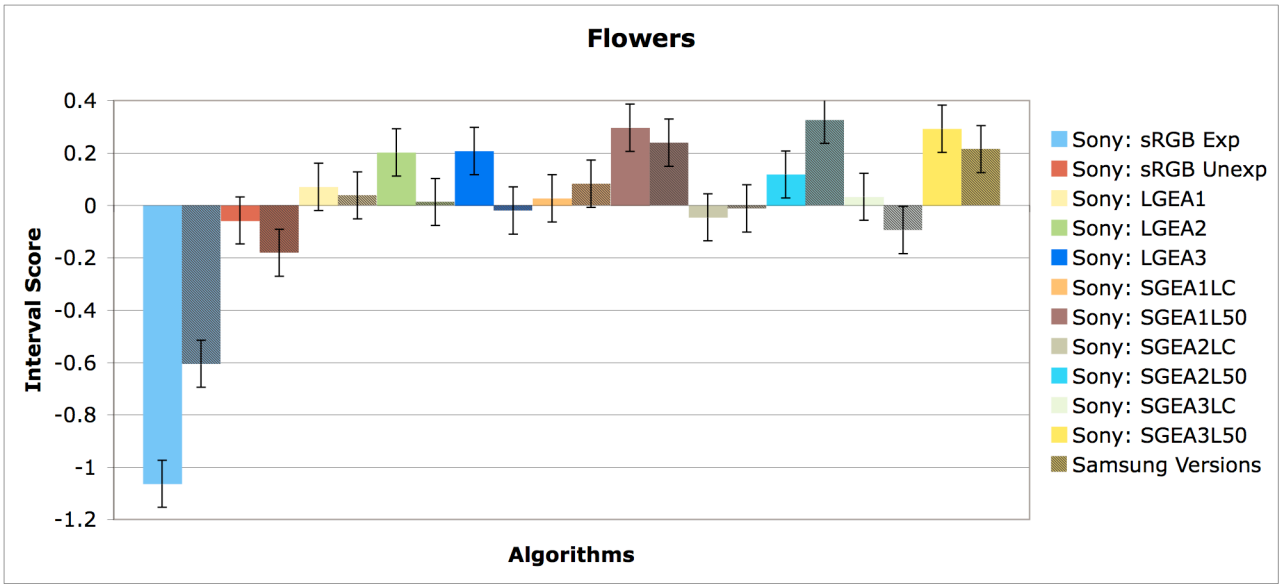

Figure 5.5. The flower scene preference results for each of the eleven algorithms, and both Sony and Samsung displays, are displayed for the average observer.

Interestingly enough, the flower scene displayed almost exact opposite results from that of both the musician and lady scenes. Here, where the original data were already very chromatic, all three sigmoidal expansion methods, extending from a lightness value of fifty, expanded the image data in the most preferable manner. LGEA2 and LGEA3, on the Sony display, were acceptable, however, the sigmoidal expansions were much preferred. This result was more significant for the Samsung display, as none of the linear expansions were preferable.

SGEA1L50 and SGEA2L50, the optimal algorithms for the flower scene, are represented by the red and blue curves, respectively, in Figure 4.42. These curves, as compared to SGEA3, resulted in the least amount of clipping in the sRGB values. SGEA3 clips the sRGB content at a lower chroma value, so that the expansion is more

drastic. Given the already colorful content of the flower scene, it appeared this other curve resulted in undesirable results due to these characteristics of the function itself.

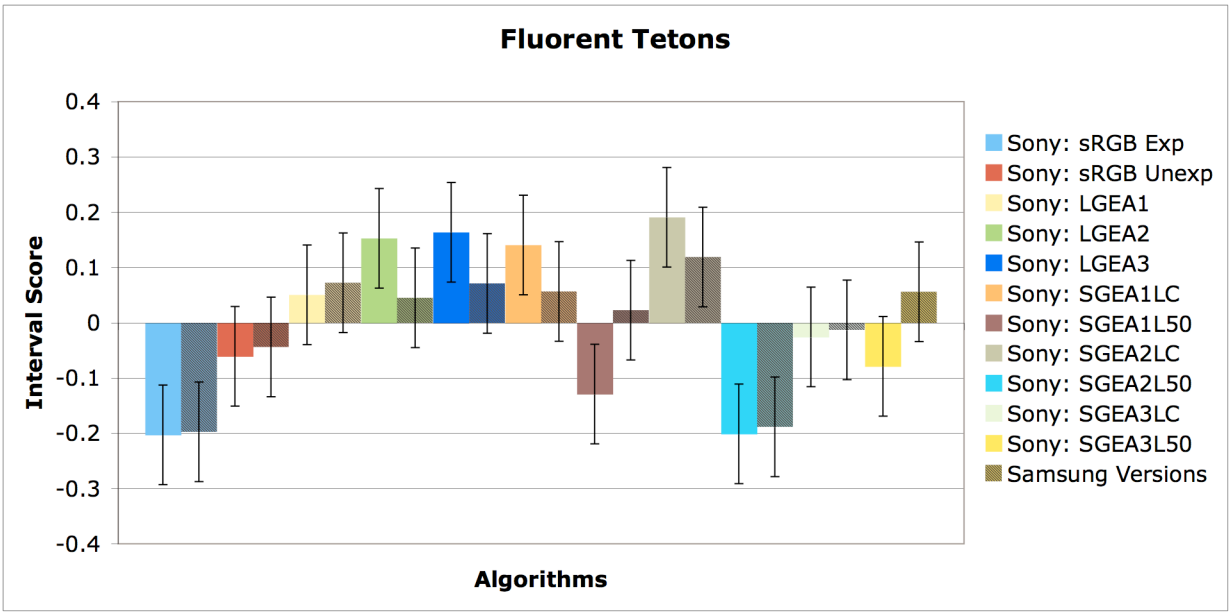

Figure 5.6. Fluorent Tetons results, averaged across observers, for each algorithm, displayed for both devices.

In the fluorent tetons scene, another scene noted for its colorfulness, the linear algorithms performed significantly better than the majority of SGEAs, with the exception of SGEA2LC. It is interesting that a significant difference between SGEAs existed, given the similarity between the sample transformations observed in Figures 4.43 and 4.44. And, furthermore, the fact that these results were consistent across displays provides additional evidence that the sigmoidal functions may perform uniquely.

However, the SGEAs in the barn image performed similarly to that of the flower image, where the barn scene is a third image recognized for its high degree of colorfulness.

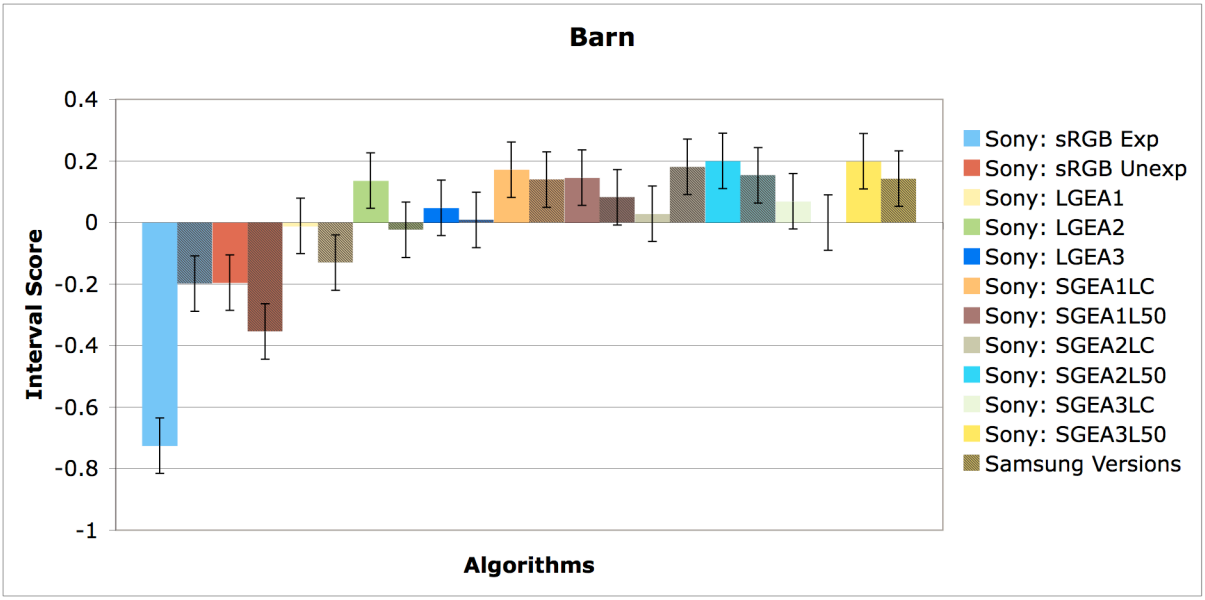

Figure 5.7. The preference results for the barn image for each algorithm and both display evaluations, average across observers.

The SGEAs performed well in this image, as they were significantly preferred over each LGEA except LGEA3. However, there is no statistically significant difference between either mapping direction. Since this image was colorful under sRGB, these colors would be mapped close to the boundary in the output display gamut. However, observers appeared to prefer the additional color, as the sRGBOrig was still disliked. Despite that the additional colorfulness was received well, the sRGB Exp was the least preferred across algorithms. However, this may be a contrast issue, as the linearly stretched version seemed to desaturate the image at the same time. Therefore, it was important to consider both lightness and chroma within the GMAs.

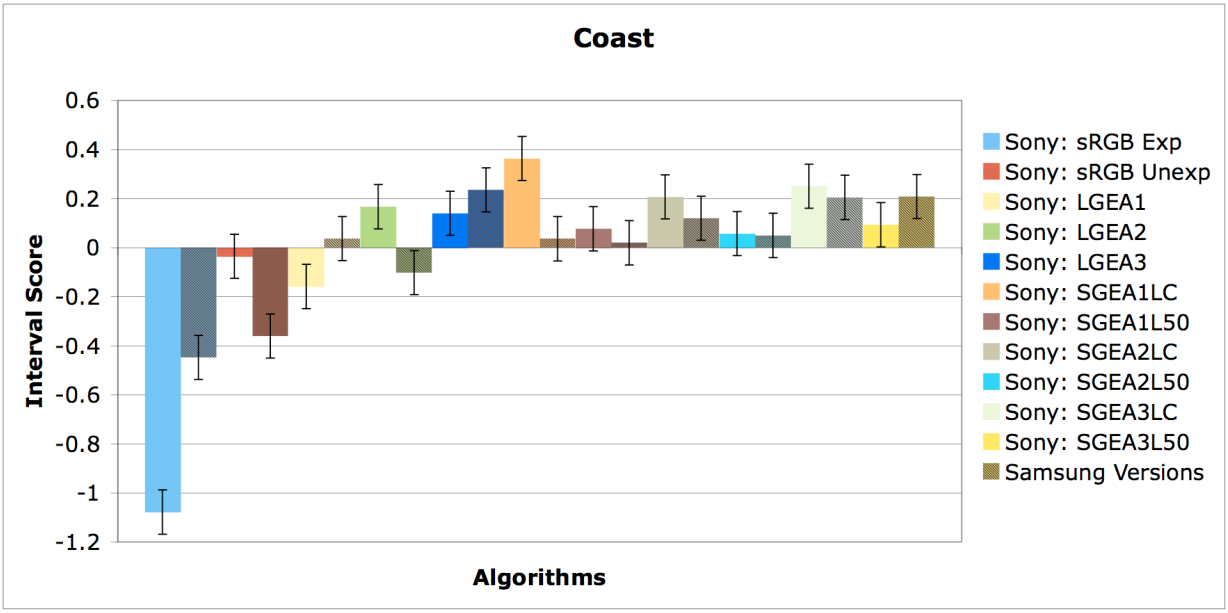

Figure 5.8. The coast scene is represented in terms of interval scores of preference.

In the coast scene, the results were much more dispersed. The significant observations were that the two controls were least preferable, and the SGEAs extending from a reference point of a lightness equal to 50 resulted in undesirable reproductions on the Sony display. This reference point, as compared to maintaining constant lightness, resulted in a few artifacts due to the large change in lightness compared to change in chroma (indicated for a few values in Figures 4.17 and 4.18). A possible explanation for this is explained through the analysis of Figure 5.9.

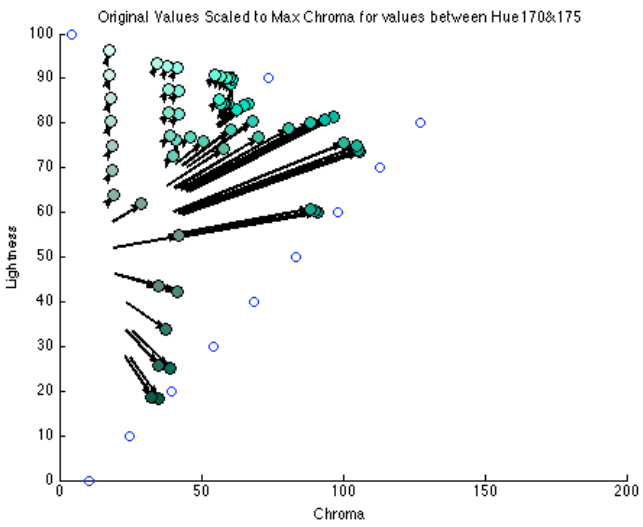

Figure 5.9 Sample transformations under SGEA1L50 for hue angles between 170-175.

The maximum output chroma is much larger for mid-level lightness values than at low or high lighnesses for the mapping direction from L* equal to 50. For example, in the given range of hue angles between 170 and 175˚, the maximum output chroma is approximately 125. Therefore, depending on the lightness and chroma coordinates, any point with a mid-level lightness has the potential to be drastically expanded in colorfulness, due to the sigmoidal function dependent on the chroma. When this occurs, and the chroma is significantly increased, the corresponding lightness does not increase at the same rate, due to the constraint of the reference point of lightness equal to 50. As a result, the overall lightness of the images does appear to decrease slightly, as the color increase is more extreme than the overall increase in lightness contrast. This effect for this mapping direction may have influenced the preference results, particularly for images comprised mostly of mid-lightness values. This effect possibly influenced the fog image, which is recognized for its overall low saturation.

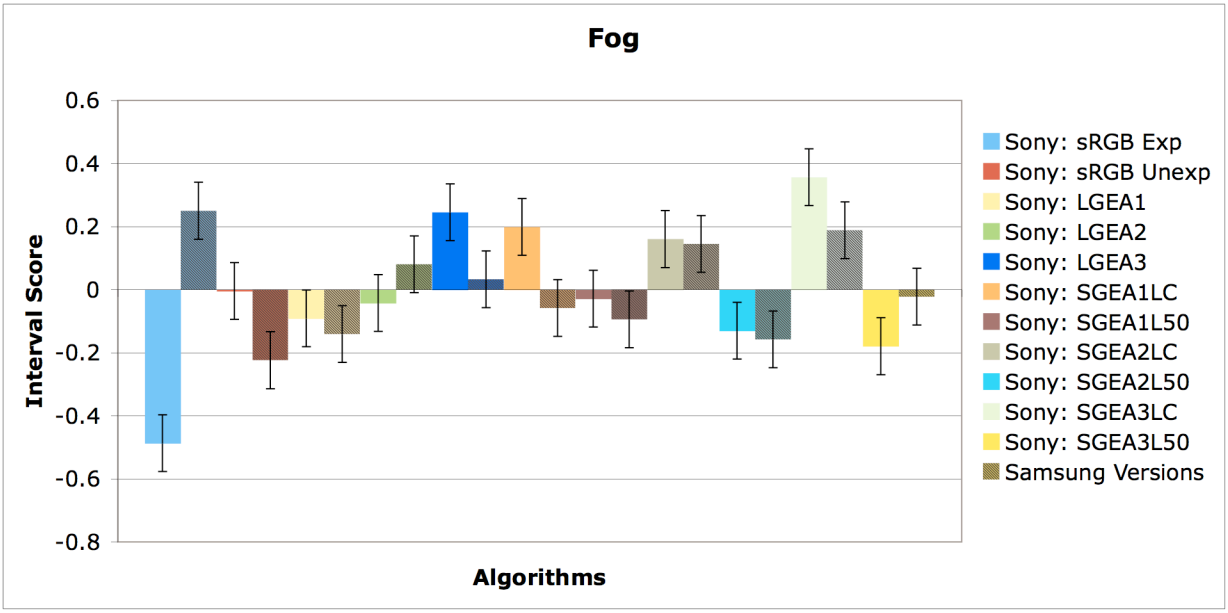

Figure 5.10. Preference interval scores for the fog image, for each of eleven algorithms and two displays and across twenty observers.

This image resulted in clear trends against the mapping direction extending from L* = 50, yet favoring SGEAs maintaining lightness. Similar reasoning could be to blame for this image, as in the Coast image, since it did not appear to be a result of the mapping function in general. Another interesting result, for this image only, was that the evaluation on Samsung display resulted in the sRGBExp version holding its own with the other algorithms. This only occurred for this image, and was most likely a result of the original overall low saturation the image maintained.

Finally, the average results, averaged across observers and images, are displayed in Figure 5.10.

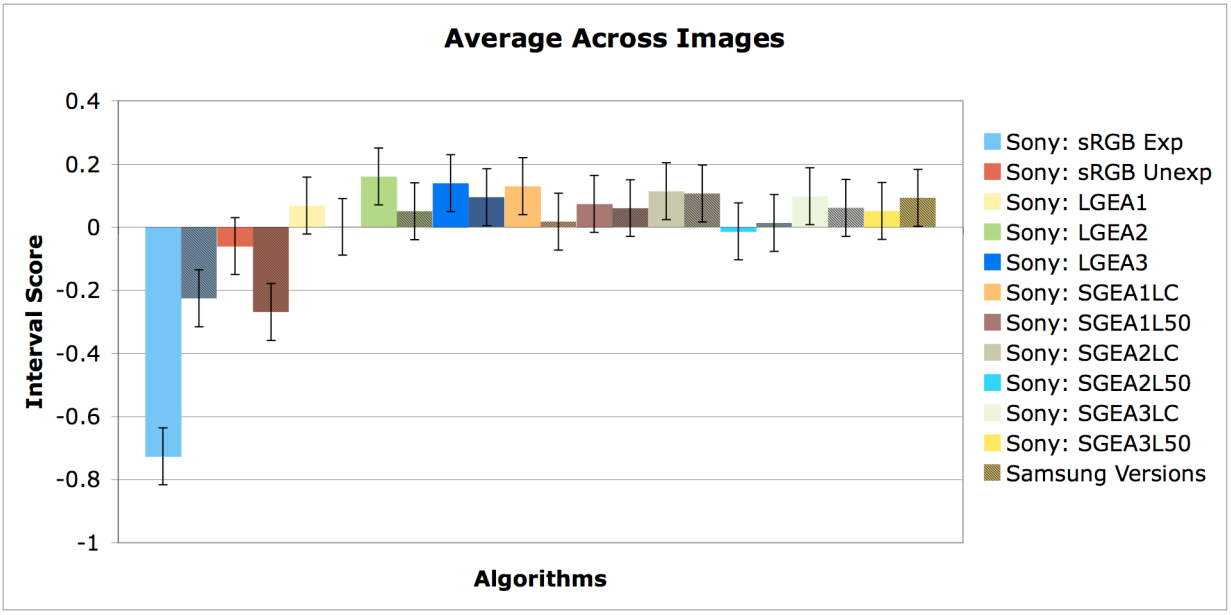

Figure 5.11. Average results for both Sony and Samsung displays.

This image illustrates the difficulty in selecting one algorithm for implementation in a wide-gamut display. However, through analyzing the individual images certain patterns were established, such that further development of a couple of these algorithms should provide an ideal algorithm that could be incorporated into the display.

6. Conclusions

Upon analyzing the preference results based on ten scenes, eleven algorithms and two displays, averaged over twenty observers for each evaluation, one of the most pronounced conclusions regarded the high degree of scene dependency the algorithms maintained. Although the SGEAs are a step in the right direction, there is still improvement necessary so that a more widespread, easily applicable, algorithm is developed that produces preferable reproductions for a wide variety of image content.

Still, all three SGEAs performed well across all images. For images of a high degree of colorfulness, SGEAs extending from L* equal to 50 produced pleasing reproductions. In addition, maintaining constant lightness for high contrast images performed well too. The scenes chosen for flesh tones, however, were consistent in that a slight increase in color, resulting from the LGEAs, was ideal across observers.

If a recommendation for one algorithm is desired, SGEA1L50 would be suggested. This algorithm was highly preferred when the results were averaged across all images and observers. In addition, this algorithm was preferred over its counterparts for many of the representative images emphasized earlier. In addition, the observer preference for this version was not display dependent. The SGEAs in general, but particularly SGEA1L50 is a good basis for improving linear expansion, and with a few minor alterations, could be the optimal reproduction method for mapping images under current sRGB standards to wide-gamut displays.

By comparing two unique display technologies, the applicability of the results becomes evident. Although there are some differences between the displays, most often they correlate with one another. Therefore, by continuing research in the development of

a gamut extension algorithm, and possibly adjusting a few of the methods incorporated in this study, a GEA applicable to multiple display technologies will be attainable.

Many recent studies have provided solid evidence that viewers enjoy more color within their display. With the technology flourishing, the need for an optimal algorithm is becoming more apparent. This study has provided an excellent basis for this desired algorithm, and with relatively minor tweaking, will be capable of providing viewers world-wide with more satisfying images.

7. References

[3M, 2008]
LCD Optics 101, 3M, http://solutions.3m.com/wps/portal/3M/en_US/Vikuiti1/BrandProducts/secondary/optics101/, 2008.

[Anderson et al.; 2007]
Anderson, H. E.K. Garcia and M.R. Gupta, Gamut Expansion for Video and Image Sets, Computational Color Imaging Workshop, 1-4, 2007.

[Bang and Choh; 2007]
Bang, Y and HK Choh , Print Color Enhancement for a Wide Gamut Source, *JIST*, 4305, 1-14, 2007.

[Bartleson; 1984]
Bartleson CJ, Measuring differences, Chapter 8, Optical Radiation Measurements, Volume 5, Chapter 8, Academic Press, 1984.

[Braun et al.; 1998]
Braun, G.J., F. Ebner, and M.D. Fairchild, Color Gamut Mapping in a Hue-Linearized CIELAB color space, *IS&T: CIC6*, 163-168,1998.

[Braun and Fairchild; 2000]
Braun, G.J. and M.D. Fairchild, General-Purpose Gamut-Mapping Algorithms: Evaluation of Contrast-Preserving Rescaling Functions for Color Gamut Mapping, *JIST*, 44, 4, 343-350, 2000.

[Braun and Fairchild; 1999]
Braun, G.J. and M.D. Fairchild, Image lightness rescaling using sigmoidal contrast enhancement functions, *Jour Elec Img*, 8, 4, 380-393, 1999.

[Day et al.; 2004]
Day, E., L. Taplin and R.S. Berns, Colorimetric characterization of a computer-controlled liquid crystal display, *Color Res Appl,* 29, 5, 365-373, 2004.

[DeCorte; 1986]
De Corte, W., Finding appropriate colors for color displays, *Color Res Appl*, 11, 56-61, 1986.

[DeMarsh and Giorgianni; 1989]
Demarsh, L.E. and E.J. Giorgianni, Color Science for Imaging Systems, *Phys. Today*, 42, 9, 42-55, 1989.

[Fairchild; 2005]
Fairchild, M.D., Color Appearance Models, John Wiley & Sons, Second Edition, 2005.

[Fedorovskaya et al.; 1997]
Fedorovskaya, E.A., H. de Ridder, and F.J.J Blommaert, Chroma variations and perceived quality of color images of natural scenes, *Color Res Appl*, John Wiley & Sons, Inc., 96-110, 1997.

[Fraser and Blatner; 2006]
Fraser, B. and D. Blatner, Adobe® Photoshop CS2: Industrial-Strength Production Techniques, Peachpit Press, Berkley, CA, 2006.

[Fraser et al.; 2005]
Fraser, B., C. Murphy, and F. Bunting, Color Management: Industrial Strength Production Techniques, Peachpit Press, Berkley, CA, Second Edition, 2005.

[Gentile et al.; 1990]
Gentile, R.S., E. Walowit and J.P. Allebach, A Comparison of Techniques for Color Gamut Mismatch Compensation, *J. Img Tech,* 16, 176-181, 1990.

[Heckaman and Fairchild; 2007]
Heckaman, R.L. and M.D. Fairchild, Beyond the Locus of Pure Spectral Color and the Promise of HDR Display Technology, *SID*, 23, 7, 22-26, 2007.

[Heckaman et al.; 2007]
Heckaman, RL et al., The Effect of Display Gamut Volume on Image Preference, IS&T: *CIC15*, 201, 2007.

[Hill et al.; 1997]
Hill, B., Th. Roger and F.W. Vorhagen, Comparative Analysis of the Quantization of Color Spaces on the Basis of the CIELAB Color-Difference Formula, *ACM Trans. Grph.,* 16, 2, 1997.

[Hollemann et al.; 2001]
Hollemann, G., B. Braun, P.Heist, J.Symanowski, U.Krause., High Power Laser Projection Displays. *SPIE Proc.*, 4294, 36-46, 2001.

[Hoshino; 1994]
Hoshino, T., Color estimation method for expanding a color image for reproduction in a different color gamut, US Patent 5, 317, 426, 1994.

[Hung and Berns; 1995]
Hung, P. and R.S. Berns, Determination of Constant Hue Loci for a CRT Gamut and Their Predictions Using Color Appearance Spaces, *Color Res Appl*, 20, 5, 285-195, 1995.

[Hunt; 2004]
Hunt, R.W.G. The Reproduction of Colour, 6th Ed., England: Wiley, 2004.

[ICC; 1996]
International Color Consortium, ICC Profile Specification, Version 4, http://www.color.org.

[IEC; 2006]
International Electrotechnical Commission, Multimedia Systems and Equipment-Colour Measurement and Management-Part 2-4- Colour Management –Extended-Gamut YCC Colour Space for video applications- xvYCC, http://webstore.iec.ch/webstore/webstore.nsf/artnum/035442, 2006.

[IEC; 2003]
IEC 61966-2-1: 1999 Multimedia systems and equipment- Colour measurement and management-Part2-1: Colour management- Default RGB colour space- sRGB Amendent 1, 2003.

[ITU-R BT.709-5; 2002] Parameter values for the HDTV standards for production and international programme exchange. April 2002.

[JEITA; 2002]
JEITA CP-3451, Exchangeable image file format for digital still cameras: Exif Version 2.2, Technical Standardization Committee on AV &IT Storage Systems and Equipment, 2002.

[Johnson; 2004]
Johnson, G. calczscore, Matlab code, 2004.

[Johnson et al.; 2004]
Johnson, G. R. Patil, E.D. Montag, M.D. Fairchild, Image Quality Scaling for Electrophotographic Prints, *SPIE Proc.,* 5294: 165-175, 2004.

[Kang et al.; 2005]
Kang, BH, MK Cho, HK Choh, and CY Kim, Perceptual Gamut Mapping on the basis of Image Quality and Preference Factors, *SPIE Proc.,* 2058, 2005.

[Kang et al.; 2003]
Kang, B.H., Morovic, J., Ronnier Luo, M., and Cho, MS., Gamut compression and extension algorithms based on observer experimental data, *ETRI*, 25: 156-170, 2003.

[Kennel; 2007]
Kennel, G., Color and Mastering for Digital Cinema: Digital Cinema Industry Handbook Series, Elsevier, Oxford, UK, 2007.

[Kerr; 2005]
Kerr, Douglas A., P.E. The sYCC Color Space, 1.1, http://doug.kerr.home.att.net/pumpkin/sYCC.pdf, 2005.

[Kim; 2007]
Kim, Moon-Cheol, Comparative color gamut analysis of xvYCC standard, Science Direct: Displays, 29, 4, 376-385, 2007.

[Kotera et al.; 2002]
Kotera, H., Suzuki, M, Mita, T., and Saito, R., Image-dependent color mapping for pleasant image renditions. *SPIE Proc.*, 4421: 463-466, 2002.

[Kotera et al.; 2001]
Kotera, H,, Mita, T. Hung-Shing, c. and Saito, R., Image-dependent gamut compression and extension, *PICS Proc.,* 288-292, 2001.

[Laird and Heynderickx; 2008]
Laird, J. and I. Heynderickx, Perceptually optimal boundaries for wide gamut TVs, *SPIE Proc*., 6807, 2008.

[Lee et al.; 2000]
Lee, C.S., C.H. Lee and Y.H. Ha, Parametric gamut mapping algorithms using variable anchor points, *IS&T*, 44,1, 68- 89, 2000.

[MacDonald, et al.; 2001]
MacDonald, L., J. Morovic and K. Xiao, Evaluation of a Colour Gamut Mapping Algorithm, *AIC*, 2001.

[MacDonald et al.; 2000]
MacDonald, L., J. Morovic and K. Xiao, A Topographic Gamut Mapping Algorithm Based on Experimental Observer Data, *IS&T:CIC8*, 311-317, 2000.

[Matsumoto et al.; 2006]
Matsumoto, T. et al., xvYCC: A New Standard for Video Systems using Extended-Gamut YCC Color Space, *SID 06*, 19:2, 1130-1133, 2006.

[Montag and Fairchild; 1998]
Montag, E.D. and M.D. Fairchild, Gamut Mapping: Evaluation of Chroma Clipping Techniques for Three Destination Gamuts, *IS&T:CIC6*, 57-61, 1998.

[Montag and Fairchild; 1996]
Montag, E.D. and M.D. Fairchild, Simulated color gamut mapping using simple rendered images, *SPIE Proc.*, 2658: 316-325, 1996.

[Moroney and Zeng; 2003]
Moroney, N. and H. Zeng, Field trials of CIECAM02 color appearance model, http://www.hpl.hp.co.uk/personal/Nathan_Moroney/cie-2003-moroney.pdf, 2003.

[Morovic and Luo; 2001]
Morovic, J. and M.R. Luo, The Fundamentals of Gamut Mapping, *JIST*, 45, 3, 283-290, 2001.

[Morovic and Luo; 1998]
Morovic, J. and M.R. Luo, Verification of Gamut Mapping Algorithms in CIECAM97s Using Various Printed Media, *IS&T:CIC6*, 53-56, 1998.

[Muijs et al.; 2008]
Subjective Evaluation of Gamut Extension Methods for Wide-Gamut Displays, *J. Elec. Img*, 2008.

[Nielson and Stokes; 1998]
Nielsen, M. and M. Stokes, The Creation of the sRGB ICC Profile, *IS&T:CIC6*, 253-257, 1998.

[Poynton; 2003]
Poynton, C. Digital Video and HDTV: Algorithms and Interfaces, Elsevier, San Francisco, CA, 2003.

[Poynton; 1997]
Poynton, C. Frequently Asked Questions About Color, http://www.poynton.com/PDFs/ColorFAQ.pdf, 1997.

[Reinhard et al.; 2007]
Reinhard et al., Image display algorithms for high- and low-dynamic-range display devices., *SID*, 15, 12, 997-1014, 2007.

[Ridder and Blommaert; 1995]
Ridder, H., and Blommaert F.J.J., Naturalness and image quality: chroma and hue variation in color images of natural scenes, *SPIE Proc.*, 2411, 51-61, 1995.

[Sakurai et al.; 2007]
Sakurai, M., R.L. Heckaman, M.D. Fairchild, T. Nakatsue, Y. Shimpuku, Relationship between Color Appearance and Color Gamut of the Display, *IDW*, VHF5-2, 2007.

[Samadani and Li; 2006]
Samadani, R. and G. Li, Geometrical Methods for Lightness Adjustment in YCC Color Space, *SPIE Proc.*, 6058, 605809-1-6 , 2006.

[Samsung; 2008]
Samsung, DLP tv: HL-T5087S, http://www.samsung.com/us, (2008).

[Spaulding and Braun; 2005]
Spaulding, K. and Gus Braun, Metrics for Comparison of Color Encodings, Proc. CIETC8-05, 2005.

[Stokes et. al; 1996]
Stokes, M. et al., A Standard Default Color Space for the Internet- sRGB, International Electrotechnical Commission (IEC/4WD 61966-2-1),Version 1.10, 1996.

[Stone et al.; 1988]
Stone, M.C., W.B. Cowan and J.C. Beatty, Color Gamut Mapping and the Printing of Digital Color Images, *ACM Trans. Gph.,* 7, 4, 249-292, 1988.

[TI; 2008]
Texas Instruments. How DLP Technology works. www.dlp.com, 2008.

[Wen; 2005]
Wen, S., Display gamut comparison with number of discernible colors, *Jour Ele Img*, 15, 4, 043001-1-8, 2005.

[Wolski et al.; 1994]
Wolski, M., J.P.Allebach and C.A. Bouman, Gamut Mapping: Squeezing the Most out of Your Color System, *IS&T: CIC2*, 89-92, 1994.

[Zeng; 2005]
Zeng, H., Color Encoding for Gamut Extension and Bit-depth Extension, *SPIE Proc.*, 5637, 6-13, 2005.